Regeneratively and Passively Constrained Control of Vibratory Networks

by

Eric Warner

A dissertation submitted in partial fulfillment
of the requirements for the degree of
Doctor of Philosophy
(Civil Engineering)
in The University of Michigan
2017

Doctoral Committee:

Associate Professor Jeffrey T. Scruggs, Chair
Professor Jerome P. Lynch
Associate Professor Jason P. McCormick
Assistant Professor Chinedum E. Okwudire

Eric Warner

erwarner@umich.edu

ORCID iD: 0000-0002-0954-6750

To my soon-to-be wife Lyla, my parents Vernon and Janice, and my friends and family who have helped me get to this point

ACKNOWLEDGEMENTS

First and foremost I would like to thank my advisor Jeffrey Scruggs. Five years ago, Jeff sold me on this new Systems Program and the work we would be doing within it. Throughout my time here, Jeff has been there for me every step of the way. Whether it was help with homework, practice preliminary exams, weekly research meetings, or just talking about control and future projects, Jeff was always available and cared about every aspect of my education. I could honestly say I would be nowhere near where I am today without his guidance and effort towards my progress as an academic and a professional.

I would also like to thank my dissertation committee Jerome Lynch, Jason McCormick, and Chinedum Okwudire. Their guidance and advice helped shape the direction my research has gone and enlightened me about essential questions I had not yet considered. They allowed me to consider my work from another perspective and therefore broaden the spectrum of what I was considering.

I would also like to thank my fiancée Lyla. Lyla has supported me in countless ways in both my professional development and more importantly my emotional well-being. Simply being able to see her at the end of stressful days made the problems of the day seem insignificant. Her love and support has allowed me to grow as a person and as a student, and I will be forever grateful to how much she's done for me.

To my parents Vernon and Janice, thank you for the constant support and advice throughout the last five years. You've raised me to be the man I am today, and I will

continue to try to make you proud. Thank you as well to my brothers Christopher and Jeffrey, whose (sometimes without warning) visits made me feel closer to home and whose confidence ("Eric you're smart, you'll be fine") in me helped me out in stressful times. Thank you to the rest of my extended family as well, who continually asked me when I'd be moving closer to home and pretended to care about my research. Thanks to Buffy and Fred, my future in-laws, for their love and support throughout my time here.

I'd also like to thank my lab-mates for their support throughout my time here, especially Rudy Nie and Brenden Ritola. We've shared many classes together, and working alongside you guys made impossible homeworks seem possible and concepts easier to understand. Thank you as well to the rest of the GG Brown Crew; Dan, Malcolm, Andy, Nephi, Sean, Yilan, Jon, Mitch, Paul to name a few. The comradery between us, whether it is IM sports, fantasy football, or dinners and drinks have made my experience here unforgettable.

Lastly, I would like to thank the funding agencies which have supported me throughout my time in Ann Arbor. More specifically, I would like to thank The University of Michigan Rackham Graduate School for the Rackham Merit Fellowship and The National Science Foundation for funding through awards CMMI-0747563 and CMMI-1235732. Their generosity allowed me to pursue my degree and research I am passionate about.

TABLE OF CONTENTS

LIST OF FIGURES

Figure

ABSTRACT

Regeneratively and Passively Constrained Control of Vibratory Networks

by
Eric Warner

Chair: Jeffrey Scruggs

This dissertation is focused on the control of vibratory networks. Mechanical examples of vibratory systems include a civil structure, automobile, and a cantilever beam. These systems are excited by external disturbances such as earthquakes, wind, or uneven road elevations. Both passive and active control laws can be utilized to suppress vibrations in these networks. Each type of control law possesses inherent advantages and drawbacks. Active control provides the highest performance but is expensive, relies on an external power source, and is complicated to implement and maintain. Passive control devices (composed of springs, inertial elements, dashpots) represent the cheapest option and provide energy-autonomy, but have inferior performance when compared to an active control device. Due to their reliability and low cost, passive control technologies set the baseline for comparison for other, more sophisticated technologies. On the other hand, although it yields superior performance, active control presumes availability of unlimited energy, which may be an impractical or unreliable assumption. This dissertation examines a new class of control technologies, called regenerative control systems. A regenerative control system

theoretically possesses energy-autonomy, but does so with better performance when compared to a passive control system. However, regenerative control devices are more expensive than passive and therefore the improved performance they attain must warrant utilization.

A regenerative control device is assumed to be connected to a large energy storage device (battery, supercapacitor, etc). At times, the control device will draw energy from the energy storage device in order to actuate the network. At other times, the control device converts mechanical energy from the network into electrical energy and replenishes the energy in the storage device. The regenerative controller is constrained such that, on average, it generates more energy than it expends. This constraint, which is a relaxation of a passive control law constraint, ensures the local energy storage device never completely depletes.

One of the main focuses of this research is to develop theory which can can solve for optimal regenerative and passive control laws. Optimizing control laws for both types of technology, in the context of the same problem, allows for a fair comparison. The regenerative control design problem can be formulated as a convex optimization and therefore can be solved easily with many commercial solvers. Passively constrained control design is a nonconvex problem and a new technique, Iterative Convex Over-Bounding (ICO) is proposed and developed to solve this nonconvex optimization. We show that optimal regenerative control outperforms optimal passive control if parasitic losses are sufficiently small. We also propose a technique to quantify how large the parasitics can be for a regenerative controller to still outperform a passive controller for a given problem.

CHAPTER 1

Introduction

For many decades, vibration suppression has remained relevant in control systems research, with many advancements made in the field which span numerous branches of engineering [49]. Although mechanical or electrical control devices for vibration suppression were introduced over one hundred years ago [21], there continue to be significant technological advances. The purpose of a control device is to suppress vibration in a mechanical system which is being externally excited. A common control device is composed of a mass, spring, and an optimal level of damping. For a simple example, see Figure 1.1a, which shows a simple mechanical system being excited by a base acceleration a, producing movement in the network x. The control device, i.e., the mass, spring, and dashpot on top of the structure, then aims to suppress the vibrations induced in the mechanical structure.

The simplest choice of control device is a spring-mass oscillator [37,38]. One such instance of this is a tuned mass-dampers (TMD) [1,12], which is utilized in buildings. Additionally, pendulum-type absorbers have been implemented in various studies as well as practical applications [22, 107]. In the civil engineering field [44], control devices of this nature have been applied to tall buildings [46, 48, 68] and bridges [94] which undergo excitation from earthquakes and wind loading. Large structures have

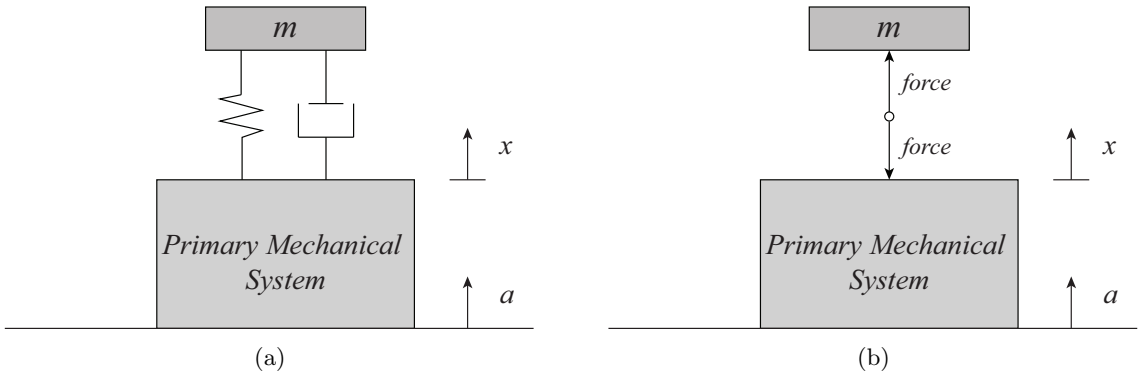

Figure 1.1: Simple Vibration Suppression Applications, which show a Controller Composed of Mechanical Components (a) and a Force Over a Reactionary Mass (b)

also been controlled via base isolation systems [58] and semi-active devices, such as magnetorheological (MR) dampers [18] or variable orifice dampers [57, 69, 93]. Another type of control device utilizes a force which acts against a reactionary mass (see Figure 1.1b) rather than springs, masses, and dashpots. These types of devices often require control algorithms, which in some cases originate from classical control techniques [40, 56, 97]. Other studies have implemented fuzzy control logic and neural networks [23, 40]. Control algorithms have also been implemented via Linear-Quadratic Gaussian (LQG) techniques [59, 63, 82, 108], a type of optimal control. Other branches of engineering, which utilize the same theory, include vibration suppression of automotive suspension systems [45], flexible beams and plates in aerospace structures [6], and prosthetic limbs in biomedical applications [99]. Both types of control devices in Figure 1.1 will be explored in more depth in the coming sections. For a more detailed list of past work, theoretics, and applications, see the survey paper [98].

To visualize a few examples of vibration suppression across various applications, see Figure 1.2. Shown in Figure 1.2a is a structure under an earthquake excitation, in Figure 1.2b a quarter-car model moving along an uneven road, and in Figure 1.2c a base excited flexible cantilever beam. Each is excited by an exogenous disturbance

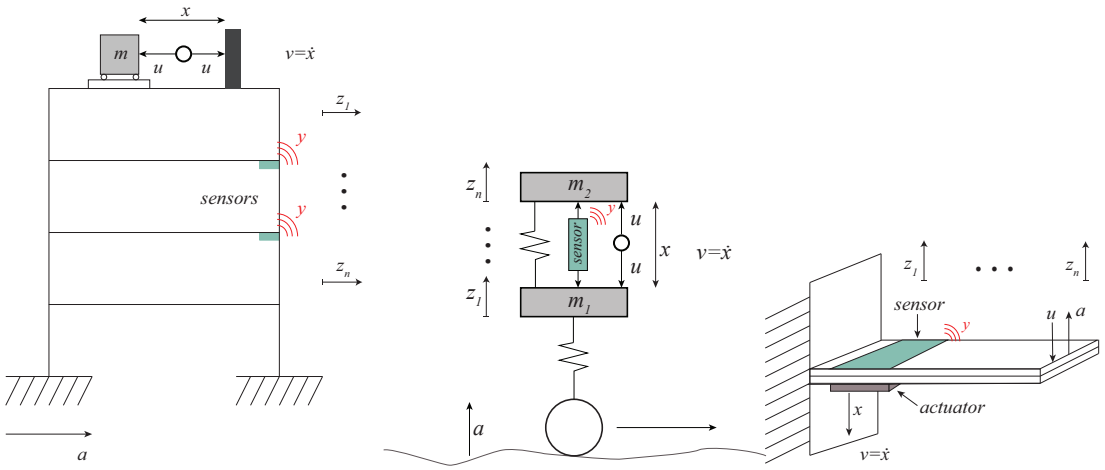

(a) Example Structural Vibration Suppression

(b) Example Quarter Car Model Vibration Suppression

(c) Example Piezoelectric Beam Vibration Suppression

Figure 1.2: Example Vibration Suppression Applications

a. This disturbance can be random (in the case of the earthquake and force), or something that can be more precisely known, such as the road elevation for the quarter-car model. The system then has the ability to incorporate sensors, which allow for an output y to be measured, where y is one or more response quantities (displacement, velocity, acceleration, etc.). Sensors are not necessarily required for examples such as Figure 1.1a, but do become necessary for applications such as Figure 1.1b and Figure 1.2 and allow for a larger domain of feedback laws to be implemented. The control device applies a control force u based on present and past values of y. This feedback law between y and u is optimized to minimize a performance output z, which is a vector of response quantities deemed important. The control device velocity is defined as v.

A subset of controllers uses only device velocity as feedback; i.e., $y = v$. Called collocation, this has certain advantages for stability robustness of active control, and is characteristic of all passive control systems [83]. Figure 1.3 shows a block diagram of the input-output systems introduced in Figures 1.2 and 1.1. As shown, the inputs are a and u into the network, producing the outputs z, v, and y. The feedback output

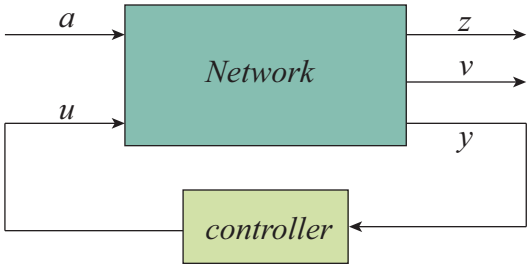

Figure 1.3: Block Diagram Representation of Control Process

y feeds into the controller block, which generates a control force u to be applied to the network in order to actuate the network. The objective of the controller is to minimize the effect of the vibrations, more specifically to minimize the characteristics of the network in the performance objective z.

At this point, an important distinction arises between the feedback law (also called control law) and the control device. The feedback law is the mathematical relationship between the input y and the output u, usually generated via an optimization problem. The control device is the hardware which realizes this optimized control law in the physical application. Often, it is assumed that if a feedback control law is utilized, feedback sensors and electronic control hardware are required. However, mechanical components (springs, dashpots, inertial elements) can also impose a feedback law.

Consider the two control device types shown in Figure 1.4. In Figure 1.4a, the control device (passive network) employs the previously mentioned mechanical components. In Figure 1.4b, the control device (actuator in the figure) utilizes an electronic feedback law which is computed via measurements from sensors (e.g., accelerometers, piezoelectric devices, etc.). Both the control device composed of exclusively mechanical components in Figure 1.4a and the one composed of a combination of mechanical and electrical components in Figure 1.4b realize feedback control laws. In Figure 1.4a, feedback is imposed via the dynamics and constitutive relations of

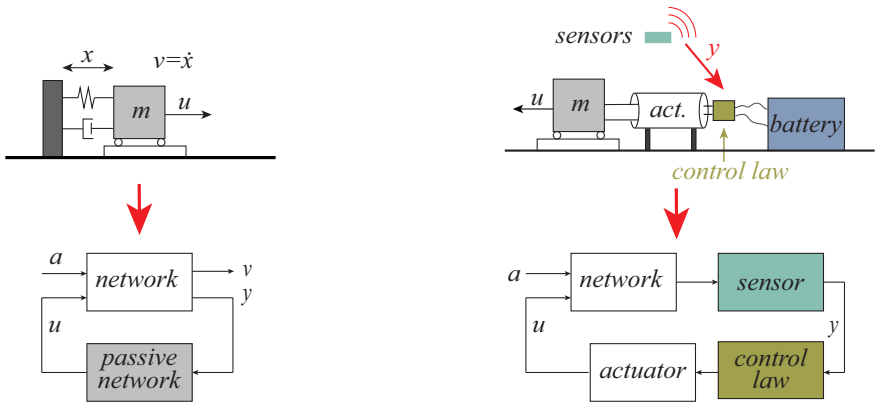

(a) Passive Controller Components

(b) Active Controller Components

Figure 1.4: Example Controller Structural Setup

the mechanical components and in Figure 1.4b feedback is imposed via the electronic law. Additionally, a given control law does not imply a unique control device. Both control device types in Figure 1.4 can realize the same control law, as long as the control law does not violate the physical limitations of the hardware. Various types of hardware (hydraulic actuator, ball-screw actuator, etc.) possess physical limitations such as force or velocity limits and sensor delay. Additionally, these devices operate on differing energy sources (local energy, gird power supply, mechanical energy), which further limit the performance of the control device. These limitations are imposed by limiting the domain of controller and therefore the domain of the optimization in the feedback law. These differing hardware implementations offer diverse capabilities, which are reflected in the feasibility of a control law given the hardware.

In mechanical passive control applications, the mechanical components are aligned such that a control law is realized, i.e., Figure 1.4a. The passive controller is constrained such that, at all times, the net energy is out of the network and into the control device. An example structural passive implementation is the pendulum TMD in Tapei 101 in Taiwan. Passive controllers represent the most cost effective and prac-

tical option for many control applications, due to their relative simplicity and lack of reliance on external power.

The controller in Figure 1.4b requires sensors to relay information on movement of the system and software to compute the control law based off these readings. Electric energy, generated from an external grid or local power source, is utilized to power the sensors and software and converted into mechanical energy to actuate the network via the hardware. This actuation can be achieved via an active unconstrained control device, variable stiffness, variable damping, or any law desired, depending on the physical limitations of the hardware and energy available. Those cases which energy comes from the external grid and is therefore "unlimited" are commonly referred to as active control. Active controllers, due to their unlimited energy supply, represent the largest control domain and can therefore achieve the highest performance.

Figure 1.5a shows two different realizations of active control. One transducer utilizes electrical energy storage and the other uses hydraulic energy storage. The actuators, utilizing this external energy, can then produce a control input u which

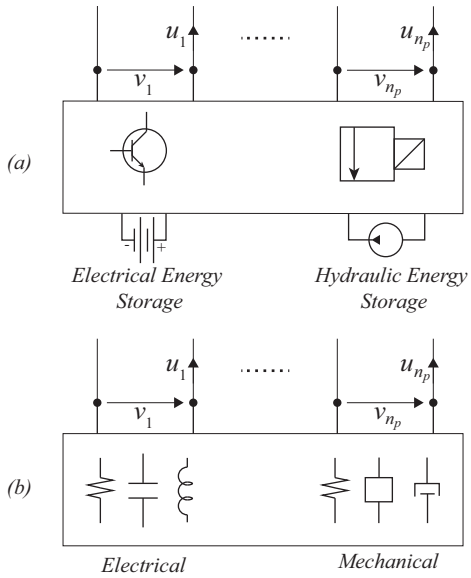

Figure 1.5: Example control technologies, showing two forms of electrical storage and active control (a) and two forms of passive control (b)

suppresses vibrations in the network. Two examples of passive control technology are shown in Figure 1.5b. This technology can be comprised of mechanical (springs, dashpots, inertial elements) and electrical (inductors, resistors, capacitors) components. Regardless of the type of device (mechanical, electrical), the components are configured such that a desired control law is realized. Both passive realizations are also independent of external power and utilize local energy to control the network.

Both active and passive control laws aim to minimize some performance output of a network subject to an exogenous disturbance. However, due to the presence of external power and the ability to realize any control law within the physical limits of the control device, in general the domain of the active controller is much larger than that of the passive controller. Any passive control can be realized via an active controller, but the inverse does not hold.

Ultimately, the goal is to design a control device which can be realized in practical applications. With ever-evolving technology, vibration suppression techniques parallel advances in applicable engineering fields (e.g., automobile, aerospace, and sensor technology). In these practical applications, economic burden and efficiency are the main factors which motivate the implementation of a controller. The control technology must balance performance with space, mass, electronic, and energy limitations to warrant utilization. As shown in previous paragraphs, power and energy requirements play a major role in the efficiency and performance of the control technology.

This research aims to explore the middle ground between active and passive control technologies, a controller which can achieve performance similar to an active controller, but without requiring power grid reliability. In the work presented, this theoretical controller is called a regenerative controller. Throughout this work, the

practicality and efficiency of the regenerative controller is assessed. To do so, the optimal performance of a regenerative controller relative to active and passive controllers must be evaluated.

1.1 Active Control vs. Passive Control

Active control, while achieving the highest performance, possesses limitations. One such limitation is the controller performance in events where the external power source cannot be relied upon (such as an earthquake or natural disaster hitting a civil structure). Without an unlimited power source, the control law realized will be sub-optimal and performance will suffer. Additionally, an active controller has high cost associated with its installation and maintenance. This motivates the use of a controller which does not require an electric grid. In these cases, unlimited energy storage is not required and local energy storage (such as a battery or supercapacitor) is utilized. While technologically advantageous, local energy utilization will limit the domain of feasible controllers and will therefore hinder control performance.

Passive controllers, as mentioned previously, are one way to achieve energy-autonomy via mechanical components such as springs, dashpots, and inertial elements. Passive implementations have been widely utilized in structural contexts. Mechanical tuning devices, such as tuned-mass dampers, are prevalent in vibration engineering [39] as well as civil structures [96]. Passive networks can also be optimized via network synthesis [95]. Passive network theory has also been utilized in electrical contexts, such as vibration suppression via electrical shunt circuits [8, 36, 70].

For reference, consider Figure 1.6. The parameters a, y, and z are as previously defined for the network $\mathcal{N}$. Additionally, we assume the system is controlled through n_p ports, via a vector of potential variables v and a vector of flow variables u. As

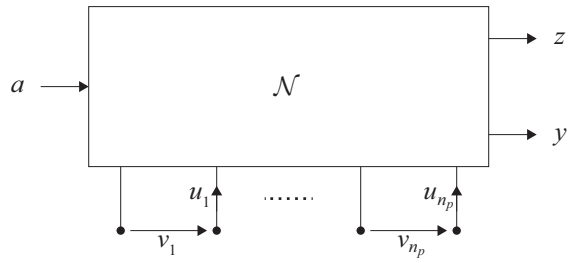

Figure 1.6: Diagram of system under consideration

mentioned, in a mechanical context, u is a force vector and v is a vector of velocities. Analogously, in an electrical context, u is a vector of currents and v is a vector of voltages. As stated, in passive controller optimization the collocation of the measurement output y and velocities (or voltages) v is assumed, i.e., $y = v$. The control strategy then consists of designing a controller $\mathcal{K} : y \to u$ such that the performance output z^2 is minimized. The energy delivered from the system $\mathcal{N}$ to the control device over the time span $t \in [0, T]$ is

$$E(T) = \int_0^T u(t)^T v(t) dt \tag{1.1}$$

and the domain of passive controllers is defined as all controllers that, at every time and for any exogenous disturbance, have extracted more energy from the system than injected, i.e., $E(T) \leq 0 \ \forall \ T, v$.

Equivalently, the domain of passive controllers is limited to those which are Strictly Positive Real (SPR). One advantage of an SPR controller is that, unlike Positive Real (PR) and active controllers, it satisfies the passivity theorem. This states that the closed-loop negative feedback connection of a passive system and a strictly passive system is always stable. Therefore, the assumption must be made that the network is passive as well. This means that when there is no exogenous disturbance, the network cannot deliver energy but rather absorbs energy, i..e $E(T) \geq 0 \ \forall \ T, v$. This assumption is mild considering structures and systems in various control fields

(automotive, aerospace, etc.) are inherently passive and do not explicitly require a stabilizing control law. Had these structures not been passive, the stability of the structure, automobile, or aerospace component could not be guaranteed. A passive controller, while more limited in its domain, guarantees a level of robustness an active controller simply cannot match. This robustness is advantageous when the network parameters are not precisely known or there is damage or degradation to the system which changes network characteristics.

However, passive controllers are not ideal for a number of reasons. The passive constraint may hinder the performance of the closed-loop system compared to an active controller or other such controllers which utilize external power. Passive realizations are also implemented via hardware design, which poses its own set of problems. Even simple passive control laws become composed of elaborate schemes of mechanical or electrical components and are therefore hard to realize in practice. With this complicated design comes a lack of adaptability in the system if there are changes in the network $\mathcal{N}$ or the disturbance characteristics. From the passivity theorem the closed-loop system is guaranteed to be stable, however changes in network or disturbance characteristics render a passive controller sub-optimal. Due to the limitations of active and passive systems, it is therefore more desirable to develop a control law that possesses the performance benefits of an active controller with the energy autonomy of a passive controller. In this vein, a regenerative controller is proposed.

1.2 Regenerative Control

In [53], Margolis and Jolly proposed a device called a *regenerative actuator* which was utilized on automotive suspensions. This work primarily focused on hydraulic

realizations in which the energy is stored in an accumulator. This idea has been advanced within automotive suspensions [66, 75], aerospace applications [80], civil structural applications [32, 74, 89, 104], and application-independent contexts [72]. The regenerative control device is connected to a local energy supply, which in this work will be assumed to be a battery or supercapicitor. When energy is being released from the network, rather than losing that energy to heat, friction, etc., the device uses this energy to replenish the local energy supply. The controller can then, at a later time, use the energy from the supercapacitor or battery to actuate the network. This increases the domain of feasible controllers (when compared to passive) and allows for increased performance.

Consider the example of a regenerative actuation system shown in Figure 1.7. It is assumed u and v are proportional to force and velocity through a coupling factor, which we denote κ, such that $f_i = \kappa_i i_i$, $v_i = \kappa_i \dot{x}_i$. The regenerative control system interfaces the transducers, via controlled power electronics, with a supercapacitor or flywheel. The controller is able to actuate the network entirely off of stored energy in the supercapacitor (called $E_s(t)$). The regenerative system replenishes the local energy supply from energy extracted from the network via the power electronics. This implies the hardware and software collaborate in order to convert electrical to

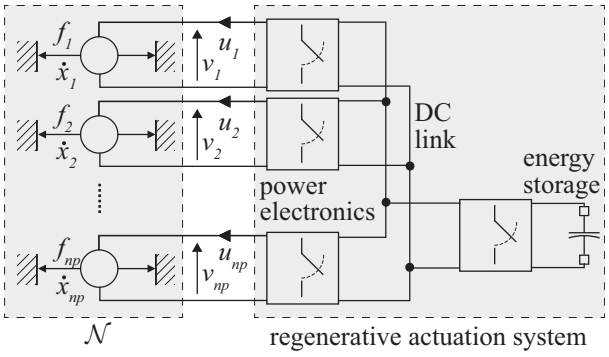

Figure 1.7: Electromechanical Example of a Regenerative Actuation System

mechanical energy and vice versa.

At the end of some time span $t \in [0, T]$, the stored energy in the supercapacitor is

$$E_s(T) = E_s(0) - \int_0^T u^T(t)v(t)dt \tag{1.2}$$

where $E_s(0)$ is the initial storage; i.e., the pre-charge. It is assumed that this precharge is large enough such that the relative magnitude of $E_s(t)$ will drift slowly compared to the dynamics of the network $\mathcal{N}$. Mathematically, this equates to, given a characteristic time constraint $\tau > 0$ for the dynamics of $\mathcal{N}$, $|E_s(t) - E_s(t + \tau)| \ll E_s(0)$. The regenerative constraint implies that, on average, the energy is out of the network, i.e.,

$$\lim_{T\to\infty} \tfrac{1}{T} E_s(T) \geqslant 0 \tag{1.3}$$

As stated, the regenerative constraint is a relaxation of the passive energy constraint.

1.3 Using Examples to Compare Controller Domains

To illustrate the active, passive, and regenerative control domains, consider the example plots in Figure 1.8. The red line represents the initial precharge $E_s(0)$ in the battery or supercapacitor the regenerative system would possess. The dotted line represents the overall trend of the energy

$$\bar{p} = \lim_{T\to\infty} \tfrac{1}{T} E_s(T) \tag{1.4}$$

The first plot shows a case which can be regenerative but not passive. Since there are points where the energy dips below its initial value (i.e., $E(T) > 0$ for some T), this cannot be realized with a passive controller. However, the long term trend of the energy is out of the network and into the control device, and therefore a regenerative

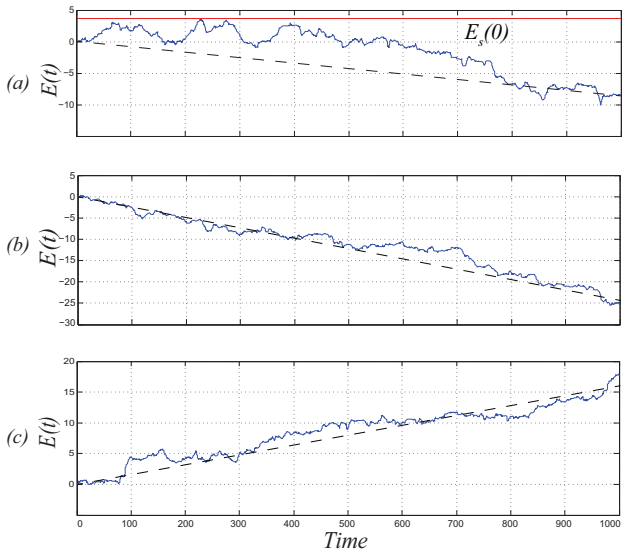

Figure 1.8: Example energy plots for system to be shown later. The dotted line represents the overall trend of the energy

control law is feasible. Figure 1.8b shows a case which can be either passive or regenerative, since $E(T) < 0 \ \forall T$ and the power flow is, on average, positive. Figure 1.8c shows the case where the controller cannot be either regenerative or passive, but can correspond to an active controller. This plot has a long term trend of energy out of the system, and as shown there comes a point where the local energy $E(t)$ reaches zero. At this point, the regenerative controller requires energy from storage to realize its control law, but the battery or supercapacitor has no energy to provide. Therefore, the controller would have to extract energy, and performance of the control law would suffer. This example clearly shows a subset of controllers which are regenerative but not passive, implying a larger domain of regenerative controller.

For an additional example, consider Figure 1.9. This system is purely illustrative, and not necessarily of practical interest. The system is a two degree-of-freedom structure with springs, inertial elements, and dampers non-dimensionalized. The structure is assumed have mass and spring values of one and a damper value of two. The controller is placed between the first and second degree of freedom and

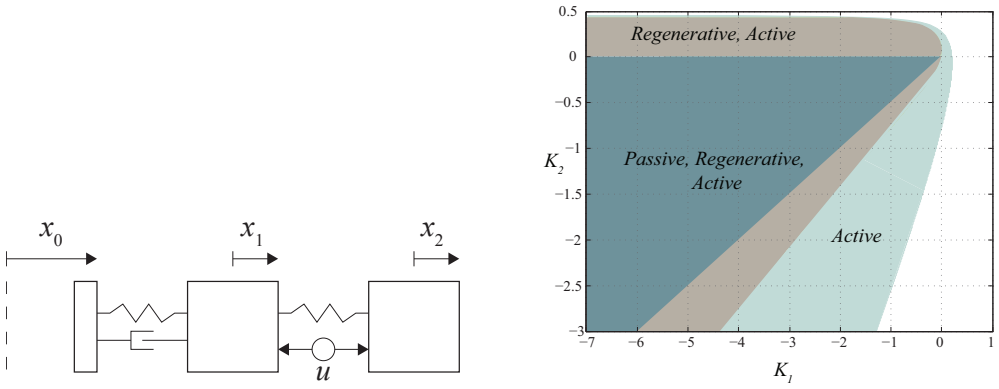

(a) System Setup for Toy Example (b) Domain of Feasible Controllers

Figure 1.9: Two Degree-of-Freedom Example

the base acceleration is assumed to be a stationary stochastic process. Additionally, feedback collocation ($y = v$) is assumed. The exogenous disturbance is assumed to be stochastic and generated via white noise passed through the filter

$$\mathcal{G}(s) = \frac{s\omega_n^2}{s^2 + 2\xi\omega_n s + \omega_n^2} \tag{1.5}$$

where $\omega_n = 2$, $\xi = 0.125$. The controller is assumed to be connected via feedback and of the form

$$\mathcal{K}(s) = \frac{K_1 s + K_2}{s^2 + 2\xi_k\omega_k s + \omega_k^2} \tag{1.6}$$

where $\omega_k = 1$, $\xi_k = 0.25$, and $\{K_1, K_2\}$ are controller gains.

Figure 1.9b shows the feasibility domain for the three types of control technologies (i.e., active, passive, regenerative). As expected, active control, which only requires closed-loop stability, has the largest domain. The regenerative controller has a larger domain than passive, including regions with positive K_2 values. This positive K_2 region (with negative K_1) corresponds to a right-half-plane zero, a violation of the SPR conditions required for a passive controller. This example merely illustrates sub-domains of K_1, K_2 values (not necessarily optimal controllers) which correspond

to the three controller types. Depending on how the performance objective is defined, it could very well be the case that the optimal $\{K_1, K_2\}$ lies in the intersection of the regenerative, passive, and active regions. Nonetheless, this example demonstrates that any passive controller can be realized via a regenerative system, and that, likewise, any regenerative controller can be realized by an active system.

Throughout the work presented, the feasibility and practicality of a regenerative controller has been justified when compared to the baseline passive model. This comparison was done over varying performance measures, types of passive controller (suboptimal/optimal), and disturbance/network domains. In order to make the most meaningful comparison, extensive work has also been completed to find a globally optimal, practical passive controller.

1.3.1 Outline of the Duration of the Report

We set out to find the answers to a few basic questions in the rest of the report.

- How is a regenerative controller theoretically optimized?
- Is there an efficient way to solve for an optimal passive controller?
- How does the performance of a regenerative controller compare to that of passive and active controllers?
- What are the obstacles and complications associated with the practical implementation of the regenerative controller?
- How does a regenerative controller perform when the characteristics of a system are not precisely known?

If successful, the regenerative controller represents a new type of controller that can realistically be implemented in vibration design and an advancement in feedback law design and controller performance.

The rest of this dissertation is outlined as follows: Chapter 2 will go through the network modeling assumptions being used for much of the report and the assumptions being made throughout the report. Chapter 3 will generate the regenerative constraint in a convex form and then account for parasitics. It will then show that a regenerative controller, through a coordinate transformation, can be optimized without conservatism. Lastly, using a number of examples, a regenerative controller will be compared to an optimal active controller. Chapter 4 will optimize a passive controller in two ways. First, we propose a sub-optimal but convex technique, whereby the zeros of the optimal regenerative controller are adjusted to the closest possible passive controller. An example of this will be shown for the same two degree-of-freedom structure from the regenerative chapter. Next, an optimal passive controller will be found with minimal conservatism via nonconvex optimization. Numerous examples of this, when compared to an optimal regenerative controller, will be shown for various performance measures and number of applications. Chapter 5 is a more general and in-depth investigation on nonconvex optimization techniques for problems like passivity-constrained control. In Chapter 6, an optimal regenerative controller is found over an uncertain polytopic parameter domain. The sensitivity of performance to disturbance uncertainty is shown in an example. In Chapter 7, conclusions are made about the work that has been done and future directions are proposed.

CHAPTER 2

Network Characterization

This chapter will act as a reference point for all future chapters. Unless explicitly stated otherwise, the matrices, vectors, and expressions defined in this chapter are the ones utilized in future chapters. This chapter also sets out to showcase a number of example systems, which are employed throughout the rest of the report. If something is changed within the systems, it will be noted in future sections. Lastly, this chapter aims to display the optimization problems which will be solved for the regenerative and passive control laws. Proofs and definitions are also accompanied throughout to show the reasoning and thought behind each of the assumptions and decisions made.

2.1 State Space Characterization

We assume our passive dynamic network $\mathcal{N}$ is a finite dimensional Linear Time Invariant (LTI) system of the form

$$\mathcal{N} = \begin{cases} \dot{x}_N &= A_N x_N + B_{Nu} u + B_{Na} a \\ v &= C_{Nv} x + D_{Nv} u \\ y &= C_{Ny} x + D_{Ny} u \\ z &= C_{Nz} x + D_{Nza} a + D_{Nzu} u \end{cases} \tag{2.1}$$

Linearity is assumed because most of the application bases to this type of work (structures, car-model, piezo-beam), although never completely linear, can be accurately

approximated by linear systems. Furthermore, mild nonlinearities can be accommodated using the techniques in Chapter 5. Time-invariance and finite-dimensionality are also assumed, as again for the application bases of this type of work these qualities can be assumed without a great deal of conservatism introduced. These qualities also serve to simplify the mathematical characterization and allow for an optimization problem to be solved efficiently. The disturbance $a(t)$ is assumed to be a realization of a finite-dimensional Gauss-Markov process of the form

$$\mathcal{A} = \left\{ \begin{array}{rl} \dot{x}_A = & A_A x_A + B_A w \\ a = & C_A x_A \end{array} \right. , \quad S_w(\omega) = I \tag{2.2}$$

where $w(t)$ is a white noise signal and $S_w(\omega)$ is the power spectrum of $w(t)$. This representation implies white noise is passed through the filter $H_A(s) = C_A[sI - A_A]^{-1}B_A$ and then fed into our system via the exogenous disturbance a. This type of formulation allows us to set the bandwidth and intensity of the disturbance spectrum in a state-space formulation. We assume a Gauss-Markov model to allow for a finite dimensional disturbance state space representation. Systems $\mathcal{N}$ and $\mathcal{A}$ can be augmented such that the state vector $x = [x_N \quad x_A]^T$, which forms the augmented system $\mathcal{P}$ (which will be called the plant) such that

$$\mathcal{P} = \left\{ \begin{array}{rl} \dot{x} = & Ax + Bu + B_w w \\ v = & Cx + Du \\ y = & C_y x \\ z = & C_z x + D_z u \end{array} \right. \tag{2.3}$$

with appropriate definitions for A, B, etc. Additionally, E is a matrix with full column rank whose columns span the controllable subspace for the pair (A, B), i.e.,

$$\mathcal{R}\{E\} = \mathcal{R}\left\{ \begin{bmatrix} B & AB & \dots & A^{n-1}B \end{bmatrix} \right\} \tag{2.4}$$

We make the following assumptions regarding $\mathcal{P}$:

- *A1*: $\mathcal{N}$ is asymptotically stable and $u \mapsto v$ is weak strict positive real (WSPR). This implies there exists some $P_N = P_N^T > 0$ such that, for appropriately sized L and M matrices,

$$\begin{bmatrix} A_N^T P_N + P_N A_N & \bullet \\ B_{Nu}^T P_N + C_{Nv} & D_{Nv}^T + D_{Nv} \end{bmatrix} = - \begin{bmatrix} L \\ M \end{bmatrix} \begin{bmatrix} L \\ M \end{bmatrix}^T \leqslant 0 \tag{2.5}$$

  with (A_N, L^T) observable [10]. The (1,1) term of (2.5) ensures that $\mathcal{N}$ is asymptotically stable. The other WSPR terms, combined with the (1,1) term, allow for passivity conditions to hold for $\mathcal{N}$. Therefore, (2.5) implies the network $\mathcal{N}$ is passive, i.e., $E(T) \geq 0 \; \forall \; T, u$ for $\mathcal{N}$ when $w(t) = 0$.

- *A2*: a is stationary. This assumption aids in future proofs and allows for the regenerative controller constraint to be modeled as a convex LMI.

- *A3*: $\mathcal{A}$ is minimal

These assumptions allow for some implications to be made regarding $\mathcal{P}$. *A1* implies that A_N is Hurwitz and *A2*-*A3* imply that A_A is Hurwitz.

Lemma 1: If *A1*-*A3* hold, then for any $R > 0$ such that $R \geq -(D^T + D)$, $\exists P = P^T, L, W$ such that (A, L^T) is observable and

$$\begin{bmatrix} A^T P + PA & \bullet \\ B^T P - C & -R \end{bmatrix} = - \begin{bmatrix} L \\ W \end{bmatrix} \begin{bmatrix} L \\ W \end{bmatrix}^T \tag{2.6}$$

$$E^T P E > 0 \tag{2.7}$$

Moreover, $A - BR^{-1}(B^T P - C)$ is asymptotically stable.

Proof. We partition the system to isolate the subspace controllable from $\mathcal{N}$, i.e.,

$$A = \begin{bmatrix} A_{11} & A_{12} \\ 0 & A_{22} \end{bmatrix} \qquad P = \begin{bmatrix} P_{11} & P_{12} \\ P_{12}^T & P_{22} \end{bmatrix} \tag{2.8}$$

$$B = \begin{bmatrix} B_1 & 0 \end{bmatrix}^T \qquad C = \begin{bmatrix} C_1 & C_2 \end{bmatrix} \tag{2.9}$$

$$E = \begin{bmatrix} I & 0 \end{bmatrix}^T \tag{2.10}$$

As a note, A_{11} is assumed to span the controllable subspace and A_{22} is assumed to span the uncontrollable subspace. Using this redefinition, (2.6) becomes:

$$\begin{bmatrix} A_{11}^T P_{11} + P_{11} A & \bullet & \bullet \\ \Phi & \Theta + \Theta^T & \bullet \\ B_1^T P_{11} - C_1 & B_1^T P_{12} - C_2 & -R \end{bmatrix} = - \begin{bmatrix} L_1 \\ L_2 \\ W \end{bmatrix} \begin{bmatrix} L_1 \\ L_2 \\ W \end{bmatrix}^T \tag{2.11}$$

where $\Phi = P_{12} A_{11} + A_{12}^T P_{11} + A_{22}^T P_{12}$, $\Theta = P_{22} A_{22} + P_{12}^T A_{12}$. From *A1* and since A_{11}, B_1, C_1, D are a realization of $\mathcal{N}$, we know $\exists\ P_{11} = P_{11}^T > 0, W \in \mathbb{R}^{m \times p}, L \in \mathbb{R}^{n \times p}$ such that

$$\begin{bmatrix} A_{11}^T P_{11} + P_{11} A_{11} & \bullet \\ B_1^T P_{11} - C_1 & -R \end{bmatrix} = - \begin{bmatrix} L_1 \\ W \end{bmatrix} \begin{bmatrix} L_1 \\ W \end{bmatrix}^T \tag{2.12}$$

and the matrix equality can be reformulated as

$$\begin{bmatrix} - \begin{bmatrix} L_1 \\ W \end{bmatrix} \begin{bmatrix} L_1^T & W^T \end{bmatrix} & \bullet \\ \begin{bmatrix} \Phi & P_{12} B_1 - C_2^T \end{bmatrix} & \Theta + \Theta^T \end{bmatrix} = - \begin{bmatrix} L_1 \\ W \\ L_2 \end{bmatrix} \begin{bmatrix} L_1 \\ W \\ L_2 \end{bmatrix}^T \tag{2.13}$$

With the first block of (2.13) satisfied, we turn our attention toward the lower portion. Looking at the (1,2) block of (2.13), we see that there must $\exists P_{12}, L_2$ such that:

$$\begin{bmatrix} \Phi^T \\ B_1^T P_{12} - C_2 \end{bmatrix} = - \begin{bmatrix} L_1 \\ W \end{bmatrix} L_2^T \tag{2.14}$$

If this holds, it is easy to see that the column and row rank of (2.13) is limited to the (1,1) block. Choose

$$L_2^T = -W^T (W W^T)^{-1} [B_1^T P_{12} - C_2] \tag{2.15}$$

The first row becomes:

$$[P_{12} A_{11} + A_{12}^T P_{11} + A_{22}^T P_{12}]^T = L_1 W^T (W W^T)^{-1} [B_1^T P_{12} - C_2] \tag{2.16}$$

Re-arranging terms, this equates to:

(2.17)

$$[A_{11}^T - L_1 W^T (WW^T)^{-1} B_1^T] P_{12} + P_{12} A_{22} + [P_{11} A_{12} + L_1 W^T (WW^T)^{-1} C_2] = 0$$

This equation is a Sylvester equation and has a unique solution if and only if the eigenvalues of $A_{11}^T - L_1 W^T (WW^T)^{-1} B_1^T$ and $-A_{22}$ are mutually exclusive. Assumptions *A2-A3* imply A_{22} is asymptotically stable. Therefore, $A_{11}^T - L_1 W^T (WW^T)^{-1} B_1^T$ must be shown to be stable. Since $A_{11}^T - L_1 W^T (WW^T)^{-1} B_1^T$ is a square matrix, we take the transpose and aim to prove $A_{11} - B_1 (WW^T)^{-1} W L_1^T$ is stable.

To show this, consider that when the Positive Real Lemma is satisfied for $\mathcal{N}$, it will also be satisfied when increasing the feed-through term D. Therefore, we can say $A_{11} - B_1 R^{-1} (B_1^T P_{11} - C_1)$ is stable. Using the relationships in (2.12), $A_{11} - B_1 (WW^T)^{-1} (W L_1^T)$ can now be guaranteed to be stable. Therefore, the Sylvester equation conditions hold, which means P_{12} can be found. To find P_{22}, consider the (2,2) term of (2.11), which states:

(2.18)
$$P_{22} A_{22} + A_{22}^T P_{22} = -L_2 L_2^T - P_{12}^T A_{12} - A_{12} P_{12}$$

Since A_{22} is asymptotically stable, P_{22} possesses a unique solution. □

By means of a more intuitive explanation, the controllability constraint $E^T P E > 0$ was required due to the nature of our system $\mathcal{P}$. Since $\mathcal{P}$ includes $\mathcal{A}$, there are disturbance states which are uncontrollable. The standard Positive Real Lemma requires minimality, and we have generalized this lemma to non-minimal systems.

2.2 Objective Function

The control law optimization is done in an multi-objective LQG context, such that a performance measure

$$J \triangleq \mathcal{E}\{z_i^2\}_{i=1,\ldots,n_z} \tag{2.19}$$

is used. It should be noted that $z \in \mathbb{R}^{n_z}$, i.e., multi-objective control is assumed. Within this assumption, there are many variations of z that are valid problem objectives and can be solved. The user can specify the optimization objective as $min(\text{trace}(zz^T))$ or $min(\|zz^T\|)$, for example. This would allow characteristics of the system (displacement, velocity, acceleration, etc.) to be multiplied within the objective function. n_z can also be any value, which allows for the performance variable z to span from a scalar value to any number of dimensions. For the structural application, multi-objective control allows for the optimization objective to span multiple degrees-of-freedom and physical characteristics of the structure (acceleration, velocity, displacement, control force).

2.3 Example System

2.3.1 Structural Example

In many of the examples presented, the three degree-of-freedom structure shown in Figure 2.1 is used. This was a representative, albeit simplified, approximation for a structural system. The structure possessed enough dimensions in order to show an interesting problem while still being intuitive, as it only possessed three degrees-of-freedom. The system is non-dimensionalized with springs and masses equal to 1 and dashpots set to 0.01. The controller is assumed to be placed between the base and first degree-of-freedom. The base acceleration $a = \ddot{x}_0$ is assumed to be a stationary stochastic disturbance with power spectral density defined as $S_a(\omega)$. This power

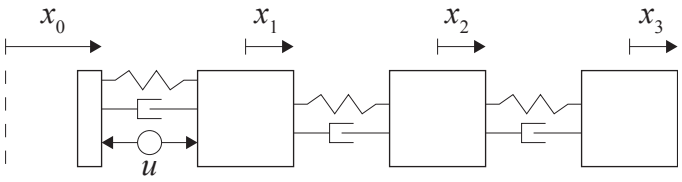

Figure 2.1: System Diagram for Examples

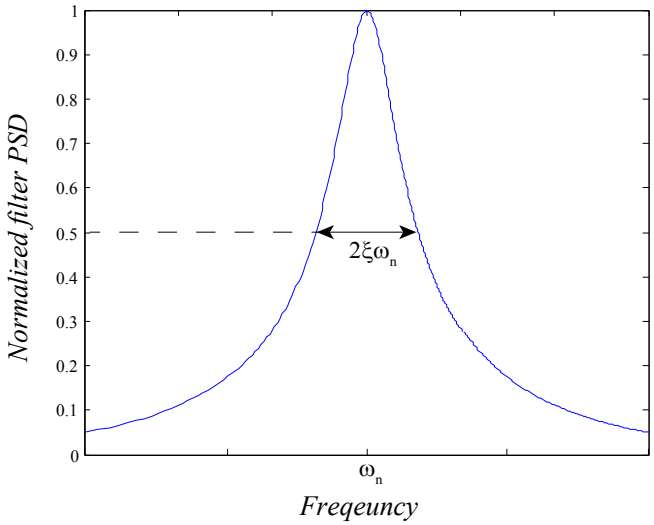

Figure 2.2: Power Spectral Density of Base Acceleration

spectral density is Gauss-Markov and serves as a filter between the white noise w and exogenous input a. The transfer function of $S_a(\omega)$ is defined as

$$S_a(\omega) = \frac{\omega^2}{(\omega^2 - \omega_n^2)^2 + (2\xi\omega_n\omega)^2} \tag{2.20}$$

This translates to a filter centered at ω_n which has an approximate half-power bandwidth of $2\xi\omega_n$, shown in Figure 2.2. This Gaussian filter was selected because we felt it representative of the broadest range of external excitations. It provided a compact transfer function, and therefore saved complications in future optimization problems. In the state space systems mentioned in $\mathcal{N}$ and $\mathcal{A}$, the matrices, in this example, would be of the form

$$A_N = \begin{bmatrix} 0_{d\times d} & I_{d\times d} \\ -M^{-1}K & -M^{-1}C \end{bmatrix} \qquad C_{Nv} = C_{Ny} = \begin{bmatrix} 0_{1\times d} & 1 & 0 & 0 \end{bmatrix} \tag{2.21}$$

$$B_{Nu} = \begin{bmatrix} 0_{d\times 1} & 1/m_1 & 0 & 0 \end{bmatrix}^T \qquad B_{Na} = \begin{bmatrix} 0_{d\times 1} & -1_{d\times 1} \end{bmatrix}^T \tag{2.22}$$

$$A_A = \begin{bmatrix} 0 & \omega_n \\ -\omega_n & -2\xi\omega_n \end{bmatrix} \qquad B_A = \begin{bmatrix} 0 \\ 1 \end{bmatrix}, C_A = \begin{bmatrix} 0 & 1 \end{bmatrix} \tag{2.23}$$

where $d = 3$ and

$$M = \begin{bmatrix} m_1 & 0 & 0 \\ 0 & m_2 & 0 \\ 0 & 0 & m_3 \end{bmatrix} \qquad K = \begin{bmatrix} k_1 + k_2 & -k_2 & 0 \\ -k_2 & k_2 + k_3 & -k_3 \\ 0 & -k_3 & k_3 \end{bmatrix} \tag{2.24}$$

$$C = \begin{bmatrix} c_1 + c_2 & -c_2 & 0 \\ -c_2 & c_2 + c_3 & -c_3 \\ 0 & -c_3 & c_3 \end{bmatrix} \tag{2.25}$$

where m_1, k_1, c_1 refers to the mass, stiffness, and damping of the first DOF, and so on for m_2, c_2, k_2, m_3, k_3, c_3. Additionally, it was assumed that $D_{Na} = D_{Ny} = 0$. The matrices C_z and D_z are user-chosen system properties such as absolute acceleration, relative displacement, control force, or relative velocity. From this point, all of the network matrices should be defined and the augmentation of the network and disturbance should be trivial.

2.3.2 Quarter Car Model

A quarter car model example was also utilized in examples throughout the dissertation. The model is shown in Figure 2.3. For this model, the network $\mathcal{N}$ and disturbance characterization A are defined as in (2.21)-(2.23), with the only changes $d = 2$ and

$$C_{Nv} = C_{Ny} = \begin{bmatrix} 0_{1\times d} & -1 & 1 \end{bmatrix} \qquad B_{Nu} = \begin{bmatrix} 0_{d\times 1} & -1/m_1 & 1/m_2 \end{bmatrix}^T \tag{2.26}$$

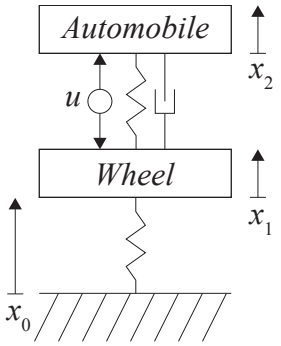

Figure 2.3: Quarter Car Model for Examples

The system matrices are defined as:

$$M = \begin{bmatrix} m_1 & 0 \\ 0 & m_2 \end{bmatrix} \qquad K = \begin{bmatrix} k_1 & -k_1 \\ -k_1 & k_1 + k_2 \end{bmatrix} \tag{2.27}$$

$$C = \begin{bmatrix} c & -c \\ -c & c \end{bmatrix} \tag{2.28}$$

where $m_1 = 345\ kg$, $m_2 = 140\ kg$, $k_1 = 18,000\ kg/m$, $k_2 = 200,000\ kg/m$, and $c = 1000\ N \cdot s/m$. It is again assumed that there are no feed-through terms, i.e, $D_{N_a} = D_{N_y} = 0$. The disturbance parameters in $\mathcal{A}$ are the same as defined in the previous section, with ω_n=10.

2.3.3 Half Car Model

In addition to the quarter car, a half car model example was also utilized in examples throughout the paper. The system is shown in Figure 2.4, which now includes four independent degrees of freedom $\{x_1, x_2, x_3, \Phi\}$. As a note, the dependent values $\{x_4, x_5\}$ are defined by the constitutive relationship

$$x_4 = x_3 - l_1\Phi \tag{2.29}$$

$$x_5 = x_3 + l_2\Phi \tag{2.30}$$

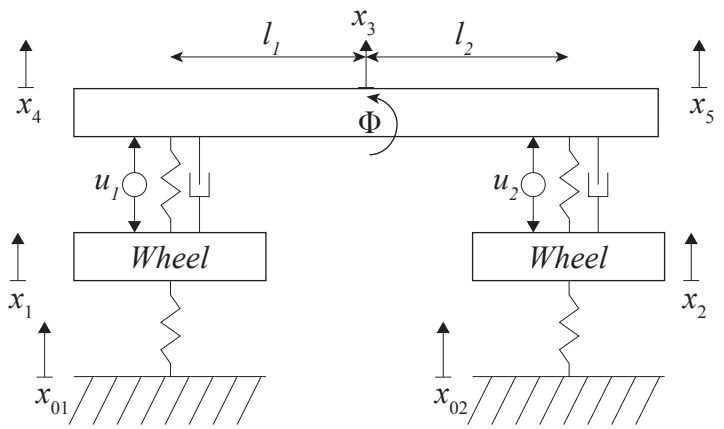

Figure 2.4: Half Car Model for Examples

with all derivations stemming from this relationship. With this in hand, we can define our state vector

$$x = \begin{bmatrix} x_s & \dot{x}_s \end{bmatrix}^T \tag{2.31}$$

where

$$x_s = \begin{bmatrix} x_1 & x_2 & x_3 & \Phi \end{bmatrix}^T \tag{2.32}$$

This implies that we are now considering the angle of the automobile as a state variable. Without the angle included (i.e., considering $x_4,\ x_5$ as state variables) in the performance vector, the angular acceleration could be very large in the automobile. This would create extreme discomfort for passengers and possible torque damage to the structure of the automobile.

One major change is now we have two exogenous inputs $x_{01},\ x_{02}$ on the front and back wheels, respectively. Since this is a model of the front and back wheels of an automobile, the disturbance of the back wheel will be a time delayed version of the disturbance on the front wheel. Therefore, we now have two exogenous disturbance systems, which we will call $\mathcal{A}$ and $\mathcal{A}_D$, where $\mathcal{A}_D$ is the time delayed version of $\mathcal{A}$.

$\mathcal{A}_D$ is defined as:

$$\mathcal{A}_D = \begin{cases} \dot{x}_D = & A_D x_D + B_D a \\ a_D = & C_D x_D \end{cases} \tag{2.33}$$

Trying to completely derive this delayed system is outside the scope of this dissertation and will not be covered. Instead, we will use a Padé approximant for the time-delayed system. Any number of states could be selected for the approximate transfer function, with each state increasing accuracy but also creating a more complex model. For our purposes, a two-state system was able to approximate the time-delayed transfer function well. This is shown in the Bode diagram in Figure 2.5. As a note, in our examples we assume $\omega_n = 100$ and $\xi = 0.25$. This frequency is around five to ten times higher than the natural frequencies of the system. We assumed automobile designers would ensure road disturbances would not excite the natural frequencies of the automobile. The magnitudes of the disturbance and approximated time-delayed models are identical. The approximation does create a slight phase offset, but this offset is quite small in our area of frequency interest $(\omega_n \pm \xi\omega_n)$.

Another aspect to consider is the amount of time the delay is assumed to take. To find this time, we used the simple equation

$$T = \frac{Len}{V} \tag{2.34}$$

where $Len = l_1 + l_2$ and V is the velocity of the automobile. V was chosen as roughly 40 mph for a realistic estimate. Therefore, A_D was implemented as a second-order Padé approximant.

Given this augmented state vector, we now set $d = 4$ and apply some changes to the matrices outlined in (2.21)-(2.23). For ease of representation, we will denote the A_A matrix in (2.23), utilized in the structural and quarter-car models, as a_a for this

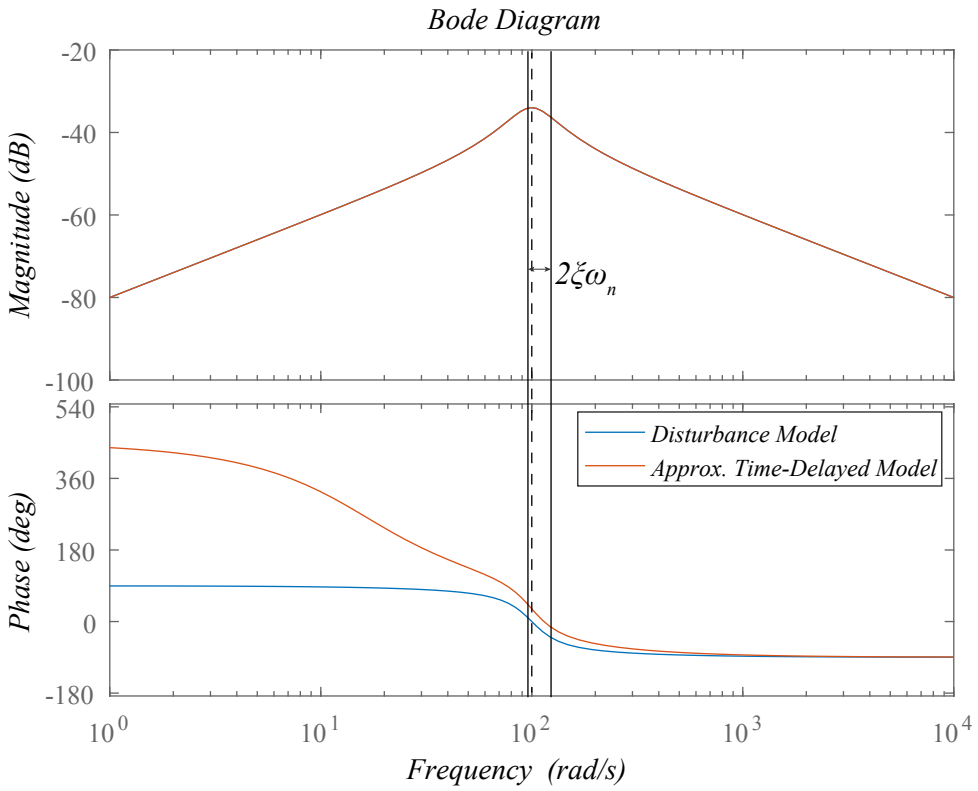

Figure 2.5: Bode Diagram of Disturbance Model and Time-Delayed Approximation

example. The same holds for B_A (b_a in this example) and C_A (c_a in this example). While A_N stays the same (with $d = 4$), we now set

$$A_A = \begin{bmatrix} a_a & 0_{n_a \times n_d} \\ B_D c_a & A_D \end{bmatrix} \qquad C_{Nv} = C_{Ny} = \begin{bmatrix} 0_{2\times d} & L \end{bmatrix} \tag{2.35}$$

$$B_{Nu} = \begin{bmatrix} 0_{d\times 2} \\ L/M \end{bmatrix} \qquad B_{Na} = \begin{bmatrix} 0_{d\times 2} \\ -G/M \end{bmatrix} \tag{2.36}$$

$$B_A = \begin{bmatrix} b_a & 0_{n_d \times 1} \end{bmatrix}^T \qquad C_A = \begin{bmatrix} c_a & 0_{1\times n_d} \\ 0_{1\times n_a} & C_D \end{bmatrix} \tag{2.37}$$

where

(2.38)

$$M = \begin{bmatrix} m_1 & 0 & 0 & 0 \\ 0 & m_2 & 0 & 0 \\ 0 & 0 & m_3 & 0 \\ 0 & 0 & 0 & J \end{bmatrix}, K = \begin{bmatrix} k_1 + k_4 & 0 & -k_4 & k_4 l_1 \\ 0 & k_2 + k_5 & -k_5 & -k_5 l_2 \\ -k_4 & -k_5 & k_4 + k_5 & -k_4 l_1 + k_5 l_2 \\ k_4 l_1 & -k_5 l_2 & -k_4 l_1 + k_5 l_2 & k_4 l_1^2 + k_5 l_2^2 \end{bmatrix}$$

$$C = \begin{bmatrix} c_4 & 0 & -c_4 & c_4 l_1 \\ 0 & c_5 & -c_5 & -c_5 l_2 \\ -c_4 & -c_5 & c_4 + c_5 & -c_4 l_1 + c_5 l_2 \\ c_4 l_1 & -c_5 l_2 & -c_4 l_1 + c_5 l_2 & c_4 l_1^2 + c_5 l_2^2 \end{bmatrix},$$

$$L = \begin{bmatrix} -1 & 0 & 1 & -l_1 \\ 0 & -1 & 1 & l_2 \end{bmatrix}^T, G = \begin{bmatrix} k_4 & 0 & 0 & 0 \\ 0 & k_5 & 0 & 0 \end{bmatrix}^T$$

n_a is the number of states in a_a, n_d is the number of states in A_D, J is the moment of inertia of the automotive body, and the m, c, k subscripts correspond to the various degrees of freedom. l_1 is the distance from the center of gravity of the automobile to the center of the front wheels, and l_2 is the same distance but to the back wheels. As shown with the above, there are now two force inputs $u_1,\ u_2$ as well as two exogenous inputs $x_{01},\ x_{02}$.

Similar to the quarter car model the parameters were set as $m_1 = m_2 = 140\ kg$, $m_3 = 690\ kg$, $k_1 = 18,000 kg/m$, $k_2 = 22,000\ kg/m$, $k_3 = k_4 = 200,000\ kg/m$, $c_1 = 1000 N \cdot s/m$, $c_2 = 1100\ N \cdot s/m$, $J = 1222\ Kg \cdot m^4$, $a = 1.3\ m$, and $b = 1.5\ m$. It is again assumed that there are no feed-through terms, i.e, $D_{N_a} = D_{N_y} = 0$.

2.4 Passive Control Domain

In order for the controller to be passive, a few conditions must be satisfied. First, the domain of passive controllers is defined as:

(2.39) $$K_P = \{\mathcal{K} : y \to u \big| E(T) \leqslant 0, \forall T \geqslant 0,\ \forall a,\ y, v, \in \mathcal{L}_2\}$$

Therefore, the passive controllers are defined as those such that $\mathcal{K} \in K_P$. As mentioned, the domain of passive controllers are limited to those which are Strictly Positive Real (SPR). This allows for the transfer function to be realized using imperfect elements, such as capacitors, conductors, and resistors in an electrical context. SPR controllers, along with a passive network, allow for the passivity theorem to be satisfied. For the passive controller to be SPR, it must, along with $y = v$, satisfy the following conditions:

1. $\mathcal{K}(s)$ is real for real s and is analytic for $Re\{s\} \geq 0$
2. $Re\{\mathcal{K}(j\omega)\} < 0, \quad -\infty < \omega < \infty$
3. $\lim\limits_{\omega \to \infty} \omega^2 Re\{\mathcal{K}(j\omega)\} < 0$

2.5 Regenerative Control Domain

The domain of feasible regenerative control laws is defined as

$$K_R = \{\mathcal{K} : y \to u \,\Big|\, \lim_{T\to\infty} \tfrac{1}{T} E_s(T) \geqslant 0, \forall a \in \mathcal{A}\} \tag{2.40}$$

In our work, we assume $a(t)$ to be stochastic, in which $\mathcal{A}$ is a set of stationary stochastic sequences with known spectrum $S_a(\omega)$. The domain of regenerative controllers is reformulated as

$$K_R = \{\mathcal{K} : y \to u \big|\ \mathcal{E}\{u^T v\} \leqslant 0, a \sim \mathcal{A}\} \tag{2.41}$$

where $\mathcal{E}(\bullet)$ denotes the expectation in stationarity.

2.6 Optimal Passive and Regenerative Control Problems

With the passive and regenerative control domains precisely defined, it is possible to define the problem goal. To start, the passive controller problem goal will be

defined. The passive controller, optimized in Chapter 4, seeks to satisfy:

$$\text{Min: J } = \max_{i\in\{1\ldots n_z\}} \mathcal{E}\left\{(C_{zi}x + D_{zi}u)^2\right\} \tag{2.42}$$

$$\text{Over: } \{A_K, B_K, C_K, D_K\} \tag{2.43}$$

$$\text{Subject to: } \mathcal{K} \in K_P \stackrel{\triangle}{=} \{\mathcal{K} : \int_0^T u^T(t)v(t)dt \leq 0\} \tag{2.44}$$

The regenerative controller, found in Chapters 3 and and 6, seeks to:

$$\text{Min: J } = \max_{i\in\{1\ldots n_z\}} \mathcal{E}\left\{(C_{zi}x + D_{zi}u)^2\right\} \tag{2.45}$$

$$\text{Over: } \{A_K, B_K, C_K, D_K\} \tag{2.46}$$

$$\text{Subject to: } \mathcal{K} \in K_R \stackrel{\triangle}{=} \{\mathcal{K} : \mathcal{E}\{u^T v\} \leq 0\} \tag{2.47}$$

As a note, we assume the size of $\{A_K, B_K, C_K, D_K\}$ is the same as $\{A, B, C, D\}$. This assumption is made throughout the paper and is a source of conservatism for the controller design in all subsequent chapters. These two optimization problems become the baseline for the controllers found in the next three chapters. Regardless of notation, change of coordinates, or added complexity, the problem goal of each controller remains the same. Once both controllers are found, the respective values of J can be found, thus allowing for a comparison of the regenerative and passive controllers.

CHAPTER 3

Regenerative Controller

In this section, an optimization procedure for a regenerative controller is formulated and solved, and an example regenerative controller is shown. To do this, the regenerative constraint $\mathcal{E}\{u^T v\} < 0$ must first be reformulated as a condition that can be solved efficiently using LMI methods. In Section 3.1, a theorem is proposed which reformulates the constraint. Additionally, the parasitics, which hinder the system's conversion from mechanical to electrical energy, must be characterized. Section 3.2 utilizes a technique from [88], which characterizes a mathematical formulation for these parasitics and applies this formulation to the regenerative constraint. Lastly, in section 3.3, an optimization technique for a regenerative controller is developed. The problem is initially non-convex, but, utilizing a coordinate transformation, a convex LMI is recovered. An example is then shown on a three degree-of-freedom structure with one and two transducers, a quarter car model, and a half car model.

3.1 Optimal Power Generation

The regenerative energy constraint $\mathcal{E}\{u^T v\} < 0$ is reformulated as

$$\lim_{T\to\infty} \frac{1}{T}\int_0^T u^T(t)v(t)dt < 0 \quad \Rightarrow -\mathcal{E}\{u^T v\} > 0 \quad \Rightarrow -\mathcal{E}\{u^T(Cx+Du)\} > 0 \tag{3.1}$$

We then define

$$\bar{p} \triangleq -\mathcal{E}\{u^T(Cx + Du)\} > 0 \tag{3.2}$$

A $\bar{p}$ value less than zero implies overall energy is being extracted from the system, and $\bar{p} > 0$ implies the long term trend of the energy is being extracted from the network. The first step towards generating a regenerative controller is to be able to enforce the regenerative constraint, i.e. $\mathcal{E}\{u^T v\} < 0$. To do so, consider reformulating the regenerative constraint as proposed in [88] via the following theorem.

Theorem 1: Assume $\mathcal{N}$ to be WSPR and that $R \triangleq -\frac{1}{2}(D + D^T) > 0$. Then

$$\bar{p} = \bar{p}_0 - \mathcal{E}\{(u - Fx)^T R(u - Fx)\} > 0 \tag{3.3}$$

where $\bar{p}_0 = -B_w^T T B_w > 0$, $F = -R^{-1}(\frac{1}{2}C + B_u^T T)$, and $T = T^T$ satisfies the Riccati equation

$$0 = A^T T + TA - (\tfrac{1}{2}C^T + TB_u)R^{-1}(\tfrac{1}{2}C^T + TB_u)^T \tag{3.4}$$

Moreover, the controller $u = Fx$ is stabilizing. It should be noted that in order for (3.4) to have a stabilizing solution, the system $\mathcal{N}$ must be WSPR.

Proof. For some $T = T^T$ and $\psi = x^T T x$, from Itô calculus it is a standard result that:

$$\frac{d}{dt}\mathcal{E}\{\psi\} = \mathcal{E}\{x^T T(Ax + Bu)\} + \mathcal{E}\{(Ax + Bu)^T Tx\} + \mathrm{tr}\{B_w^T T B_w\} \tag{3.5}$$

This can be rewritten in the following matrix form:

$$\frac{d}{dt}\mathcal{E}\{\psi(t)\} = \mathcal{E}\left\{ \begin{bmatrix} x \\ u \end{bmatrix}^T \begin{bmatrix} A^T T + TA & TB \\ B^T T & 0 \end{bmatrix} \begin{bmatrix} x \\ u \end{bmatrix} \right\} + tr\{B_w^T T B_w\} \tag{3.6}$$

Now, impose stationarity (i.e., *A2* from Chapter 2):

$$0 = \mathcal{E}\left\{ \begin{bmatrix} x \\ u \end{bmatrix}^T \begin{bmatrix} A^T T + TA & TB \\ B^T T & 0 \end{bmatrix} \begin{bmatrix} x \\ u \end{bmatrix} \right\} + tr\{B_w^T T B_w\} \tag{3.7}$$

Add and subtract $\bar{p} = \mathcal{E}\{u^T v\}$:

$$\bar{p} = \mathcal{E}\left\{ \begin{bmatrix} x \\ u \end{bmatrix}^T \begin{bmatrix} A^T T + TA & \frac{1}{2}C^T + TB \\ \frac{1}{2}C + B^T T & R \end{bmatrix} \begin{bmatrix} x \\ u \end{bmatrix} \right\} + \bar{p}_0 \tag{3.8}$$

Using the definition for F, this can be alternatively expressed via a Schur compliment as:

$$\bar{p} = \mathcal{E}\left\{ \begin{bmatrix} x \\ \bar{u} \end{bmatrix}^T \begin{bmatrix} A^T T + TA - F^T R F & 0 \\ 0 & R \end{bmatrix} \begin{bmatrix} x \\ \bar{u} \end{bmatrix} \right\} + \bar{p}_0 \tag{3.9}$$

where F is defined above and $\bar{u} = u - Fx$.

At this point, it becomes advantageous to utilize the modified version of the PRL outlined in (2.6)-(2.7) applied to the matrix in (3.8). Since the disturbance realization is uncontrollable, the range space of the matrix E will be the range space of the first n_x rows and columns of A, where n_x is the dimension of x_N. The last n_a, the dimension of x_A, rows and columns of A will be uncontrollable. The positive real lemma outlined in (2.6)-(2.7) can be reformulated as the Riccati equation

$$A^T P + PA + (B^T P - \hat{C})^T R^{-1} (B^T P - \hat{C}) = -LL^T + LW^T (WW^T)^{-1} WL^T \tag{3.10}$$

where $\hat{C} = -\frac{1}{2}C$. The right hand side of (3.10) can now be recast as a negative semi-definite matrix, i.e., $\exists P = P^T$ such that

$$A^T P + PA + (B^T P - \hat{C})^T R^{-1} (B^T P - \hat{C}) \leq 0 \tag{3.11}$$

$$E^T P E > 0 \tag{3.12}$$

This can be reformulated, via a Schur Compliment, as a convex LMI. Via [4], given $R > 0$, the set of solutions to the LMI include the case when (3.11) is an equality. Therefore $\exists\ \hat{P} = \hat{P}^T$ such that

$$A^T \hat{P} + \hat{P} A + \left[B^T \hat{P} - \hat{C} \right]^T R^{-1} \left[B^T \hat{P} - \hat{C} \right] = 0 \tag{3.13}$$

$$E^T \hat{P} E > 0 \tag{3.14}$$

Moreover, $A + BR^{-1}(B^T\hat{P} - \hat{C})$ is stable. Defining $T = -\hat{P}$, the above is equivalent to (3.4) and $(A + BF)$ is stable. Utilizing this fact, (3.9) is equivalent to

$$\bar{p} = \mathcal{E}\left\{ \begin{bmatrix} x \\ \bar{u} \end{bmatrix}^T \begin{bmatrix} 0 & 0 \\ 0 & R \end{bmatrix} \begin{bmatrix} x \\ \bar{u} \end{bmatrix} \right\} + \bar{p}_0 \tag{3.15}$$

which is equivalent to (3.3).

□

Using the above theorem the regenerative constraint (3.1) can be expressed as

$$\mathcal{E}\left\{(u - Fx)^T R(u - Fx)\right\} < \bar{p}_0 \tag{3.16}$$

3.2 Accounting for Parasitics

With any regenerative controller, a major limiting factor is the parasitics involved, which manifest themselves in the transfer of mechanical to electrical energy and vice versa. These losses will occur irrespective of what technology is used (e.g., hydraulic, electronic, etc.) or level of power is being absorbed. The above power generation terms assume a perfect system (i.e., no parasitics), but this will not hold in real-life applications. There will be losses throughout the power electronics, which utilize high-bandwidth tracking at each of the transducers via pulse width modulation or hysteretic switching control. The entirety of the parasitics involved would require a

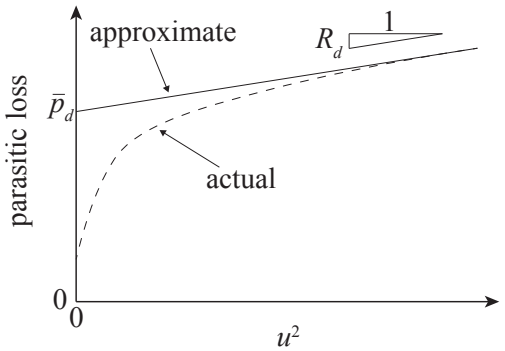

Figure 3.1: Parasitics Approximation

deep understanding of the electronics used and would result in a complex characterization, so a conservative model will be used. Using a model proposed by [88] and advanced by [104], the parasitics are over-bounded by a combination of conductive losses and static losses which are irrespective of the level of power. It can be shown that for many systems that these losses can be approximated as a function of the current u, and manifest themselves in a semi-concave curve that is a function of u^2. Figure 3.1 shows the semi-concave curve in question, and the approximation being done. This approximation has values $\{\bar{p}_d, R_d\}$ which parametrize a function linear in u^2 . $\bar{p}_d$ is the static power consumption and R_d is the transmission resistance matrix. This allows for a conservative approximation of the parasitic loss model as

$$\mu(u(t)) = \bar{p}_d + u^T(t) R_d u(t) \tag{3.17}$$

This alters (3.2) to

$$\bar{p} = -\mathcal{E}\left\{u^T(Cx + Du)\right\} - \mathcal{E}\{\bar{p}_d + u^T R_d u\} \tag{3.18}$$

Which, in the optimization procedure, modifies R to be

$$R = -\tfrac{1}{2}(D + D^T) + R_d \tag{3.19}$$

and $\bar{p}_0$ to be

$$\bar{p}_0 = -B_w^T T B_w - \bar{p}_d \tag{3.20}$$

Throughout much of the following work, the regenerative controller will be optimized over varying values of $\bar{p}_d$ and R_d. As the parasitics increase, the performance of the regenerative controller suffers. Therefore, the parasitic parameters are the main hindrance of the performance of the regenerative controller.

3.3 Regenerative Controller Optimization

The controller $\mathcal{K}$ is assumed to be linear time invariant, strictly proper, finite-dimensional, and of the form

$$\mathcal{K} = \begin{cases} x_K &= A_K x_K + B_K y \\ u &= C_K x_K + D_K y \end{cases} \tag{3.21}$$

With this controller in hand, the closed loop system state vector is defined as $\hat{x} = [x \;\; x_K]^T$ with the associated state space equations

$$\mathcal{T} = \begin{cases} \hat{x} &= \hat{A}\hat{x} + \hat{B}w \\ z &= \hat{C}_z\hat{x} \\ r &= \hat{C}_r\hat{x} \end{cases} \tag{3.22}$$

where $r = u - Fx$ and

$$\hat{A} = \begin{bmatrix} A + BD_KC_y & BC_K \\ B_KC_y & A_K \end{bmatrix}, \qquad \hat{B} = \begin{bmatrix} B_w \\ 0 \end{bmatrix} \tag{3.23}$$

$$\hat{C}_z = \begin{bmatrix} C_z + D_zD_KC_y & D_zC_K \end{bmatrix} \qquad \hat{C}_r = \begin{bmatrix} -F + D_KC_y & C_K \end{bmatrix} \tag{3.24}$$

For the controller, the feed-through term is assumed to be zero, i.e., $D_K = 0$. To minimize the system cost J via a regenerative controller, the following theorem is proposed.

Theorem 2: Controller $\mathcal{K}$ is stabilizing, regenerative, and has performance $J < \gamma$ if and only if there exist matrices $P = P^T \geqslant 0$, $Q = Q^T \geqslant 0$ such that

$$\begin{bmatrix} \hat{A}^TP + P\hat{A} & \bullet \\ \hat{B}^TP & -I \end{bmatrix} < 0 \tag{3.25}$$

$$\begin{bmatrix} \gamma & \bullet \\ \hat{C}_{zi}^T & P \end{bmatrix} > 0 \quad , \quad i \in \{1 \dots n_z\} \tag{3.26}$$

$$\begin{bmatrix} Q & \bullet \\ \hat{C}_r^T & P \end{bmatrix} > 0 \tag{3.27}$$

$$\bar{p}_0 + \mathrm{tr}\{QR\} < 0 \tag{3.28}$$

Proof. To frame the optimization problem as a series of convex LMIs, first define

$$\hat{S} = \mathcal{E}\left\{ \begin{bmatrix} xx^T & xx_K^T \\ x_K x^T & x_K x_K^T \end{bmatrix} \right\} > 0 \tag{3.29}$$

$\hat{S}$ is positive definite due to $\hat{A}$ being Hurwitz. Then, $\exists P = P^T > 0,\ Q = Q^T \geqslant 0$ such that $\hat{S}$ simultaneously satisfies the following inequalities:

$$\hat{A}\hat{S} + \hat{S}\hat{A}^T + \hat{B}\hat{B}^T = 0 \tag{3.30}$$

$$\hat{C}_z \hat{S} \hat{C}_z^T = J \quad , \quad i \in \{1 \dots n_z\} \tag{3.31}$$

$$\text{tr}\left\{ \hat{C}_r \hat{S} \hat{C}_r^T R \right\} = -\bar{p}_0 \tag{3.32}$$

We can now find a $S > \hat{S}$ such that $J < \gamma$ if and only if $\exists P = P^T > 0, Q = Q^T \geqslant 0$ such that

$$\hat{A}S + S\hat{A}^T + \hat{B}\hat{B}^T < 0 \tag{3.33}$$

$$\hat{C}_z S \hat{C}_z^T < \gamma \quad , \quad i \in \{1 \dots n_z\} \tag{3.34}$$

$$\text{tr}\left\{ \hat{C}_r S \hat{C}_r^T R \right\} < -\bar{p}_0 \tag{3.35}$$

Taking the Schur compliment of the three LMIs above and defining $P = S^{-1}$, one yields (3.25)-(3.28). Since S is positive definite, it is invertible. □

The objective is to minimize γ over the optimization domain $\{A_K, B_K, C_K, P, Q\}$ subject to (3.25)-(3.28). The above optimization presents two problems, initially that the first LMI in non-convex. Additionally, the optimization variables $\{A_K, B_K, C_K\}$ are realization dependent. To alleviate both of these issues, a method proposed by Scherer [87] is utilized. The variables P and P^{-1} are redefined as

$$P = \begin{bmatrix} Y & \bullet \\ N^T & \times \end{bmatrix} \qquad P^{-1} = \begin{bmatrix} X & \bullet \\ M^T & \times \end{bmatrix} \tag{3.36}$$

where $X, Y \in \mathbb{R}^{n\times n}$ and $\times$ is a term that is unnecessary to define. With this new definition of P, P^{-1} the constraints (3.25)-(3.27) can be shown to be of the form

$$\begin{bmatrix} \Delta_1 + \Delta_1^T & \bullet & \bullet \\ A^T + \tilde{A}^T & \Delta_2 + \Delta_2^T & \bullet \\ B_w^T & B_w^T Y & -I \end{bmatrix} < 0 \tag{3.37}$$

$$\begin{bmatrix} \gamma & \bullet & \bullet \\ XC_{zi}^T + \tilde{C}^T D_{zi}^T & X & \bullet \\ C_{zi}^T & I & Y \end{bmatrix} > 0, \qquad i \in \{1 \dots n_z\} \tag{3.38}$$

$$\begin{bmatrix} Q & \bullet & \bullet \\ \tilde{C}^T - XF^T & X & \bullet \\ -F^T & I & Y \end{bmatrix} > 0 \tag{3.39}$$

$$\bar{p}_0 + \mathrm{tr}\{QR\} < 0 \tag{3.40}$$

where the new variables $\{\tilde{A}, \tilde{B}, \tilde{C}\}$ are of the form

$$\tilde{A} = NA_K M^T + NB_K C_y X + YBC_K M^T + YAX \tag{3.41}$$

$$\tilde{B} = NB_K \tag{3.42}$$

$$\tilde{C} = C_K M^T \tag{3.43}$$

and

$$\Delta_1 = AX + B\tilde{C} \tag{3.44}$$

$$\Delta_2 = YA + \tilde{B}C_y \tag{3.45}$$

The optimization problem is now convex and realization-independent. The objective is to minimize γ over the optimization domain $\{\tilde{A}, \tilde{B}, \tilde{C}, X, Y, Q\}$ subject to (3.37)-(3.40). Since this problem is convex, the solution can be found efficiently through standard LMI solvers [9]. It should be noted that M, N can be found via the relationship $MN^T + XY = I$ once the solution to the above optimization is found. The

controller characteristics $\{A_K, B_K, C_K\}$ can be found via the relationships described in (3.41)-(3.43).

Additionally, it is necessary to define noise in the feedback output y. It is assumed y is corrupted by white noise with a spectral intensity matrix Ξ. This ensures a finite controller and merely adjusts (3.25) to

$$\begin{bmatrix} \Delta_1 + \Delta_1^T & \bullet & \bullet & \bullet \\ A^T + \tilde{A}^T & \Delta_2 + \Delta_2^T & \bullet & \bullet \\ B_w^T & B_w^T Y & -I & \bullet \\ 0 & \tilde{B}^T & 0 & -\Xi^{-1} \end{bmatrix} \tag{3.46}$$

An interesting note is that this problem can be easily modified to a power generation optimization. All one would need to do is fix some value of γ and change the objective such that it minimizes $\bar{p}$. Once this convex optimization is run, optimal regenerative controller characteristics $\{\tilde{A}^*, \tilde{B}^*, \tilde{C}^*, Y^*, X^*\}$ are obtained and thus the original controller characteristics $\{A_K^*, B_K^*, C_K^*\}$ can be found.

3.3.1 Example

To formulate an example, consider the three-degree of freedom structure shown in Figure 2.1 with all system values as stated in Chapter 2. In the power spectral density of the base accelerations, it is assumed the natural frequency $\omega_n = 1$ and damping ratio $\xi = 0.125$. As a note, for all other examples, it is assumed $\xi = 0.25$. The fictitious noise was assumed to be of value $\Xi = 1e-6$ for all examples. The performance vector is defined as

$$z = \begin{bmatrix} x_2 - x_1 & \ddot{x}_3 + \ddot{x}_0 & u \end{bmatrix}^T \tag{3.47}$$

and

$$y = v = \dot{x}_1 - \dot{x}_0 \tag{3.48}$$

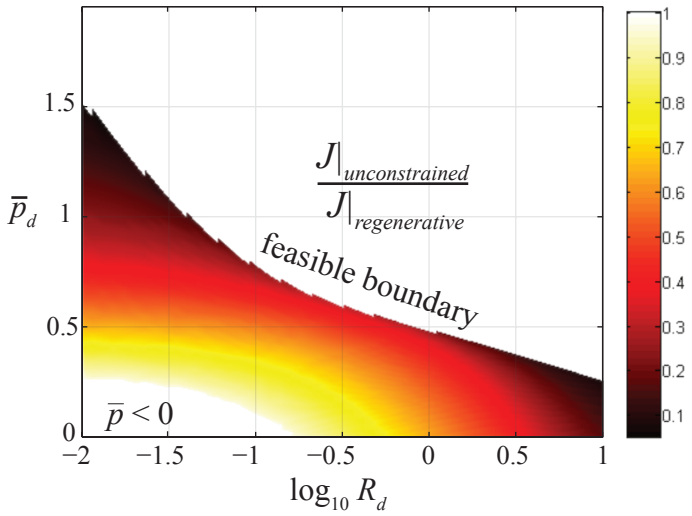

Figure 3.2: Surface Plot of Performance Ratio of Active vs. Regenerative Control over the Parasitics

Figure 3.2 shows a surface plot of the performance ratio

$$\frac{J|_{unconstrained}}{J|_{regenerative}} \tag{3.49}$$

This ratio is being plotted as a function of the parasitic parameters $\bar{p}_d$ and R_d. The unconstrained controller does not change over the parasitic parameters, but the regenerative controller performance will deteriorate over the parasitics. If the ratio is high, the regenerative controller has similar performance to the unconstrained active controller. As parasitics increase and the performance of the regenerative controller decreases, this ratio lowers and the active controller possess a larger advantage compared to the regenerative controller/ The first thing to note is the feasible boundary of the regenerative controller. Even if the sole objective of the regenerative controller was power generation, it would be unable to overcome the parasitics constraints and therefore is not feasible. Additionally, the region in white corresponds to a performance ratio of one, and therefore the regenerative controller is able to replicate the performance of an active controller.

An interesting dichotomy is the relationship between power generation and dis-

turbance rejection in the regenerative controller. As the parasitics increase, the hardware parasitics limit the controller so much that it exclusively focuses on power generation, which in term severely hampers the control performance. As it hits the feasible boundary, the regenerative controller is unable to generate any power, even when that is its sole focus. As the parasitics decrease, the controller can focus on implementing control and performance can mirror an optimal LQG controller. The positive power generation comes as a byproduct of the LQG control algorithm i.e., the regenerative constraint does not need to be explicitly enforced. As the parasitics increase, the performance ratio drops as the constraint $\bar{p} \leqslant 0$ becomes activated and the ratio drops until it hits the boundary. However, for low enough parasitics, the regenerative controller is able to replicate active LQG unconstrained control performance. This is significant because it means that, for capable electronics, there is no drop-off between a regenerative and active controller.

The plot in Figure 3.3 shows the performance ratio of an active to a regenerative controller for various performance objectives, given the same system specified in Chapter 2. The first row corresponds to a performance vector of

$$z = \begin{bmatrix} \ddot{x}_1 + \ddot{x}_0 & \ddot{x}_2 + \ddot{x}_0 & \ddot{x}_3 + \ddot{x}_0 & \alpha u \end{bmatrix}^T \tag{3.50}$$

where α is the ratio for which the control input is multiplied and $\ddot{x}_i + a$ is the absolute acceleration of the i^{th} degree of freedom. In the first column of all plots, $\alpha = 1$, and in the second $\alpha = 0.1$. The case $\alpha = 0.1$ corresponds to the case when there is not as large a reliability on control force. This could be the case if the supercapicator (for the regenerative controller) was very large, or the springs, dashpots, and masses could handle a very large control force requirement. Or in the case when the other performance measure vector terms have an increased importance. The second row

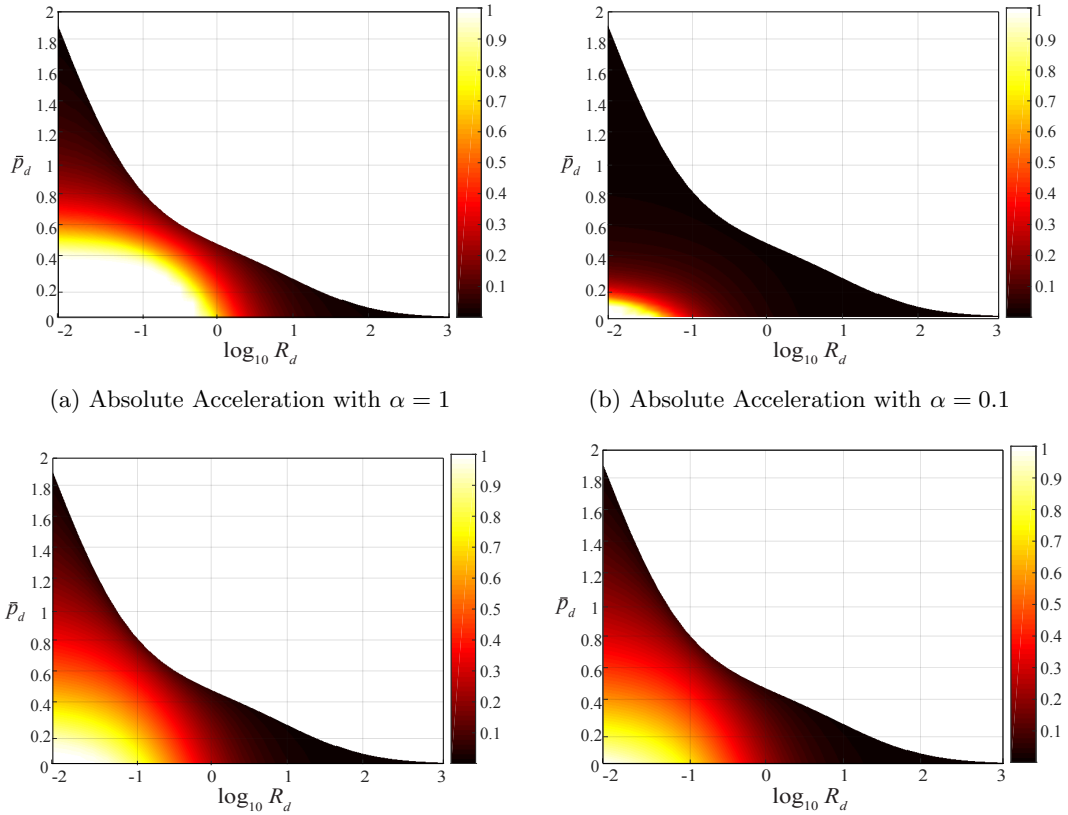

(a) Absolute Acceleration with $\alpha = 1$

(b) Absolute Acceleration with $\alpha = 0.1$

(c) Relative Displacement with $\alpha = 1$

(d) Relative Displacement with $\alpha = 0.1$

Figure 3.3: Surface Plot of Active vs. Regenerative Performance Ratio, of 3 DOF, One Input Structure for Different Performance Variables

of Figure 3.3 corresponds to a performance vector of

$$z = \begin{bmatrix} x_1 & x_2 & x_3 & \alpha u \end{bmatrix}^T \tag{3.51}$$

where x_i is relative displacement of the i^{th} degree-of-freedom and α is the same as the previous row.

It is interesting to note the change in performance over the various performance objectives and α values. The regenerative controller is able to replicate the performance of an active controller for a much larger region when $\alpha = 1$. One explanation for this result is that when $\alpha = 0.1$, the control device can utilize a much larger force output without a great force penalty in the cost function. This allows for a much more effective active controller. However, when a regenerative controller is

implemented, parasitics are introduced. When $\alpha = 0.1$ and more control force is utilized, the parasitic parameter R_d has a much higher effect and therefore cost is diminished.

Additionally, there is a much larger discrepancy in the α values in the absolute acceleration case compared to the relative displacement case. One possible rationale for this is that a controller, when focusing on the acceleration of the structure, requires a much larger force to minimize the cost. A large amount of control force required would then produce this large discrepancy.

3.3.2 Two Transducers Examples

The third set of examples, Figure 3.4, consists of a system with two transducers, shown in Figure 3.4a. Again the springs and masses are non-dimensionalized at value one and the dashpots are of value 0.01. The power spectral density of the exogenous disturbance can again be characterized as in (4.25). In this example, the feedback laws are again collocated, but now y is a vector of the form

$$y = v = \begin{bmatrix} \dot{x}_1 - \dot{x}_0 \\ \dot{x}_2 - \dot{x}_1 \end{bmatrix} \tag{3.52}$$

The performance vector for the first row is now

$$\begin{bmatrix} \ddot{x}_1 + \ddot{x}_0 & \ddot{x}_2 + \ddot{x}_0 & \ddot{x}_3 + \ddot{x}_0 & \alpha u_1 & \alpha u_2 \end{bmatrix}^T \tag{3.53}$$

and for the second row

$$\begin{bmatrix} x_1 & x_2 & x_3 & \alpha u_1 & \alpha u_2 \end{bmatrix}^T \tag{3.54}$$

Once again, the first column corresponds to the case when $\alpha = 1$ and the second column corresponds to $\alpha = 0.1$. and the exogenous disturbance filter is the same as in the case with one transducer. It is interesting to note the lessened area of feasible control laws. Because there are now two transducers, the effect of the parasitic

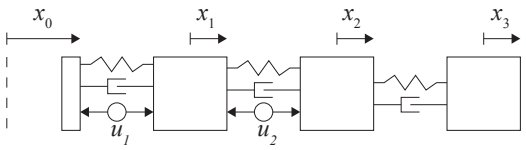

(a) System Description

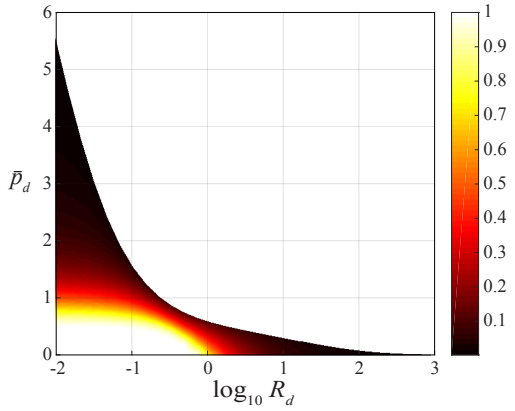

(b) Absolute Acceleration of Two Transducer System with $\alpha = 1$

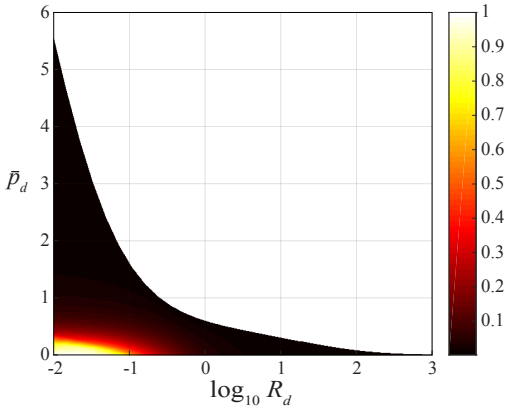

(c) Absolute Acceleration of Two Transducer System with $\alpha = 0.1$

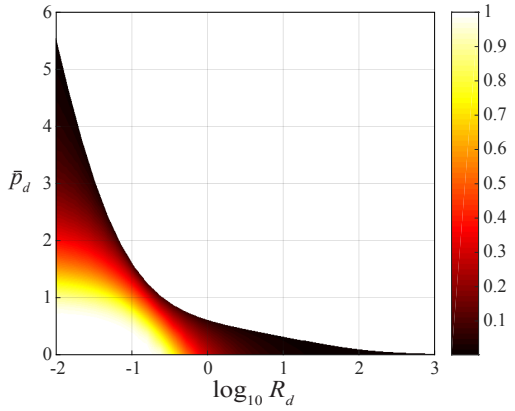

(d) Relative Displacement of Two Transducer System with $\alpha = 1$

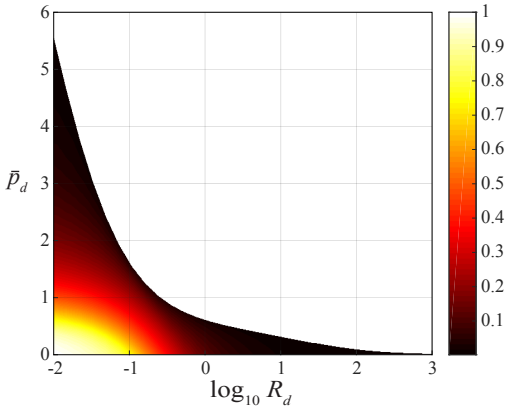

(e) Relative Displacement of Two Transducer System with $\alpha = 0.1$

Figure 3.4: Surface Plot of Active vs. Regenerative Performance Ratio, of 3 DOF, Two Transducer Structure

parameters $\{\bar{p}_d, R_d\}$ is much higher. There is once again a large discrepancy between the two absolute acceleration plots, but there is also now a more noticeable difference in when α changes value. When $\alpha = 1$, the two transducers must control the system without a large amount of control force, and therefore the regenerative controller can replicate the performance of the active controller for a much larger region.

3.3.3 Quarter Car Model Example

Figure 3.5 shows an example on the quarter car model from Figure 2.3 when $\omega_n = 10$ and $\xi = 0.25$. The mass, stiffness, and damping values are as defined in Chapter 2.3.2, and the performance vector z values is composed of the absolute acceleration of x_2 and the control force u, i.e.,

$$z = \begin{bmatrix} \ddot{x}_2 & \alpha u \end{bmatrix}^T \tag{3.55}$$

Since, in automotive examples, the acceleration of the wheel is not important to the comfort of the occupants, $\ddot{x}_1$ was not included. The columns represent different values of α, which multiplies by the force input u in the performance vector. To note, for both the Quarter and Half car models $\alpha \in \{0.01, 0.1\}$ rather than $\{0.1, 1\}$. The lower weights on force vectors allowed for a more interesting result to be obtained, as when $\alpha = 1$ little to no control force was applied.

These examples showcase an interesting, new result for the regenerative controller. When $\alpha = 1$ less control force is utilized, and therefore the dynamic parameter R_d has a much lower effect on the performance of the regenerative controller. The

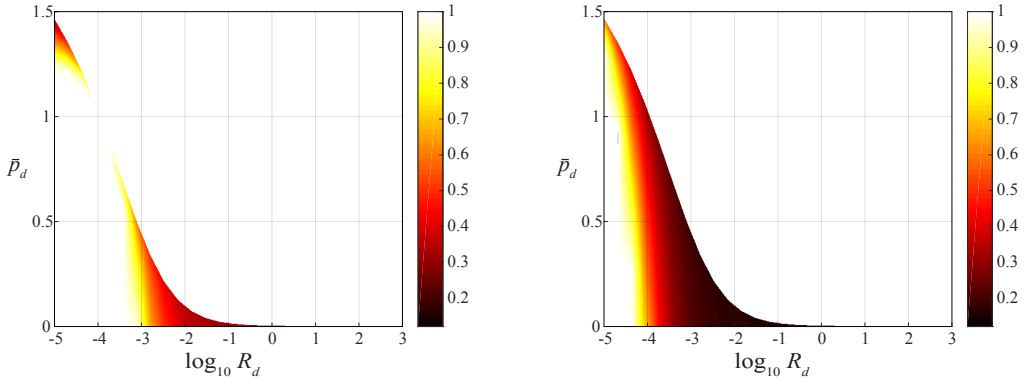

(a) Absolute Acceleration of Quarter Car Model System with $\alpha = 0.1$

(b) Absolute Acceleration of Quarter Car Model System with $\alpha = 0.01$

Figure 3.5: Surface Plot of Active vs. Regenerative Performance Ratio for Quarter Car Model System

static parameter p_d is the only one which significantly decreases the performance of the controller. Additionally, for a lower R_d value the performance barely suffers as the parasitic values reach the feasibility line. This would seem to suggest that the controller need not apply a large amount of force to control the system effectively. When $\alpha = 0.1$, the performance is much more dependent on the dynamic parameter R_d. In this scenario, the control law can utilize a larger amount of force without as large of penalty in the cost function.

Overall, for this example, the regenerative controller is able to replicate the performance of an active controller much more effectively. However, much like the two transducer case, the feasibility region is much more narrow than the one transducer structural case. This introduces an interesting dichotomy between the two types of examples. The quarter car model example does not need a large amount of control force, and therefore have a much larger area of active controller replication. However, the quarter car example provides a much more narrow feasibility area for the parasitic parameters. The single transducer structural example provides a much larger feasibility region but a smaller area of active controller replication.

3.3.4 Half Car Model Example

Figure 3.6 shows examples on the half car model from Figure 2.4. As a reminder, $\omega_n = 100$, which is roughly five to ten times higher than the largest natural frequency of the system. Also, $\xi = 0.25$. The mass, stiffness, and damping values are as defined in Chapter 2.3.3, and the performance vector z values are

$$z = \begin{bmatrix} \ddot{x}_3 & \theta & \alpha u_1 & \alpha u_2 \end{bmatrix}^T \tag{3.56}$$

The columns represent different values of $\alpha \in \{0.01, 0.1\}$, which multiplies by the force input u in the performance vector. For the results, it would appear as though

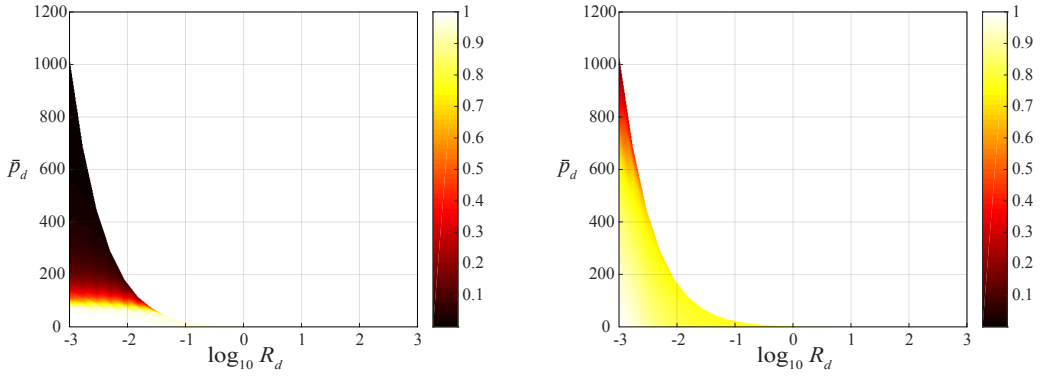

(a) Absolute Acceleration of Half Car Model System with $\alpha = 0.1$

(b) Absolute Acceleration of Half Car Model System with $\alpha = 0.01$

Figure 3.6: Surface Plot of Active vs. Regenerative Performance Ratio for Half Car Model System

there is a very small window of replication of performance of the regenerative controller. However, if the parasitic parameters are kept within reasonable levels, the regenerative controller can replicate the performance of the active controller quite effectively. The regenerative controller can generate power for large values of $\bar{p}_d$, and therefore the majority of the area shown in Figure 3.6 has a very low ratio. In reality there is a much larger area of feasibility and a much larger area of replication, as there is now a much larger potential for static power loss.

The examples in this chapter showcase the comparison between active and regenerative control laws over a variety of examples. These examples differ in scope and results, but it is clear that, for low enough parasitics, in general a regenerative controller can replicate an unconstrained active control law. This would seem to suggest a regenerative controller can outperform a passive controller.

CHAPTER 4

Passive Control

As mentioned, the passive controller serves as a baseline comparison for the optimal regenerative controller due to its practicality and cost efficiency. However, the passive controller has a limited domain and therefore its performance suffers. The comparison of regenerative and passive controllers allows for a more detailed understanding of the effectiveness and practicality of the regenerative control network.

Much work has been done to optimize an SPR controller in an LQG context. Lozano-Leal and Joshi [67] wrote a benchmark paper which, by adjusting the weights in the LQG optimization, produce an SPR controller. This was advanced and leveraged in numerous other papers [35, 60, 61]. However, the problem type in [67] arises only in special occasions and is not applicable to many structural systems. When this special circumstance does not hold, the control problem is non-convex and the methods presented will not produce a closed-form solution. It is even unclear under which circumstances the optimal controller has a finite dimension [14]. Previous work has also optimized SPR controllers with conservatism on all controller characteristics but the observer [26, 91, 92] or regulator [20]. Even with the added conservatism, the optimization problem is non-convex and over-bounding techniques must be used.

The passive controller is assumed to be of the form

$$\mathcal{K}_p = \begin{cases} \dot{x}_p &= A_p x_p + B_p y \\ u &= C_p x_p + D_p y \end{cases} \tag{4.1}$$

In order to enforce the SPR conditions in a state-space sense, the Kalman-Yakubovich-Popov (KYP) Lemma was developed. This lemma states that if $\mathcal{K}_p$ is SPR if and only if $\exists\ W_p = W_p^T > 0$ such that

$$\begin{bmatrix} A_P^T W_p + W_p A_p + \lambda W_p & W_P B_P + C_p^T \\ B_p^T W_p + C_p & D_p^T + D_p^T \end{bmatrix} \leq 0 \tag{4.2}$$

for some $\lambda > 0$ holds.

With no assumptions regarding the controller, it is easy to see this LMI is non-convex. The optimization domain is $\{W_p, A_p, B_p, C_p, D_p\}$, which creates nonlinearities in three out of four terms in (4.2). This fundamental nonconvexity proves to be a difficult problem, and the reason many researchers make assumptions regarding characteristics of the controller. In order to find the optimal passive controller, two methods have been implemented. The first consists of moving the zeros of the regenerative controller to find the closest possible passive controller. In this method, the controller variables A_p, B_p are assumed to be the same as the regenerative controller, which introduces conservatism into the optimization. In the next method, the passive controller is optimized with no conservatism, save for the specification of the controller dimension. The moving of zeros method is compared to a regenerative controller thorough a simple example, and the optimal passive controller is compared to an optimal regenerative controller via a number of examples.

4.1 Moving of Zeros

This section aims to find the distance between passive and regenerative controllers, i.e., how close a passive controller is to an optimal regenerative controller. That is,

what is the closest $\mathcal{K}_p \in K_P$ to the optimized regenerative controller $\mathcal{K}^* \in K_R$? To obtain this passive controller, the optimization procedure will seek to define some tolerance ϵ_0 such that $\|\mathcal{K}_p - \mathcal{K}^*\|_\infty < \epsilon_0$, where $\mathcal{K}^*$ has the transfer function $C_K^*(sI - A_K^*)B_K^*$, i.e., the regenerative controller optimized in the previous chapter. We define some tolerance ϵ_0 such that we can conclude $\mathcal{K}^*$ is "effectively passive" if $\epsilon < \epsilon_0$. If $\epsilon > \epsilon_0$, there is a distance between the two controllers. To visualize this, consider the case where $Re\{\mathcal{K}^*(j\omega)\} < 0$ except at a few frequencies which are not significant, such as a few high frequencies where $|\mathcal{K}^*(j\omega)|$ is very small. In this case, it would be conceivable to find a passive system very close (within ϵ_0) to this system which will give closely related performance. If this passive controller has a similar form and therefore comparable performance, it would lesson the practicality of the regenerative controller.

4.1.1 Derivation

The goal becomes to find a passive realization $\mathcal{K}_p \in K_P$ which minimizes $\|\mathcal{K}_p - \mathcal{K}^*\|_\infty$. There is some additional conservatism introduced, as it is assumed $A_p = A_K^*$ and $B_p = B_K^*$. This amounts to moving the transfer function zeros of the regenerative realization, while maintaining the poles. With this assumption, via the Bounded Real Lemma, we have that $\|\mathcal{K}_p - \mathcal{K}^*\|_\infty < \epsilon$ if there exists $T_p = T_p^T$ such that

$$\begin{bmatrix} A_K^{*T}T_p + T_pA_K^* & \bullet & \bullet \\ B_K^{*T}T_p & -\epsilon I & \bullet \\ C_p - C_K^* & D_p & -\epsilon I \end{bmatrix} < 0 \tag{4.3}$$

Additionally, for the controller $\mathcal{K}_p$ to be passive there must exist a $W_p = W_P^T > 0$ such that

$$\begin{bmatrix} A_K^{*T}W_p + W_pA_K^* & \bullet \\ B_K^{*T}W_p + C_p & D_p^T + D_p \end{bmatrix} < 0 \tag{4.4}$$

The optimization goal becomes to minimize ϵ over $\{C_p, D_p, T_p, W_p\}$ subject to (4.3), (4.4). This optimization is convex, but it is also realization-specific. To alleviate this dependence, consider rewriting the above regenerative control parameters in terms of the non-dimensionalized optimal regenerative controller characteristics $\{\tilde{A}^*, \tilde{B}^*, \tilde{C}^*\}$ and transforming the passive parameters such that $\tilde{C}_p = C_p M^T$, $\tilde{D}_p = D_p$. From this point, one can show the above optimization is equivalent to finding $\tilde{T}_p = \tilde{T}_p^T > 0, \tilde{W}_p = \tilde{W}_p^T > 0$ (see Appendix for proof) such that

$$\begin{bmatrix} \bar{A}^T\tilde{T}_pG + G^T\tilde{T}_p\bar{A} & \bullet & \bullet \\ \tilde{B}^{*T}\tilde{T}_pG & -\epsilon I & \bullet \\ \tilde{C}_p - \tilde{C}^* & \tilde{D}_p & -\epsilon I \end{bmatrix} < 0 \tag{4.5}$$

$$\begin{bmatrix} \bar{A}^T\tilde{W}_pG + G^T\tilde{W}_p\bar{A} & \bullet \\ \tilde{B}^{*T}\tilde{W}_pZ + \tilde{C}_p & \tilde{D}_p^T + \tilde{D}_p \end{bmatrix} < 0 \tag{4.6}$$

where

$$\bar{A} = \tilde{A}^* - \tilde{B}^*C_yX^* - Y^*B_u\tilde{C}^* - Y^*AX^* \tag{4.7}$$

$$G = I - Y^*X^* \tag{4.8}$$

Our optimization goal is now to minimize ϵ over the optimization domain $\{\tilde{C}_p, \tilde{D}_p, \tilde{T}_p, \tilde{W}_p\}$ subject to (4.5), (4.6). This reformulation alleviates the necessity to find M, N. These can be found using the relationship $I - Y^*X^* = MN^T$ once the optimization is complete. It should be noted that the X^*, Y^* values are the variables generated in the regenerative control optimization. M and N in turn would be used to find A_K, B_K, C_K.

One thing to note is that (4.5)-(4.6) requires $\bar{A}G^{-1}$ to be Hurwitz. $\bar{A}G^{-1}$ being non-Hurwitz means the optimal regenerative controller is open-loop unstable. For obvious reasons the zeros of an open-loop unstable transfer function cannot be moved to form a passive transfer function. Therefore, any unstable regenerative controller will not have a passive counterpart and is shown as such.

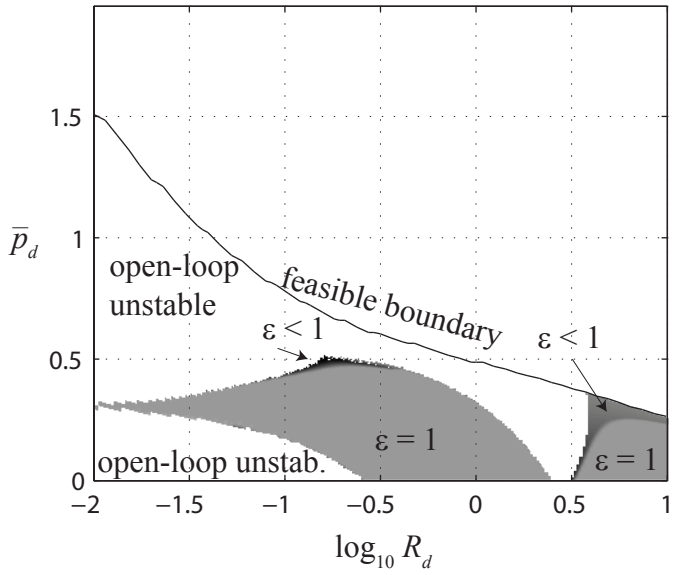

Figure 4.1: Surface Plot of ϵ Values over Parasitics with Open-Loop Unstable Regions Shown

4.1.2 Example

To formulate an example, the three-degree of freedom structure shown in Figure 2.1 is again considered. In the power spectral density of the base accelerations, it is again assumed the natural frequency $\omega_n = 1$ and damping ratio $\xi = 0.125$. The performance vector is again defined as in (3.47) and $y = v$ is defined as in (3.48).

Figure 4.1 is a surface plot which shows the ϵ value over the parasitic region normalized by $\|K^*\|_\infty$ i.e.,

$$\frac{\|\mathcal{K}_p - \mathcal{K}^*\|_\infty}{\|\mathcal{K}^*\|_\infty} \tag{4.9}$$

It is interesting to note that for much of the region, the optimal regenerative controller is open-loop unstable and therefore no passive controller can be realized. Additionally, a good portion of the region $\epsilon = 1$, which implies that at its peak value the regenerative controller is negative real, and the passive controller $\mathcal{K}_p$ is merely set equal to zero. There are a few regions where a passive controller can be optimized (and $\epsilon < 1$), but for the most part the passive controller was not able to

be optimized. This, at the very least, shows that the two controllers are inherently different. The regenerative controller can occupy a domain which a passive controller simply cannot. This passive to regenerative performance ratio will be investigated in the next section, but for now the comparison of the two controllers is unclear.

4.2 Optimal Passive Control

With the optimization strategy presented previously (i.e., the moving of zeros), we found the regenerative and passive controllers appear to be inherently different and determined some characteristics of a regenerative controller. While giving an initial intuition, the complete comparison of the two controllers remains to be seen.

The work presented in this section will attempt to optimize a passive controller without any assumptions regarding the controller matrices (other than dimension). Comparing the optimal regenerative controller $\mathcal{K}^* \in K_r$ with an optimal passive counterpart allows for a more complete comparison. It is assumed the controller is SPR; however, this assumption is mild, since any passive controller can be reformulated as an SPR function.

To enforce $\mathcal{K} \in K_P$, the first step is the positive-real lemma outlined in (4.2). The closed-loop stability constraint (3.25) and cost constraint (3.26) additionally become constraints in the optimization. Therefore, the closed loop LQG performance $J < \gamma$ if and only if there exist $W_p = W_p^T, P = P^T$ such that (4.2), (3.25), (3.26) hold.

Once again, the controller characterization is realization dependent. To alleviate this, the method proposed in [87] is again utilized. But, unlike the regenerative case, this transformation does not produce a convex set of LMIs (see Appendix Section

7.2.2 for proof). The optimization LMIs are transformed into the new constraints

(4.10)

$$\begin{bmatrix} AX + XA^T + B\tilde{C} + (B\tilde{C})^T + B_w B_w^T & \bullet \\ B_w B_w^T + \tilde{A} + (AZ + B\tilde{D}B^T Z)^T & B_w B_w^T + ZA^T + AZ + \tilde{B}B^T Z + (\tilde{B}B^T Z)^T \end{bmatrix} < 0$$

(4.11)

$$\begin{bmatrix} X & \bullet & \bullet \\ Z & Z & \bullet \\ C_z X + D_z \tilde{C} & C_z Z + D_z \tilde{D} B^T Z & Q \end{bmatrix} > 0$$

(4.12)

$$\begin{bmatrix} \Psi^T Z(I - YX) + (I - XY)Z\Psi & \bullet \\ (\tilde{B}^T - YB\tilde{D})^T Z(I - YX) + \tilde{C} - \tilde{D}C_y X & \tilde{D}^T + \tilde{D} \end{bmatrix} < 0$$

(4.13)

$$Z > 0$$

where $Z = Y^{-1}$ and

(4.14)

$$\Psi = \tilde{A} - YAX - \tilde{B}C_y X - YB\tilde{C} - YB\hat{D}C_y X$$

The optimization goal is to minimize γ over the optimization domain $\{\tilde{A}, \tilde{B}, \tilde{C}, \tilde{D}, Y, X, Z\}$ subject to (4.10)-(4.13). The obvious problem is the non-convexity culminating in a quad-linear term together in two terms of the (1,1) term of (4.12). There is no coordinate transformation or reformulation which will recover convexity in the passive controller optimization, which means non-convex methods must be implemented.

4.2.1 Iterative Convexification Over-Bounding (ICO) Technique

The non-convex optimization method utilized here stems from methods which were proposed simultaneously by de Oliveira [16] and Shimomura [91]. These techniques were updated in [90] with the use of weighting matrices. The derivations and methodology have been given their own Chapter, Chapter 5. The general idea behind the method is to solve a non-convex problem via a series of convex, over-bounding problems. It takes many iterations, but will converge to an optimal point.

The reader is directed towards Chapter 5.1.2 to see the methods which are applied to the LMI equations within the current chapter.

4.2.2 Optimal Passive Controller with Non-Convex Optimization

Utilizing the ICO principle, the optimization LMIs (3.37), (3.38), (4.12) can be over-bounded to create convex LMIs. It should be noted that in the regenerative formulation, (3.37), (3.38) are convex after the coordinate transformation. However, in this formulation, we have redefined $\tilde{A} \leftarrow Z\tilde{A}$, $\tilde{B} \leftarrow Z\tilde{B}$, and $P \leftarrow YPY$. This creates nonconvexities in the originally convex (3.37), (3.38). Additionally, define $\mathcal{G}_0(S,R) = S_0R^T + RS_0^T + SR_0^T + R_0Q^T - Q_0R_0^T - R_0Q_0^T$ and $\Theta = B_wB_w^T$. For the full proof, see the Appendix, but to preserve brevity the LMIs (3.37), (3.38) are reformulated as the convex constraints

(4.15)

$$0 > \begin{bmatrix} \left(\begin{bmatrix} \Theta + AX + XA^T + B\tilde{C} + \tilde{C}B^T & \bullet \\ \Theta + \tilde{A} + ZA^T & \Theta + ZA^T + AZ \end{bmatrix} + \mathcal{G}_0 \left(\begin{bmatrix} 0 \\ ZB \end{bmatrix}, \begin{bmatrix} B\tilde{D} \\ \tilde{B} \end{bmatrix} \right) \right) & \begin{bmatrix} 0 \\ (Z - Z_0)BW_{10} \end{bmatrix} & \begin{bmatrix} B(\tilde{D} - \tilde{D}_0) \\ (\tilde{B} - \tilde{B}_0) \end{bmatrix} \\ \bullet & -2W_{10} + W_1 & 0 \\ \bullet & \bullet & -W_1 \end{bmatrix}$$

(4.16)

$$0 < \begin{bmatrix} \left(\begin{bmatrix} X & Z & (C_zX + D_z\tilde{C})^T \\ Z & Z & ZC_z^T \\ C_zX + D_z\tilde{C} & C_zZ & Q \end{bmatrix} + \mathcal{G}_0 \left(\begin{bmatrix} 0 \\ ZB \\ 0 \end{bmatrix}, \begin{bmatrix} 0 \\ 0 \\ D\tilde{D} \end{bmatrix} \right) \right) & \begin{bmatrix} 0 \\ (Z - Z_0)B \\ 0 \end{bmatrix} & \begin{bmatrix} 0 \\ 0 \\ D(\tilde{D} - \tilde{D}_0)W_{2k} \end{bmatrix} \\ \bullet & W_2 & 0 \\ \bullet & \bullet & 2W_{20} - W_2 \end{bmatrix}$$

Defining

$$T_0 = (\tilde{B}_0 - B\tilde{D}_0)^T \tag{4.17}$$

$$U_0 = (Z_0 - X_0)P_0 \tag{4.18}$$

$$V_0 = (\tilde{A}_0^T - X_0A^T - \tilde{C}_0^TB^T - X_0BT_0 \tag{4.19}$$

(4.12) is reformulated as

(4.20)

$$
\begin{aligned}
0 > &\begin{bmatrix}
U_0(\tilde{A}-AX-B\tilde{C}-V_0^T)+(\tilde{A}-AX-B\tilde{C}-V_0)^TU_0^T & \bullet & \bullet & \bullet \\
\tilde{C}+(\tilde{B}-B\tilde{D}-T_0^T)^TU_0^T & \tilde{D}+\tilde{D}^T & \bullet & \bullet \\
-W_{30}U_0^T & 0 & -W_{30}+W_3 & \bullet \\
\tilde{A}-AX-B\tilde{C}-V_0^T & \tilde{B}-B\tilde{D}-T_0^T & 0 & -W_3
\end{bmatrix} \\
&+\mathcal{G}_0\left(\begin{bmatrix} U_0(\tilde{B}-B\tilde{D}) \\ \tilde{D} \\ 0 \\ \tilde{B}-B\tilde{D} \end{bmatrix},\begin{bmatrix} -XB \\ 0 \\ 0 \\ 0 \end{bmatrix}\right)+\mathcal{G}_0\left(\begin{bmatrix} V_0P \\ T_0P \\ P \\ 0 \end{bmatrix},\begin{bmatrix} Z-X \\ 0 \\ 0 \\ 0 \end{bmatrix}\right) \\
&+\begin{bmatrix} (X-X_0)B \\ 0 \\ 0 \\ 0 \end{bmatrix}W_4\begin{bmatrix} (X-X_0)B \\ 0 \\ 0 \\ 0 \end{bmatrix}^T+\begin{bmatrix} U_0(\tilde{B}-B\tilde{D}-T_0^T) \\ \tilde{D}-\tilde{D}_0 \\ 0 \\ \tilde{B}-B\tilde{D}-T_0^T \end{bmatrix}W_4^{-1}\begin{bmatrix} U_0(\tilde{B}-B\tilde{D}-T_0^T) \\ \tilde{D}-\tilde{D}_0 \\ 0 \\ \tilde{B}-B\tilde{D}-T_0^T \end{bmatrix}^T \\
&+\begin{bmatrix} (Z-X)-(Z_0-X_0) \\ 0 \\ 0 \\ 0 \end{bmatrix}W_5\begin{bmatrix} (Z-X)-(Z_0-X_0) \\ 0 \\ 0 \\ 0 \end{bmatrix}^T+\begin{bmatrix} V_0(P-P_0) \\ T_0(P-P_0) \\ (P-P_0) \\ 0 \end{bmatrix}W_5^{-1}\begin{bmatrix} V_0(P-P_0) \\ T_0(P-P_0) \\ (P-P_0) \\ 0 \end{bmatrix}^T
\end{aligned}
$$

where one can take the Schur compliment of the last four terms in order to render an equivalent linear matrix inequality. The optimization procedure is to minimize γ over the optimization domain $\{\tilde{A},\tilde{B},\tilde{C},\tilde{D},P,X,Z\}$ subject to the now convex LMI constraints (4.15), (4.16), (4.21), and (4.13). Complicating the optimization, each of the LMI constraints require feasible starting points, such that (4.15), (4.16), (4.21) still hold when $\tilde{A}=\tilde{A}_0$, $\tilde{B}=\tilde{B}_0$, etc. Additionally, the ICO non-convex technique requires many iterations to find an optimal solution. The over-bounding technique requires convergence at a sub-optimal minimal point at each iteration. This sub-optimal point is the convexification point for the next iteration, and the cycle repeats. So this technique allows for a series of convex optimization problems

to be solved which ultimately solve a non-convex optimization problem. Therefore it can take many iterations for the optimization to converge towards the globally optimal controller. Once the controller is optimized, the values for $\{A_p, B_p, C_p, D_P\}$ can be backed out from the relationships

$$\tilde{A} = NA_PM^T + NB_PC_yX + YBC_PM^T + YAX \tag{4.21}$$

$$\tilde{B} = NB_P \tag{4.22}$$

$$\tilde{C} = C_PM^T \tag{4.23}$$

$$\tilde{D} = D_P \tag{4.24}$$

4.2.3 Optimization Design Algorithm

As stated, initial feasible optimization variables $\{\tilde{A}_0, \tilde{B}_0, \tilde{C}_0, \tilde{D}_0, X_0, Y_0, Z_0, W_{10}, \ldots W_{50}\}$ and many iterations are necessary to conduct the optimization. To generate these initial convexification points and alleviate some of the computational burden, a design technique is introduced. The iterative algorithm is described as such:

1. Minimize γ subject to (3.37), (3.38) to find an initial controller.
2. Given $\{\tilde{A}, \tilde{B}, \tilde{C}, \tilde{D}, X\}$ and $Z = Y^{-1}$ from the previous step, generate a constraint which replaces the right-hand side of (4.12) with some variable expression ϵI, where ϵ is a scalar and I is appropriately sized. The $\{\tilde{A}, \tilde{B}, \tilde{C}, \tilde{D}, X, Z\}$ values are fixed from the previous step and not optimization variables. The optimization goal is to minimize ϵ over P subject to (4.12) with the right-hand side of (4.12) set to ϵ.
3. From the previous step, feasible optimization variables $\{\tilde{A}, \tilde{B}, \tilde{C}, \tilde{D}, X, Z\}$ and a Lyapunov variable P such that the left side of (4.12) is less than some minimized constant ϵ are available. From this point, set the left-hand sides of (4.15), (4.21) to ϵI and the left-hand side of (4.16) to $-\epsilon I$, with I appropriately sized for each

constraint. For our purposes, these constraints will be named $(4.15_\epsilon,)$ (4.21_ϵ), (4.16_ϵ). It should be noted that if $\epsilon > 0$, these three LMIs are over-bounded. Use the optimization variables from Steps 1 and 2 as initial feasible points for the convexification. Now, solve the optimization problem with a fixed γ value while trying to minimize ϵ subject to (4.15_ϵ), (4.21_ϵ), (4.16_ϵ) and (4.13). Incrementally increase γ each iteration by some factor α such that $\gamma_{i+1} = (1+\alpha)\gamma_i$, where i is the iteration number, while the optimization program attempts to bring down ϵ. Continue increasing γ until $\epsilon < 0$, which overbounds each of the constraints. For each iteration, use the optimizations variables $\{\tilde{A}, \tilde{B}, \tilde{C}, \tilde{D}, X, Z, P\}$ from the last iteration as convexification points.

4. Lastly, the minimization of γ can occur. The optimzation variable values from the last iteration of Step 3 serve as the initial "convexification" points for the first iteration of Step 4. The objective is to now minimize γ over $\{\tilde{A}, \tilde{B}, \tilde{C}, \tilde{D}, X, Z, P\}$ subject to (4.15), (4.16), (4.21), (4.13). For the current iterations, the values of $\{\tilde{A}_0, \tilde{B}_0, \tilde{C}_0, \tilde{D}_0, X_0, Z_0, P_0\}$ are set to the variable values $\{\tilde{A}, \tilde{B}, \tilde{C}, \tilde{D}, X, Z, P\}$ from the previous iteration. For the first iterations, use the optimization variables from the last iteration of the previous step. At each iteration, some cost value γ_i is generated, which can be compared to the cost at the previous iteration γ_{i-1}. Continue this iteration until $\gamma_{i-1} - \gamma_i < \sigma$, where σ is some user-chosen tolerance. Due to the property of the convexification algorithm, the cost at the current iteration is guaranteed to be lower than the previous iteration, and the algorithm will converge, albeit slowly.

At the end of Step 4, a non-conservative controller $\mathcal{K}_p \in K_P$ will be generated. Due to the property of the algorithm, as the convergence algorithm gets closer to the optimal point, the convergence steps get smaller and the algorithm will move more

slowly. Nonetheless, after many iterations an optimal passive controller can be found.

4.2.4 Examples When Compared to Optimal Regenerative Controller

One Transducer Structural Example

For the first set of examples, the system used is the same as in the previous section, i.e. Figure 2.1. The only subtle difference is in the white noise filter for the exogenous input. In this case, we have changed $\xi = 0.25$, i.e., the power spectral density for the base acceleration $a = \ddot{x}_0$ is

$$S_a(\omega) = \frac{\omega^2}{(\omega^2 - 1)^2 + (0.5\omega)^2} \tag{4.25}$$

Shown in Figure 4.2 are four sets of data in the same manner as Chapter 3. Once again, the first row corresponds to a performance vector of

$$z = \begin{bmatrix} \ddot{x}_1 + \ddot{x}_0 & \ddot{x}_2 + \ddot{x}_0 & \ddot{x}_3 + \ddot{x}_0 & \alpha u \end{bmatrix}^T \tag{4.26}$$

where α is the ratio for which the control input is multiplied and $\ddot{x}_i + a$ is the absolute acceleration of the i^{th} degree of freedom. Also as in the previous chapter, the first column of all plots corresponds to $\alpha = 1$ and the second $\alpha = 0.1$.

Again, the second row of Figure 4.2 corresponds to a performance vector of

$$z = \begin{bmatrix} x_1 & x_2 & x_3 & \alpha u \end{bmatrix}^T \tag{4.27}$$

where x_i is relative displacement of the i^{th} degree-of-freedom. We again assume collocated feedback, i.e., $y = v = \dot{x}_1 - \dot{x}_0$ for the regenerative and passive cases (this is the only option in the passive case). Shown in the plots is the ratio of passive to regenerative control, i.e.

$$J_R = \frac{J_{passive}}{J_{regenerative}}$$

Therefore, a larger J_R value corresponds to a much better performance of the regenerative controller. Again, the plots are being optimized over the parasitic parameters.

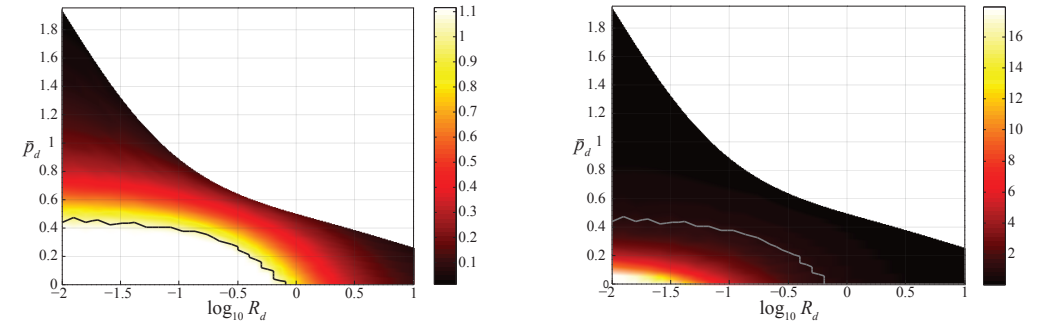

(a) Absolute Acceleration with $\alpha = 1$

(b) Absolute Acceleration with $\alpha = 0.1$

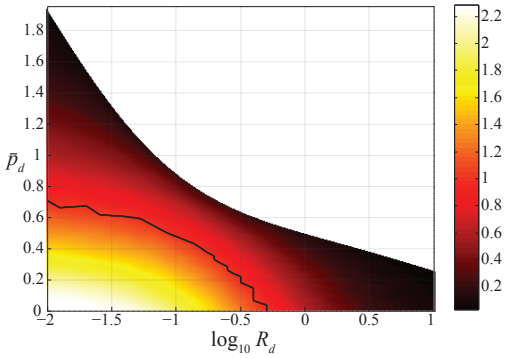

(c) Relative Displacement with $\alpha = 1$

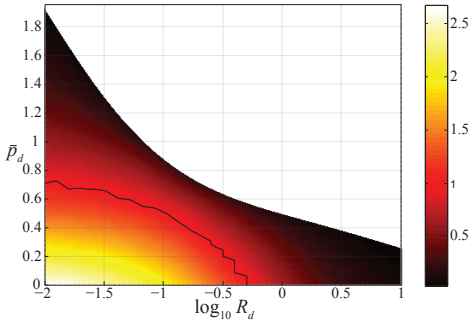

(d) Relative Displacement with $\alpha = 0.1$

Figure 4.2: Surface Plot of Active vs. Regenerative Performance Ratio, of 3 DOF, One Input Structure for Different Performance Variables

The passive controller is held constant throughout, while the regenerative controller's performance is deteriorating as the parasitics increase. As in Chapter 3, the first thing to note is the feasible boundary that each plot has. This boundary is where the regenerative controller can no longer overcome the parasitics of the electronics. Each plot also has a solid black or gray line inside of the shaded region. These are the points where $J_R = 1$, i.e., the passive and regenerative controllers have the same performance. Above this point the passive controller would be optimal, and below it the regenerative controller is optimal.

The plots clearly show that the smaller the weight on the control force, the better the regenerative performance. These smaller control force weights allow the regenerative controller to have an even larger domain and a much larger advantage over the

passive controller. In the relative displacement case when $\alpha = 0.1$, the value obtained at $\{p_d, R_d\} = \{0, 0\}$ is 2.6772, a 267.7 % improvement. In a case where displacement was more important than the control input, this would provide an almost three times better performance. This discrepancy grows more than five times as large for the absolute acceleration case with $\alpha = 0.1$. In the case where $\{p_d, R_d\} = \{0, 0\}$ the ratio of passive to regenerative cost was 17.98, or an almost 1800% improvement.

Two Transducer Structural Example

The second set of examples consists of a system with two transducers, shown in Figure 3.4a. Again the springs and masses are non-dimensionalized at value one

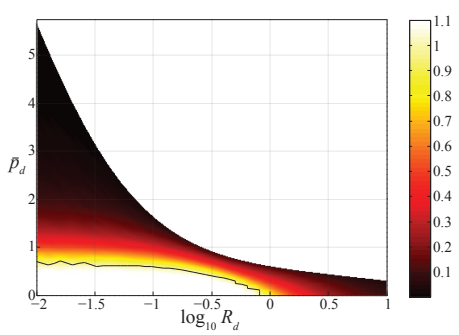

(a) Absolute Acceleration of Two Transducer System with $\alpha = 1$

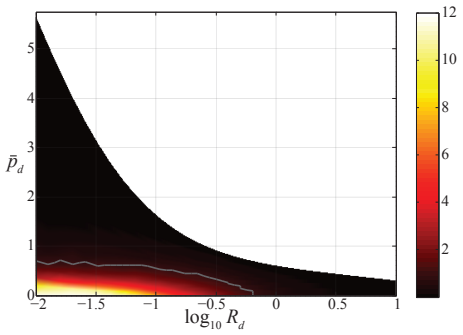

(b) Absolute Acceleration of Two Transducer System with $\alpha = 0.1$

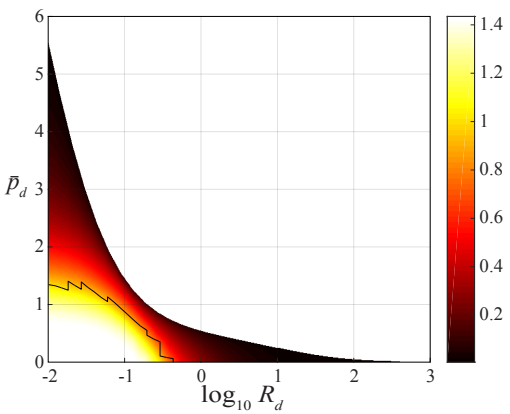

(c) Relative Displacement with $\alpha = 1$

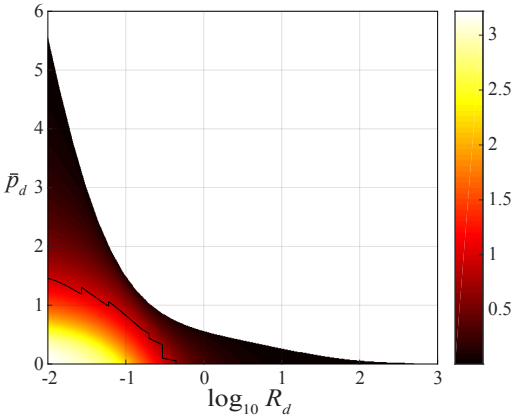

(d) Relative Displacement with $\alpha = 0.1$

Figure 4.3: Surface Plot of Active vs. Regenerative Performance Ratio, of 3 DOF, Two Transducer Structure, for Different Performance Variables

and the dashpots are of value 0.01. The power spectral density of the exogenous disturbance can again be characterized as in (4.25). In this example, the feedback laws are again collocated, but now it is a vector of the form

$$y = v = \begin{bmatrix} \dot{x}_1 - \dot{x}_0 \\ \dot{x}_2 - \dot{x}_1 \end{bmatrix} \tag{4.28}$$

The performance vectors are now

$$\begin{bmatrix} \ddot{x}_1 + \ddot{x}_0 & \ddot{x}_2 + \ddot{x}_0 & \ddot{x}_3 + \ddot{x}_0 & \alpha u_1 & \alpha u_2 \end{bmatrix}^T \tag{4.29}$$

for absolute acceleration and

$$\begin{bmatrix} x_1 & x_2 & x_3 & \alpha u_1 & \alpha u_2 \end{bmatrix}^T \tag{4.30}$$

for displacement. The exogenous disturbance filter is the same as in the case with one transducer. The ratio of passive to regenerative performance, J_R, is again shown in Figure 4.3. The first thing to note are the increased parasitics, which are due to the increased capability of the controllers to harvest energy. Therefore, the potential for static parasitics ($\bar{p}_d$) is increased. Once again, the performance vector with $\alpha = 0.1$ has a much higher regenerative performance potential. There also is an increased dependency on the transmission resistance matrix, R_d. As R_d increases, there is a decreased range of $\bar{p}_d$ values which are feasible. Nonetheless, the regenerative controller has a clear advantage over the passive system for all of the examples shown. This performance ranges from roughly 10% to 1200%, but persists throughout the various performance vectors. From these examples, it becomes clear that the regenerative controller has the ability to outclass the passive controller for low enough parasitics. In some cases (e.g. $\alpha = 0.1$) the regenerative controller has significantly lower performance than the passive controller. This would suggest allowing the controller to exert a larger amount of force provides the regenerative controller with a larger advantage compared to the passive controller.

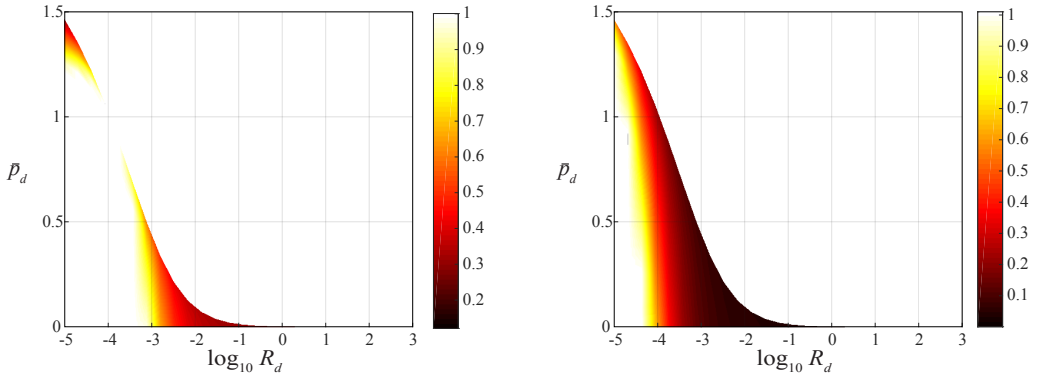

(a) Absolute Acceleration of Quarter Car Model System with $\alpha = 0.1$

(b) Absolute Acceleration of Quarter Car Model System with $\alpha = 0.01$

Figure 4.4: Surface Plot of Passive vs. Regenerative Performance Ratio for Quarter Car Model System

Quarter Car Model Example

Figure 4.4 shows an example on the quarter car model pictured in Figure 2.3 when $\omega_n = 10$. The mass, stiffness, and damping values are as defined in Chapter 2.3.2, and the performance vector z values are the same as in Chapter 3.3.3 (i.e., absolute acceleration of the body of the automobile and control force). The columns represent different values of α, which multiplies by the force input u in the performance vector.

These plots show an interesting contrast to previous examples, which show a larger increase in performance for the regenerative system. However, this performance increase decreases quickly as parasitics increase. In the quarter-car model, deterioration due to parasitics occurs much more slowly. The regenerative controller is able to replicate its performance much more effectively. However, the advantage of a regenerative controller over a passive controller is much lower than previous examples. There is little to no performance advantage across any of the plots, no matter the frequency. Additionally, the performance degradation is much more pronounced, when $\alpha = 1$, for the p_d parameter. Because $\alpha = 1$, the controller expends less control energy (to not increase the cost parameter), and the effect of the dynamic parasitic

parameter R_d is much less influential in the cost value.

Half Car Model Example

Figure 4.5 shows examples on the half car model from Figure 2.4. Once again, the mass, stiffness, and damping values are as defined in Chapter 2.3.3 and the performance vector and disturbance values are the same as in Chapter 3.3.4 . The figure is aligned the same as in previous examples, with the columns representing values of α. It is assumed the parameters for the disturbance characterization are the same as in Chapter 2.3.3.

Similar to the quarter car examples, the results in Figure 4.5 show little advantage of a regenerative control law when compared to a passive control law. However, as in previous examples the area of replication is much larger, and the advantage, albeit small, persists though a large region of the parasitic values. One thing to note is that the optimal passive control law is a ten degree-of-freedom transfer function. Using techniques developed in [11] (see Appendix), this transfer function can be realized as a series of springs, dashpots, inertial elements, and levers. However, the configuration of these mechanical components, for a ten DOF system, will be quite complex. There

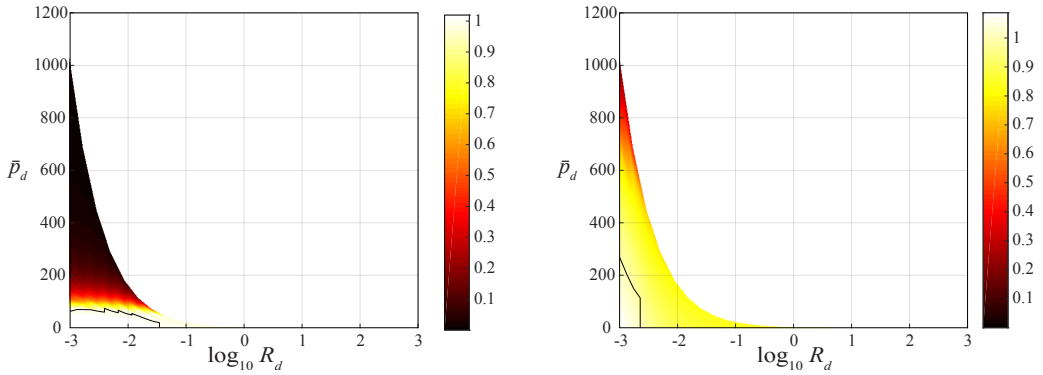

(a) Absolute Acceleration and Angle of Half Car Model System with $\alpha = 0.1$

(b) Absolute Acceleration and Angle of Half Car Model System with $\alpha = 0.01$

Figure 4.5: Surface Plot of Passive vs. Regenerative Performance Ratio for Half Car Model System

will be multiple levers which may require to be spanned across multiple wheels. This type of implementation is simply not practical, and therefore it may be advantageous to consider a different type of passive control device.

Viscous Damping Half Car Model Example

Shown in Figure 4.6 is the case when, rather than an optimal passive control law, a viscous damper is inserted where the control devices currently sit in Figure 2.4. To solve for the optimal damping values, we cycled through values of c_1^* (damping between DOF x_1 and x_4) and c_2^* (damping between DOF x_2 and x_5). We could then compute performance as:

$$J = C_z P C_z^T \tag{4.31}$$

where P is the Lyapunov matrix which solves

$$(A + \tilde{K})P + P(A + \tilde{K})^T + B_w B_w^T = 0 \tag{4.32}$$

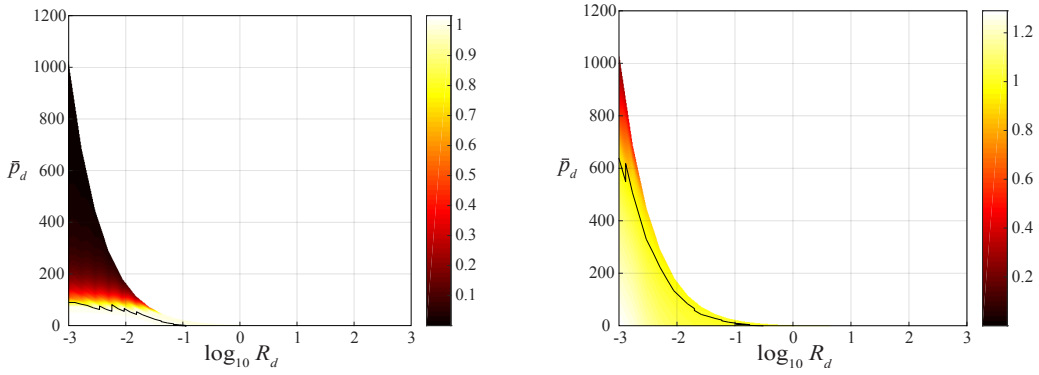

(a) Zoomed in Absolute Acceleration and Angle of Half Car Model System with $\alpha = 0.1$

(b) Zoomed in Absolute Acceleration and Angle of Half Car Model System with $\alpha = 0.01$

Figure 4.6: Surface Plot of Passive vs. Regenerative Performance Ratio for Half Car Model System

and

$$E = \begin{bmatrix} \ddot{x}_3 & \Phi & \tilde{K} \end{bmatrix}^T \tag{4.33}$$

$$\tilde{K} = \begin{bmatrix} 0 & 0 & 0 \\ 0 & -M^{-1}k & 0 \\ 0 & 0 & 0 \end{bmatrix} \tag{4.34}$$

$$k = \begin{bmatrix} c_1^* & 0 & {}^{-}c_1^* & c_1^* l_1 \\ 0 & c_2^* & -c_2^* & -c_2^* l_2 \\ -c_1^* & -c_2^* & c_1^* + c_2^* & -c_1^* l_1 + c_2^* l_2 \\ c_1^* l_1 & -c_2^* l_2 & -c_1^* l_1 + c_2^* l_2 & c_1^* l_2^2 + c_2^* l_2^2 \end{bmatrix} \tag{4.35}$$

A shown in Figure 4.6, the advantage of the optimal regenerative controller over the viscous damper is not significantly larger than that of the optimal passive control law. However, the area of advantage is much larger than that of the optimal passive controller. For the parameters selected, it appears the regenerative controller, while still advantageous, is less so than that of the structural examples.

4.2.5 Concluding Remarks

Throughout the previous examples, an optimal regenerative controller was compared to an optimal passive controller. For the structural examples, there was a clear cut advantage of the regenerative controller over its passive counterpart. This advantage ranged from 10% to 1600%, but continually persisted. The half-car model example also showcased a clear advantage, albeit on a smaller scale, for both an optimal passive control law and an optimized viscous damping force. The optimal passive control law is not practical in an automotive setting, and therefore we consider the viscous damping case. The performance advantage of a regenerative controller over an optimal viscous damping force ranged from 2% - 30%, but there was a clear advantage throughout. Additionally, for the half car model the area (over the parasitic parameters) of the regenerative control advantage was very large, and

it would seem this advantage is attainable for a large range of parasitic values. The quarter car model case showed little advantage for the regenerative controller, but the half car model is a more complex and practical version of the quarter car model. Overall, the regenerative controller showcased performance advantage throughout and is theoretically the preferred control technology.

CHAPTER 5

Iterative Convex Over-Bounding (ICO) Techniques

In the last 20 years, Linear Matrix Inequality (LMI) techniques have gained popularity in applications such as robust system analysis, topology optimization, and system performance analysis [4, 9]. By utilizing interior point methods and other convex techniques, LMI formulations have also become more common in control synthesis [24, 87]. A state-space representation of plant and controller dynamics allows for convex LMIs to be formed which encompass system and performance constraints. LMI techniques provide an efficient, practical way to solve these optimization problems via numerous LMI solvers [9].

However, as shown in Chapter 4, in many $\mathcal{H}_2$ and $\mathcal{H}_\infty$ control problems as well as robust analysis, nonconvex constraints arise. Often, these constraints are bilinear (or biaffine) matrix inequalities (BMIs) [101], which in turn make the problem NP-hard [100] to solve. Therefore, the optimization cannot be solved in polynomial time, and this inefficiency becomes increasingly noticeable as problem complexity increases. BMIs require a non-convex method for optimization, which in many cases must introduce conservatism (local vs. global optimum, validity of solution) in order to make the problem convex or reduce the time required.

To this end, both global and local optimization methods have been found. The ma-

jority of global optimization methods are some form of Branch and Bound technique. Branch and Bound is a search technique which splits the optimization domain into smaller regions, and then finds the optimization minimum constrained to each region. The algorithm, after finding its first minimum, can then selectively choose which of the other regions require searching. This method has been developed through numerous studies [5, 30, 64, 73, 102], but does not come without compromise. The problem remains NP-hard and therefore cannot be used in complex optimizations. This introduces conservatism into control problems, as limiting controller complexity may severely hinder performance.

Local optimization methods represent a much larger variety of techniques. A common method, D-K iterations, constitutes a two-step process to solve for a local optimum [7,17,31,50,51]. Each step consists of optimizing half of the control domain, while keeping the other half constant. While this method is fast, there is no guarantee it will converge to even a local solution. Even if a local optimum can be found [54], the method requires feasible starting points for variables, which is a burdensome task for more complex optimization problems. Interior point methods have also been utilized [42, 65], which incorporate a log-barrier function in order to find an optimal solution for a special class of optimization problem. Recently, path-following techniques [41, 81, 103] have gained popularity. These techniques allow for a non-convex problem to be recast as a convex one by not considering the non-convex terms. This can be done under the condition that the optimization does not advance far enough such that the non-convex terms have a noticeable impact. Rank-minimization approaches have also been researched [19, 47], but these methods are impactful for a subset of optimization problems (such as reduced-order controller design) and have no guarantee that the solution will be feasible for the original BMI. Methods such as

the projection method [33,34], min/max method [25], XY centering [52], and method of centers [31] have also been proposed, each with their own benefits and sources of conservatism. Another method developed by [62] is a gradient-based BMI optimizer which uses a modified Newton step on the dual formulation of the optimization problem. This method solves simple LMI optimization problems very quickly, but does not appear to effectively scale to more complex non-convexities. The MatLab program PenBMI utilizes this theory to solve BMI problems. While very fast and effective for simple BMI examples, when this program was scaled to the passive control optimization problems from the previous chapter, the running time was much longer than that proposed in this chapter.

Most closely related to the work of this paper are the simultaneous methods, called Iterative Convex Overbounding (ICO), proposed by Shimomura [92] and De Oliveira [16]. These propose, via completion of a square, solving the BMI constraint via a series of overbounding, convex problems (LMIs). This method was updated, via the use of weighting matrices, in [90], and applied to various control problems [105,106]. Like each of the methods mentioned, there are benefits and sources of conservatism incurred from the ICO approach. This approach is guaranteed to converge to a local optimum, does not compromise the optimization parameters, and does not split the optimization domain. However, it still takes NP time, the non-convexities are still present, ICO does require an initial feasible starting point, and it does not guarantee a global optimum.

Throughout this chapter, we aim to advance the ICO algorithm via two techniques. Both are able to find a local optimum, however the second technique improves upon convergence properties and time required for certain examples. These methods are then compared, and then a dynamic combination of these methods is

shown. An example is then shown comparing the two techniques.

5.1 Convex Over-Bounding

To explain the general principle of convex over-bounding, we illustrate it on a simple example, in which S and R are variables which must satisfy the BMI

$$Q + \mathrm{He}\{BRDSC\} < 0 \tag{5.1}$$

where Q, B, C, D are constant matrices and $\mathrm{He}\{A\} = A + A^T$. It is additionally assumed that (5.1) is satisfied when $\{R, S\}$ are instantiated at known values $\{R_0, S_0\}$, which we will call *design points*. Defining $S = S_0 + \tilde{S}$, $R = R_0 + \tilde{R}$ (where $\{\tilde{R}, \tilde{S}\}$ are finite perturbations), (5.1) is equivalent to

$$Q + \mathrm{He}\{B(R_0 + \tilde{R})D(S_0 + \tilde{S})C\} < 0 \tag{5.2}$$

Since $\{R_0, S_0\}$ is known to be feasible, there exists an open neighborhood in $\{\tilde{R}, \tilde{S}\}$ which includes $\{0, 0\}$, over which (5.2) is satisfied. Expanding (5.2), and collecting the linear terms, gives

$$Q + \mathrm{He}\{\phi(R, S) + B\tilde{R}D\tilde{S}C\} < 0 \tag{5.3}$$

where

$$\phi(R, S) = B\left(RDS_0 + R_0DS - R_0DS_0\right)C \tag{5.4}$$

5.1.1 Previous Technique

Continuing with Lyapunov BMI (5.1), the following is the convex over-bounding procedure proposed and implemented in [90, 105, 106].

Let $D = UV$ where U and V^T have full column rank. Then for some arbitrary invertible matrix L_1, (5.3) is equivalent to

$$Q + \mathrm{He}\{\phi(R, S)\} + B\tilde{R}UL_1L_1^TU^T\tilde{R}^TB^T + C^T\tilde{S}^TV^TL_1^{-T}L_1^{-1}V\tilde{S}C < \eta\eta^T \tag{5.5}$$

where

$$\eta = B\tilde{R}UL_1 - C^T\tilde{S}^TV^TL_1^{-T} \tag{5.6}$$

Noting that $\eta\eta^T \geqslant 0$, it follows that (5.5) is conservatively implied by

$$Q + \mathrm{He}\{\phi(R,S)\} + B\tilde{R}UL_1L_1^TU^T\tilde{R}^TB^T + C^T\tilde{S}^TV^TL_1^{-T}VL_1^{-1}\tilde{S}C < 0 \tag{5.7}$$

It should be noted that the conservatism vanishes when $\eta(\tilde{R},\tilde{S}) = 0$ (including the perturbation origin; i.e., $\{\tilde{R},\tilde{S}\} = \{0,0\}$) in which case (5.7) is equivalent to (5.1). Defining $W_1 = L_1L_1^T > 0$ and implementing a Schur compliment, (5.5) holds if

$$\begin{bmatrix} \mathrm{He}\{\phi(R,S)\} & \bullet & \bullet \\ (R-R_0)^TB^TU^T & -W_1^{-1} & \bullet \\ (S-S_0)CV & 0 & -W_1 \end{bmatrix} < 0 \tag{5.8}$$

Recalling that L_1 can be any arbitrary invertible matrix, we see that in (5.8), W_1 can be taken to be any positive definite matrix.

As such, setting the right-hand side of (5.5) to zero over-bounds the nonconvex constraint with a convex constraint; i.e., (5.8). It is worth emphasizing that the conservatism of (5.8) is global in the $\{\tilde{R},\tilde{S}\}$ domain, thus allowing for these perturbations to be large. This is in contrast to some other "convexifying" LMI techniques for handling nonconvex terms and unlike many iterative LMI techniques which require that the perturbations to be small.

5.1.2 New technique

Starting again from (5.3), consider that rather than being reformulated as (5.5), it can be equivalently reformulated as

$$\mathrm{He}\{\phi(R,S)\} + \alpha\alpha^T < B\tilde{R}UL_2L_2^TU^T\tilde{R}^TB^T + C^T\tilde{S}^TV^TL_2^{-T}L_2^{-1}V\tilde{S}C \tag{5.9}$$

where ϕ is defined previously and

$$\alpha = B\tilde{R}UL_2 + \tilde{S}CVL_2^{-1} \tag{5.10}$$

where L_2 is an arbitrary invertible matrix. Define $W_2 = L_2 L_2^T$, this implies that W_2 can be any positive-definite matrix, and the above inequality can be reformulated as

$$\text{He}\{\phi(R,S)\} + \beta W_2^{-1}\beta^T < B\tilde{R}UW_2U^T\tilde{R}^TB^T + C^T\tilde{S}^TV^TW_2^{-1}V\tilde{S}C \tag{5.11}$$

where

$$\beta = B\tilde{R}UW_2 + C^T\tilde{S}^TV^T \tag{5.12}$$

As in the previous method, since the right-hand side of (5.11) is positive definite, we can obtain a more conservative condition by setting the right-hand side to zero. Specifically, via a Schur compliment, (5.11) holds if

$$\begin{bmatrix} \text{He}\{\phi(R,S)\} & \bullet \\ B(R-R_0)UW_2 + C^T(S-S_0)^TV^T & -W_2 \end{bmatrix} < 0 \tag{5.13}$$

holds. This again over-bounds the nonconvex problem with a convex one. Also as with the previous over-bound, the conservatism vanishes when $\beta(\tilde{R},\tilde{S}) = 0$, and specifically at the origin in the perturbation space.

5.1.3 Interpolation (Variation) of the Two Methods

It could be the case that neither of the over-bounds discussed above performs best, but rather some linear combination of the two. First represent (5.1) equivalently as

$$Q + \text{He}\{BRU(I-\Lambda)VSC\} + \text{He}\{BRU\Lambda VSC\} < 0 \tag{5.14}$$

where Λ is an interpolation matrix, chosen to be symmetric and in the domain $0 < \Lambda < I$. If one was to utilize the first and second methods on the respective terms in (5.14), the resulting convex over-bounded constraint would be

$$\begin{bmatrix} Q + \text{He}\{\phi(R,S)\} & \bullet & \bullet & \bullet \\ U^T(R-R_0)^TB^T & -\tilde{W}_1^{-1} & \bullet & \bullet \\ V(S-S_0)C & 0 & -\hat{W}_1 & \bullet \\ \begin{pmatrix} W_2B(R-R_0)U \\ +C^T(S-S_0)^TC^T \end{pmatrix} & 0 & 0 & -\hat{W}_2 \end{bmatrix} < 0 \tag{5.15}$$

where $\tilde{W}_1 = L_1 \Lambda L_1^T$, $\hat{W}_1 = L_1 \Lambda^{-1} L_1^T$ and $\hat{W}_2 = L_2 (I - \Lambda)^{-1} L_2^T$.

In (5.15), the values of L_1, L_2, and Λ (or, equivalently, compatible values of weighting matrices $\tilde{W}_1$, $\hat{W}_1$, W_2, and $\hat{W}_2$) can be viewed as tuning parameters, chosen strategically to minimize the conservatism with which (5.15) implies (5.1). However, as we will show in Section 5.3, we can make these weighting matrices optimization parameters as well, thus reducing the importance of the values at which they are initialized.

5.2 ICO Algorithm

We now illustrate how to use convex over-bounding to optimize the values of R and S in the following simple BMI problem:

$$\{R^\star, S^\star\} = \text{sol} \begin{cases} \text{Given} & Q, B, C, D, E, F \\ \text{Minimize} & J \triangleq \text{tr}(ER) + \text{tr}(FS) \\ \text{Over} & R, S \\ \text{Subject to} & (5.1) \end{cases} \tag{5.16}$$

where it is tacitly assumed that all matrices are real, and of compatible dimension.

To solve this problem, iterative convex over-bounding is used. We assume that an initial feasible design point $\{R_1, S_1\}$ is known. Then the k^{th} iteration, for $k \geqslant 1$, is as follows:

1. Formulate convex constraint (5.15) for feasible design points $\{R_k, S_k\}$.
2. Minimize J subject to (5.15), over the optimization domain $\{R, S\}$. Note that this is a convex LMI problem with a guaranteed feasible solution, which we denote $\{R_k^\star, S_k^\star\}$.
3. Set $R_{k+1} = R_k^\star$, $S_{k+1} = S_k^\star$. Note that $\{R_{k+1}, S_{k+1}\}$ are guaranteed to be feasible because (5.15) is more conservative than (5.1) for all $\{R, S\}$.
4. Advance $k \to k + 1$ and return to step 1.

This procedure is guaranteed to converge monotonically to a local optimum $\{R^\star, S^\star\}$ for problem (5.16). As such, the non-convex problem has been replaced via a convergent series of convex subproblems.

In many cases, it may be easy to determine a feasible starting design point, $\{R_1, S_1\}$. If this is not the case, then an iterative algorithm, similar to the one above, can be used to find one. To run this algorithm, let parameters $\{R_1, S_1\}$ be specified, but not necessarily feasible for (5.1). Then step k of the feasibility algorithm consists of the following steps.

1. Determine the performance J_k associated with design point $\{R_k, S_k\}$, and formulate convex over-bounded constraint (5.15). Replace the right-hand side of (5.15) with ϵI, where I is of appropriate dimension. This modified constraint will now be referred to as (5.15_ϵ).
2. Minimize ϵ subject to (5.15_ϵ), as well as the constraint that $J < J_k(1+\delta)$ where $\delta > 0$ is a small constant. As such, the domain for the optimization is $\{R, S, \epsilon\}$. Let the optimal solutions be denoted $\{R_k^\star, S_k^\star, \epsilon_k^\star\}$.
3. Set $R_{k+1} = R_k^\star$, $S_{k+1} = S_k^\star$. If $\epsilon_k^\star < 0$ then $\{R_{k+1}, S_{k+1}\}$ are feasible, and the above algorithm can now be implemented to minimize J. Otherwise, set $k \to k+1$ and repeat.

As such, the ICO algorith in general is a two-stage optimization, in which the first stage determines a feasible design point, and the second stage determines an optimum. We make a few brief comments about its execution:

- The algorithm above referred to the interpolation of the two over-bounding methods discussed in Section 5.1 (i.e., (5.15)), but the same procedure can of course be implemented for either of the limiting cases for the interpolation; i.e., by changing (5.15) in the algorithm with either (5.8) or (5.13).

- In the feasibility stage of the algorithm, the constraint $J < (1+\delta)J_k$ is not strictly needed. However, it is useful so that when stage 2 is initiated, the performance of the initial feasible design point is not excessively large.

- In most optimization algorithms which require many iterations to converge, the optimization stops when $J_{k-1} - J_k < \epsilon$, i.e., when the change in objective function from one iteration to the next is smaller than some value. However, this method does not prove effective for the ICO algorithm. Some iterations of our algorithm produce a small change in the objective function, and then much larger changes occur in the next iteration. Therefore, stopping the algorithm when $J_{k-1} - J_k < \epsilon$ would limit the effectiveness of the algorithm and the optimality of the stopping point.

  To combat this effect, we have utilized an exponential regression function to determine convergence. This function fits an exponential curve $\hat{\gamma}(i) = \gamma_k\big((1-\alpha_k) + \alpha_k e^{-\beta_k(i-k)}\big)$ to the time serious of cost values $\{J_{k-i}, \ldots, J_k\}$, where i is an iteration time index for our curve and $\alpha_k, \beta_k, \gamma_k$ are the exponential curve parameters. To save space within this section, the derivations for $\alpha_k, \beta_k, \gamma_k$ are shown in the Appendix. This function is fit to J over the time index i, a subset of the entire optimization iteration count. This time index is large enough such that the convergence criteria are not affected by a small number of iterations which do not represent the overall trend of the cost value. Over this time interval, we can find the ratio of change in the exponential curve value via $\frac{1}{(1-\alpha_k)}$. We can now set our new convergence condition to be:

$$\frac{1}{(1-\alpha_k)} < \epsilon \tag{5.17}$$

5.3 Dynamic Adjustment of Weights

The ICO algorithm requires specification of weighting parameters L_1, L_2, and Λ. The algorithm is guaranteed to converge irrespective of how these matrices are chosen, provided they meet the stated requirements (i.e., L_1 and L_2 invertible, $0 \leqslant \Lambda \leqslant I$). However, the rate of convergence strongly depends on how they are chosen. It would therefore be convenient if the algorithm could also update these parameters upon each iteration, so as to reduce the conservatism of the convex over-bounding procedure. A dynamic value of Λ allows for the optimization procedure to shift the interpolation between the two over-bounding techniques discussed in the previous section. Meanwhile, including L_1 and L_2 in the optimization domain can be used to effectively normalize the magnitudes of the different perturbation terms (i.e., $\tilde{R}, \tilde{S}$).

One possibility for adjusting L_1, L_2, and Λ would be to use convex over-bounding on (5.15) to create a conservative LMI that is convex in $\{R, S, L_1, L_2, \Lambda\}$. However, this would result in a very complicated LMI, and here we propose a more straightforward, heirarchical way to dynhamically adjust the weighting terms in a separate optimization. To explain this, suppose that iteration k of the optimization has been completed. (For the purposes of this discussion, it is irrelevant whether the optimization is in the first (feasibility) or second (minimization) phase.) For iteration k, suppose the values of the weighting parameters used were $\{L_{1k}, L_{2k}, \Lambda_k\}$, and define the incremental changes in the optimization variables for the k^{th} iteration as

$$\tilde{R}_k^\star \triangleq R_k^\star - R_k \qquad\qquad \tilde{S}_k^\star \triangleq S_k^\star - S_k \tag{5.18}$$

Our strategy for updating the weights (i.e., for finding $\{L_{1(k+1)}, L_{2(k+1)}, \Lambda_{k+1}\}$ is to retrospectively consider $\{\tilde{R}_k^\star, \tilde{S}_k^\star\}$ and determine the weights that would have resulted in minimal conservatism of (5.15).

Consider that (5.1), evaluated at $\{R, S\} = \{R_k^\star, S_k^\star\}$, is

$$\Xi(R, S, L_1, L_2, \Lambda) < \eta_k(I - \Lambda)\eta_k^T + \gamma_k \Lambda \gamma_k^T + \chi_k \Lambda \chi_k^T \tag{5.19}$$

where

$$\eta_k = B\tilde{R}_k^\star U L_1 - C^T \tilde{S}_k^{\star T} V^T L_1^{-T} \tag{5.20}$$

$$\gamma_k = B\tilde{R}_k^\star U L_2 \tag{5.21}$$

$$\chi_k = C^T \tilde{S}_k^{\star T} V^T L_2^{-T} \tag{5.22}$$

and where Ξ is the remainder term which, upon performing three Schur complements, becomes the left-hand side of (5.15). As such, the right-hand side of (5.19) (which we recall is positive-semidefinite due to the restriction that $0 \leqslant \Lambda \leqslant I$) is the term which is conservatively set to zero to arrive at (5.15). What we wish to do now is to examine the right-hand side of (5.19), and determine new weights $\{L_1, L_2, \Lambda\}$ such that this matrix is small under some measure, thus retrospectively reducing the degree of conservatism associated with the over-bound. These new weights will then be the ones used for the next iteration; i.e., $\{L_{1(k+1)}, L_{2(k+1)}, \Lambda_{k+1}\}$.

Variations exist for algorithms to achieve this objective, depending on how one defines "small under some measure," and whether additional structure is imposed on the problem to simplify it. Here, we will incorporate several such simplifications. To begin with, we will constrain L_1 and L_2 to be symmetric. (However, a slightly more elaborate procedure could be implemented in the general case.) More importantly, we will not conduct a global optimization over $\{L_1, L_2, \Lambda\}$. Instead, we will determine sub-optimal solutions for each variable. Specifically, there are three steps in this sequence:

1. Find symmetric L_1 to minimize $\mathrm{tr}(\eta_k^T \eta_k)$. This can be done by solving the

following convex optimization

$$W_1^\star = \text{sol}\begin{cases} \text{Given} & Q, B, C, D, \tilde{R}_k^\star, \tilde{S}_k^\star \\ \text{Minimize} & \text{tr}(Z) \\ \text{Over} & Z = Z^T, W_1 = W_1^T \\ \text{Subject to} & \Delta_{1k}(Z, W_1) > 0 \end{cases} \tag{5.23}$$

where

$$\Delta_{1k}(Z, W_1) \triangleq \begin{bmatrix} \begin{pmatrix} Z + \text{He}(B\tilde{R}_k^\star D\tilde{S}_k^\star C) \\ -B\tilde{R}_k^\star U W_1 U^T \tilde{R}_k^{\star T} B^T \end{pmatrix} & \bullet \\ V\tilde{S}_k^\star C & W_1 \end{bmatrix} \tag{5.24}$$

and then finding $L_{1(k+1)} = \sqrt{W_1^\star}$.

2. Find symmetric L_2 to minimize $\text{tr}(\gamma_k^T\gamma_k + \chi_k^T\chi_k)$. This can be done by solving the following convex optimization

$$W_2^\star = \text{sol}\begin{cases} \text{Given} & Q, B, C, D, \tilde{R}_k^\star, \tilde{S}_k^\star \\ \text{Minimize} & \text{tr}(Z) \\ \text{Over} & Z = Z^T, W_2 = W_2^T \\ \text{Subject to} & \Delta_{2k}(Z, W_2) > 0 \end{cases} \tag{5.25}$$

where

$$\Delta_{2k}(Z, W_2) \triangleq \begin{bmatrix} Z - B\tilde{R}_k^\star U W_2 U^T \tilde{R}_k^{\star T} B^T & \bullet \\ V\tilde{S}_k^\star C & W_2 \end{bmatrix} \tag{5.26}$$

and then finding $L_{2(k+1)} = \sqrt{W_2^\star}$.

3. Find $\Lambda = \Lambda^T$ satisfying $0 \leqslant \Lambda \leqslant I$ and minimizing the trace of the right-hand side of (5.19), with the solutions for L_1 and L_2 from steps 1 and 2 inserted. We note that this is also a convex optimization, and define the unique solution as $\Lambda^\star$. Set $\Lambda_{k+1} = \Lambda^\star$.

We make no claim that the above constitutes a true global optimization in the $\{L_1, L_2, \Lambda\}$ domain. However, it is very straight-forward to implement, and does address the stated objectives in a qualitative sense. To see this, note that if $\text{tr}\{\eta_k^T\eta_k\}$

and $\text{tr}\{\gamma_k^T\gamma_k + \chi_k^T\chi_k\}$ are both made small, then the trace of the right-hand side of (5.19) is small irrespective of Λ, as long as $0 \leqslant \Lambda \leqslant I$.

5.4 Examples

With the two convex over-bounding techniques specified, an example can be performed to compare the effectiveness of the proposed methods. The system utilized will again be the example system from Chapter 2. In this example, we aim to find an optimal passive controller. The power spectral density parameters have been specified as $\omega = 1, \xi = 0.25$ such that

$$S_a(\omega) = \frac{\omega^2}{(\omega - 1)^2 + (0.5\omega)^2} \tag{5.27}$$

Shown in Figure 5.1 are four plots. The two rows correspond to two different system performance objectives, and the two columns correspond to different weighting factors on the control variable in the performance vector. The top row performance vectors have again been specified as

$$z = \begin{bmatrix} \ddot{x}_1 + \ddot{x}_0 & \ddot{x}_2 + \ddot{x}_0 & \ddot{x}_3 + \ddot{x}_0 & \alpha u \end{bmatrix}^T \tag{5.28}$$

and the bottom row is specified as

$$z = \begin{bmatrix} x_1 & x_2 & x_3 & \alpha u \end{bmatrix}^T \tag{5.29}$$

where $\alpha = 1$ in the first column, and $\alpha = 0.1$ in the second column. In each of these plots, we again assume co-located feedback for the passive control law, i.e., $y = v = \dot{x}_1 - \dot{x}_0$.

The examples in Figure 5.1 show mixed results. For the case when absolute acceleration is important, the previous technique provides better performing results. When relative displacement is of importance, the new technique provides much better

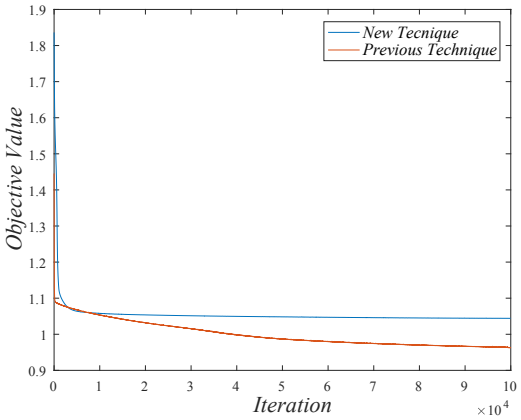

(a) Absolute Acceleration of Structural System with $\alpha = 1$

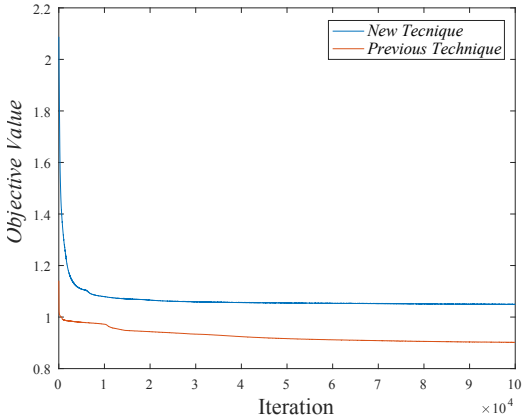

(b) Absolute Acceleration of Structural System with $\alpha = 0.1$

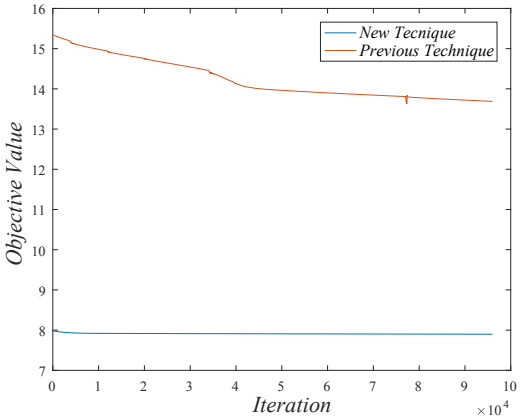

(c) Relative Displacement of Structural System with $\alpha = 1$

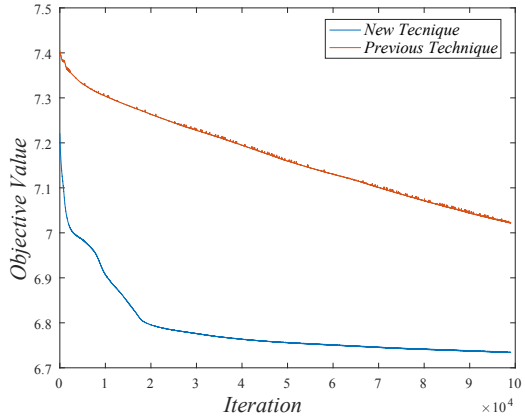

(d) Relative Displacement of Structural System with $\alpha = 0.1$

Figure 5.1: Iterative Cost Plot of One Transducer System of Variation and Prior Technique ICO Methods

performance. At the very least, we can say that the two methods provide advantages in differing scenarios. In some cases, (i.e., Figure 5.1c, the new techniques appears to converge to a lower, different optimal point. However, it should be noted that in Figure 5.1c, the usual convergence criteria had not been met when the iterations were stopped. With this knowledge known, the interpolation of the two methods can provide an advantage in deciding which algorithm to choose.

One issue within the algorithm are the "jumps" in the cost value that occur for all four cases above. These increases in objective value are caused by numerical precision issues within the optimization, one example of which is extreme values of the W

weighting parameters. The optimization could make one W term either very large or very small (depending on if W is inverted or not) to allow for large movement in the direction of one variable. The inversion (or non-inversion) of this same W parameter along another diagonal would therefore be extreme in the other direction. This movement to extrema creates numerical precision issues and inefficiencies in the convergence characteristics. The convexification algorithm, in theory, guarantees that the optimization cost will always be decreasing. However, as shown the algorithm clearly is not performing to its expected potential. This is something that must be addressed in future work, via such techniques as slack introduction or limiting the optimization in some capacity.

CHAPTER 6

Robust Optimal Regenerative Control

In the previous sections, optimal regenerative and passive controllers were found with minimal conservatism and compared. Using the methods presented, a comparison of performances was found for an assumed network and disturbance characterization. However, in a physical application, these known system parameters cannot be implicitly assumed. In any vibration suppression application, there will be unknown parameters such as sensor-actuator delay, inaccurate sensors, or incorrect characterization of the network which will all add uncertainty into the controller optimization. More specific to a regenerative controller, the parasitic parameters may not be exactly known or may deteriorate over time. In a structural context, there are a number of motivations for considering an uncertain plant and/or disturbance characterization. Impurities in materials, inaccurate characterization of exogenous disturbances, and even human error in construction could all impact the accuracy of the network model being used. Therefore, an uncertain model characterization, which accounts for these errors, becomes increasingly desirable. If a controller could be optimal over the entire range of possible system values, this robustness would prove advantageous in a physical application.

With these known parameters of the network $\mathcal{N}$ and the disturbance characteri-

zation $\mathcal{A}$, it was shown that the regenerative controller could be framed as a convex optimization problem. However, this convexity cannot be implicitly assumed in the case where the network and disturbance parameters are uncertain. For a regenerative controller optimized over known parameters, there is no evidence of any guaranteed robustness. Moreover, for low enough parasitics, the regenerative controller replicates an unconstrained active LQG control law, which historically has a very small robustness margin [13].

In our work, we have focused on uncertainties which can be characterized by a polytopic domain in the system parameter space. We additionally still maintain a number of assumptions regarding our network. We still assume that the composite plant $\mathcal{P}$ is linear, the driving point impedance $y \mapsto u$ is positive real, the internal dynamics of the plant $\mathcal{N}$ are asymptotically stable, and the parasitic parameter $R_d > 0$.

Survey papers [77, 85] outline many of the polytopic methods utilized in previous work. Almost all of these methods assume the uncertainty in parameters is linearly interpolated over N vertices, i.e.,

$$A(\alpha) = \sum_{i=1}^{N} \alpha_i A_i \tag{6.1}$$

where the weighting vector $\alpha = \{\alpha_1 \dots \alpha_N\}$ is uncertain but is assumed to be in the set

$$\Delta_N = \left\{ \alpha \in \mathbb{R}^N \,\middle|\, \sum_{i=1}^{N} \alpha_i = 1, \quad \alpha_i \geq 0 \right\} \tag{6.2}$$

We likewise make these assumptions in the work presented. For a graphical representation of a polytopic domain, see Figure 6.1. Many methods additionally assume coupled uncertainty in other, but not necessarily all, network characteristics. There is also a distinction made in literature between quadratic and robust sta-

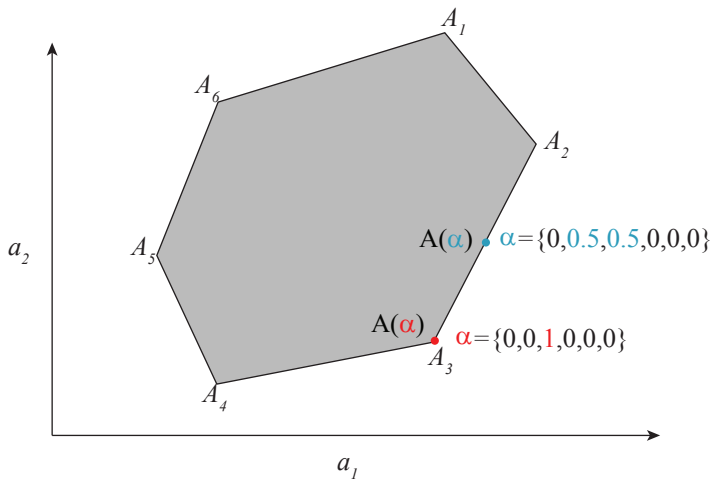

Figure 6.1: Example Uncertain Polytopic Domain

bility. Quadratic stability implies the network is stable for any, possible infinite, time-variation of the polytopic uncertain parameters. Robust stability suggests the network is stable for all possible (but time-independent) parameters within the uncertain polytope. Quadratic stability can be solved via convex LMIs, while robust stability may require a special solver or many possible iterations. It is a classical result [43] that the quadratic stability of $A(\alpha)$ is guaranteed by the existance of $P = P^T > 0$ such that

$$PA_i + A_i^T P < 0, \quad i = 1 \dots N \tag{6.3}$$

This concept was exteneded to allow the Lyapunov matrix P to be an affine function of α, via the use of additional matrix inequality constraints [27, 55, 86], as well as through the imposition of conservatism in (6.3) [29, 71, 84]. It was also found that robust stability could be guaranteed (and thus a $P(\alpha)$ could be defined for all points in the polytope) for both system stability and closed-loop performance with the addition of significantly more LMIs to the problem and the use of a custom solver [2, 3, 76, 78, 79]. Most closely related to our work was in [26], which optimizes a full-order strictly proper dynamic output feedback controller under an $\mathcal{H}_2$ performance

measure, subject to polytopic parameter uncertainty in $A(\alpha)$, as well as several other state space parameter matrices. This method allows for a coordinate transformation as in [87] which results in basis-independent controller optimization variables. This does require the introduction of some conservatism, as there are some nonlinearities in the matrix inequality constraint.

In the following section a regenerative controller is optimized over a polytopic domain, building off of the work in [26]. Due to the over-bounding methods presented in section 4.2.1, the method presented does not require any additional conservatism due to nonlinearites. First, the polytopic network will be constructed, then the regenerative constraint will be formulated in the polytopic context. Lastly, the regenerative LMI optimization will be shown with a corresponding example.

6.1 Polytopic System Characterization

The polytopic uncertainties present in the network adjust the characteristics described in $\mathcal{N}, \mathcal{A}, \mathcal{P}$ to $\mathcal{N}(\alpha), \mathcal{A}(\alpha), \mathcal{P}(\alpha)$ respectively, where $\mathcal{N}(\alpha)$ is of the form

$$\mathcal{N}(\alpha) = \left\{ \begin{array}{rl} \dot{x}_N & = A_N(\alpha)x_N + B_{Nu}(\alpha)u + B_{Na}(\alpha)a \\ v & = C_{Nv}(\alpha)x + D_{Nv}(\alpha)u \\ y & = C_{Ny}(\alpha)x + D_{Ny}(\alpha)u \\ z & = C_{Nz}(\alpha)x + D_{Nza}(\alpha)a + D_{Nzu}(\alpha)u \end{array} \right. \tag{6.4}$$

Once again, the disturbance $a(t)$ is assumed to be a stationary stochastic process characterized by a rational, strictly-proper power spectrum. This manifests itself in the polytopic network $\mathcal{A}(\alpha)$ such that

$$\mathcal{A}(\alpha) = \left\{ \begin{array}{rl} \dot{x}_A = & A_A(\alpha)x_A + B_A(\alpha)w \\ a = & C_A(\alpha)x_A \end{array} \right. , \quad S_w(\omega) = I \tag{6.5}$$

where $w(t)$ is still a white noise signal and $S_w(\omega)$ is the power spectrum of $w(t)$. Systems $\mathcal{N}$ and $\mathcal{A}$ can be again augmented (where $x = [x_N \;\; x_A]^T$) to form the new

network $\mathcal{P}(\alpha)$ such that

$$\mathcal{P}(\alpha) = \begin{cases} \dot{x} = & A(\alpha)x + B(\alpha)u + B_w(\alpha)w \\ v = & C(\alpha)x + D(\alpha)u \\ y = & C_y(\alpha)x \\ z = & C_z(\alpha)x + D_z(\alpha)u \end{cases} \tag{6.6}$$

Each parameter is assumed to be scaled by the weighting vector $\alpha \in \Delta_N$. Additionally, each parameter has N vertices which multiply by these scaling factors. It is assumed that the values of $\alpha_1, \ldots, \alpha_N$ are the same for each of the uncertain parameters. It is additionally assumed that each of the network parameters have coupled uncertainty via the value of α.

It will also be convenient to define a matrix E with full column rank (i.e., $E^T E > 0$) whose columns span the controllable subspace for (A, B), i,e.

$$span\{E\} = span\left\{ \begin{bmatrix} B & AB & \ldots & A^{n-1}B \end{bmatrix} \right\} \tag{6.7}$$

6.1.1 Positive Real Conditions

As in Chapter 2, the assumption must be made that the driving point impedance $y \mapsto u$ is positive real. However, this assumption is complicated by the polytopic uncertainty. Now, the Positive Real Lemma states that this impedance is positive real if and only if $\exists P(\alpha) = P(\alpha)^T > 0$ such that

$$\begin{bmatrix} A^T(\alpha)P(\alpha) + P(\alpha)A(\alpha) & P(\alpha)B(\alpha) - \frac{1}{2}C^T(\alpha) \\ B^T(\alpha)P(\alpha) - \frac{1}{2}C(\alpha) & -\frac{1}{2}D(\alpha) - \frac{1}{2}D^T(\alpha) \end{bmatrix} \leqslant 0 \tag{6.8}$$

This leads to the ensuing lemma, which strengthens the above inequality to a strict inequality.

Lemma 6.1.1: For each fixed $\alpha \in \Delta_N$, assume $u \mapsto v$ is positive real, $A(\alpha)$ is Hurwitz, and $R_d > 0$. Then $\exists P(\alpha) = P^T(\alpha) > 0$ with $EPE^T > 0$ such that

$$\begin{bmatrix} A^T(\alpha)P(\alpha) + P(\alpha)A(\alpha) & P(\alpha)B(\alpha) - \frac{1}{2}C^T(\alpha) \\ B^T(\alpha)P(\alpha) - \frac{1}{2}C(\alpha) & -R(\alpha) \end{bmatrix} < 0 \tag{6.9}$$

where

$$R(\alpha) = R_d - \tfrac{1}{2}D(\alpha) - \tfrac{1}{2}D^T(\alpha) \tag{6.10}$$

Proof. For a given α, let P_a satisfy (6.8). If $A(\alpha)$ is Hurwitz and $R_d > 0$, then $\exists P_b = P_b^T > 0$ such that

$$\begin{bmatrix} A^T(\alpha)P_b + P_bA(\alpha) & P_bB(\alpha) \\ B^T(\alpha)P_b & -R_d \end{bmatrix} < 0 \tag{6.11}$$

Taking $P(\alpha) = P_a + P_b$, we see that the addition of the two matrix inequalities above gives (6.9). □

Building off of this lemma, a theorem can be formulated which creates a starting-point for the development of a regenerative controller in a polytopic domain.

Theorem 6.1.1 If $\exists P = P^T > 0$ with $EPE^T > 0$, such that for $i = 1...N$,

$$\begin{bmatrix} A_i^T P + PA_i & PB_i - \frac{1}{2}C_i^T \\ B_i^T P - \frac{1}{2}C_i & -R_i \end{bmatrix} < 0 \tag{6.12}$$

then (6.9) is satisfied for any $\alpha \in \Delta$ with $P(\alpha) = P$.

Proof. Note that taking (6.9) at each of the vertices and with $P(\alpha) = P$ yields

$$\alpha_1 \begin{bmatrix} A_1^T P + PA_1 & PB_1 - \frac{1}{2}C_1^T \\ B_1^T P - \frac{1}{2}C_1 & -R_1 \end{bmatrix} + \cdots + \alpha_N \begin{bmatrix} A_N^T P + PA_N & PB_N - \frac{1}{2}C_N^T \\ B_N^T P - \frac{1}{2}C_N & -R_N \end{bmatrix} < 0 \tag{6.13}$$

Since each point in the polytope must satisfy (6.12), each matrix can be taken separately as a constraint. Since $\alpha_i \geq 0 \ \ \forall \alpha \in \Delta_N$, the α coefficient can be dropped and the result presented in (6.12) follows. □

6.2 Polytopic Regenerative Constraint

As in previous sections, the regenerative constraint can be formulated as:

$$\bar{p} \stackrel{\triangle}{=} \mathcal{E}\left\{u^T v + \mu(u)\right\} \leqslant 0 \tag{6.14}$$

where $\mu(u)$ is defined as in (3.17). Given this, the following result can be formulated.

Lemma 6.1.2: Assume $u \mapsto v$ is positive real, $A(\alpha)$ is Hurwitz, $R_d > 0$, and $P(\alpha) = P(\alpha)^T$, with $EPE^T > 0$, satisfies (6.9). Then, given some stabilizing feedback law $\mathcal{K} : y \to u$, in stationarity,

$$\bar{p} = \mathcal{E}\left\{ \begin{bmatrix} x \\ u \end{bmatrix}^T \begin{bmatrix} Q(\alpha) & S(\alpha) \\ S^T(\alpha) & R(\alpha) \end{bmatrix} \begin{bmatrix} x \\ u \end{bmatrix} \right\} - \mathrm{tr}\{B_w^T(\alpha)P(\alpha)B_w(\alpha)\} + \bar{p}_d \tag{6.15}$$

where $R(\alpha)$ is as in (6.10) and

$$Q(\alpha) = -\left(A^T(\alpha)P(\alpha) + P(\alpha)A(\alpha)\right) \tag{6.16}$$

$$S(\alpha) = -P(\alpha)B(\alpha) + \tfrac{1}{2}C^T(\alpha) \tag{6.17}$$

Proof. The first thing to note is that

$$\mu(u) = \bar{p}_d + u^T R_d u \tag{6.18}$$

and therefore

$$\mathcal{E}\left\{u^T v + \mu(u)\right\} = u^T C(\alpha)x + u^T(R_d + R_0(\alpha))u + \bar{p}_d \tag{6.19}$$

where $R_0(\alpha) = \frac{1}{2}D(\alpha) + \frac{1}{2}D^T(\alpha)$. Therefore, adding and subtracting $2\,\mathcal{E}\left\{x^T P(\alpha)(A(\alpha)x + B(\alpha)u)\right\}$ and taking the Schur compliment of the subtracted expression and (6.19) gives

(6.20)

$$\bar{p} = \mathcal{E}\left\{ \begin{bmatrix} x \\ u \end{bmatrix}^T \begin{bmatrix} 0 & \frac{1}{2}C^T(\alpha) \\ \frac{1}{2}C(\alpha) & R_d + R_0 \end{bmatrix} \begin{bmatrix} x \\ u \end{bmatrix} \right\} + \mathcal{E}\left\{ \begin{bmatrix} x \\ u \end{bmatrix}^T \begin{bmatrix} A^T(\alpha)P(\alpha) + P(\alpha)A(\alpha) & P(\alpha)B(\alpha) \\ B^T(\alpha)P(\alpha) & 0 \end{bmatrix} \begin{bmatrix} x \\ u \end{bmatrix} \right\}$$
$$-2\,\mathcal{E}\left\{x^T P(\alpha)(A(\alpha)x + B(\alpha)u)\right\} + \bar{p}_d$$

Noting it is a standard result from Itô calculus that

$$\tfrac{d}{dt}\,\mathcal{E}\{x^T P(\alpha)x\} = 2\left\{x^T P(\alpha)(A(\alpha)x + B(\alpha)u)\right\} + \mathrm{tr}\{B_w^T(\alpha)P(\alpha)B_w(\alpha)\} \tag{6.21}$$

and therefore

(6.22)

$$\bar{p} = \mathcal{E}\left\{ \begin{bmatrix} x \\ u \end{bmatrix}^T \begin{bmatrix} Q(\alpha) & S(\alpha) \\ S^T(\alpha) & R(\alpha) \end{bmatrix} \begin{bmatrix} x \\ u \end{bmatrix} \right\} - \mathrm{tr}\{B_w^T(\alpha) P(\alpha) B_w(\alpha)\} + \tfrac{d}{dt}\mathcal{E}\{x^T P(\alpha) x\} + \bar{p}_d$$

Since stationarity is assumed, $\frac{d}{dt}\mathcal{E}\{x^T P(\alpha) x\} = 0$ and the proof is complete. □

Using the previous result, a theorem can be developed which establishes an expression for the regenerative constraint. This theorem can also conveniently be expressed at the vertices of the polytope rather than at all points within the polytope (i.e. $A(\alpha)$). To preserve brevity, it was assumed the term B_w to be invariant, although this result can be extended when this does not hold.

Theorem 6.1.2: Let B_w be invariant for $\alpha \in \Delta$ and let $K : y \to u$ be any stabilizing feedback law. Then $\bar{p} < 0$ for all $\alpha \in \Delta$ if $\exists P = P^T > 0$,with $EPE^T > 0$, such that, for $i = 1...N$,

(6.23)
$$\begin{bmatrix} Q_i & S_i \\ S_i^T & R_i \end{bmatrix} > 0$$

(6.24)
$$\mathcal{E}\left\{x^T \hat{Q}_i x\right\} + \mathcal{E}\left\{\|u - G_i x\|_{R_i}^2\right\} < \bar{p}_0$$

where $\|q\|_{R_i}^2 = q^T R_i q$ for some $q \in \mathbb{R}^{n_p}$, and

(6.25)
$$Q_i = -A_i^T P - P A_i \qquad S_i = -PB_i + \tfrac{1}{2} C_i^T$$

(6.26)
$$R_i = R_d + \tfrac{1}{2} D_i + \tfrac{1}{2} D_i^T \qquad \hat{Q}_i = Q_i - S_i R_i^{-1} S_i^T$$

(6.27)
$$G_i = -R_i^{-1} S_i^T \qquad \bar{p}_0 = \mathrm{tr}\{B_w^T P B_w\} - \bar{p}_d$$

Proof. The proof follows directly from Lemma 6.1.2 and Theorem 6.1.1. We have sufficient conditions as (6.23) and

(6.28)
$$\mathcal{E}\left\{ \begin{bmatrix} x \\ u \end{bmatrix}^T \begin{bmatrix} Q_i & S_i \\ S_i^T & R_i \end{bmatrix} \begin{bmatrix} x \\ u \end{bmatrix} \right\} < \bar{p}_0$$

which can be reformulated as (6.24). □

Note is that the variable P found, which satisfies the conditions of Theorem 6.1.2, will not necessarily be unique. The equality (6.15) suggests that, in principle, all solutions should be equivalent. Therefore, it is not obvious which solution of P would be the optimal one. In the following work, P^* is denoted as the feasible solution that minimizes $\bar{p}_0$, i.e. the solution that generates the most power from the system. To solve for P^*, the optimization problem

$$P^\star = \text{sol}\begin{cases} \text{Minimize:} & \text{tr}\{B_w^T P B_w\} \\ \text{Over:} & P = P^T > 0 \\ \text{Subject to:} & (6.23), i = 1...N, , (6.7) \end{cases} \tag{6.29}$$

is solved. From this point forward, it is assumed $\hat{Q}_i, G_i$, and $\bar{p}_0$ are evaluated with $P = P^*$.

6.3 Robust Optimal Regenerative Control

As in the case of the regenerative controller without uncertainty, a finite-dimensional, linear time-invariant, and strictly proper controller is assumed of the form

$$\mathcal{K}_U = \begin{cases} \dot{x}_U &= A_U x_U + B_U y \\ u &= C_U x_U + D_U y \end{cases} \tag{6.30}$$

As in (2.3), the state is augmented to the form $x = [x_N \; x_A]^T$ and therefore the closed loop system is formulated as

$$\mathcal{T} = \begin{cases} \dot{\hat{x}} = & \hat{A}(\alpha)\hat{x} + \hat{B}w \\ z = & \hat{C}_z(\alpha)\hat{x} \\ r = & \hat{C}_r(\alpha)\hat{x} \end{cases} \tag{6.31}$$

where $r = u - G(\alpha)x$ and

$$\hat{A}(\alpha) = \begin{bmatrix} A(\alpha) + B(\alpha)D_U C_y(\alpha) & B(\alpha)C_U \\ B_U C_y(\alpha) & A_U \end{bmatrix}, \qquad \hat{B} = \begin{bmatrix} B_w \\ 0 \end{bmatrix} \tag{6.32}$$

$$\hat{C}_z(\alpha) = \begin{bmatrix} C_z(\alpha) + D_z(\alpha)D_U C_y(\alpha) & D_z(\alpha)C_U \end{bmatrix} \tag{6.33}$$

$$\hat{C}_r(\alpha) = \begin{bmatrix} -G(\alpha) + D_U C_y(\alpha) & C_U \end{bmatrix} \tag{6.34}$$

In this optimization, it is assumed $D_U = 0$, i.e., no feed-through term. The goal now becomes to optimize $\{A_U, B_U, C_U\}$ such that the covariance of the performance output $J = \max_{i=1...n_z} \mathcal{E}\{z_i^2\}$ is minimized subject to $\bar{p} < 0$, all over the uncertain polytopic domain $\alpha \in \Delta_N$. To do this, the following theorem is proposed:

Theorem 6.3.1: For a given controller $\mathcal{K}_U$ in the form of (6.30), $J < \gamma$ and $\bar{p} < 0$ if there exist $T = T^T, Z_i = Z_i^T$ such that, for $i = 1, \ldots, N$,

$$\begin{bmatrix} \hat{A}_i^T T + T\hat{A}_i & T\hat{B}_i \\ \hat{B}_i^T T & -I \end{bmatrix} < 0 \tag{6.35}$$

$$\begin{bmatrix} \gamma & \hat{C}_{z_{ij}} \\ \hat{C}_{z_{ij}}^T & T \end{bmatrix} > 0 \quad , \quad j \in \{1...n_z\} \tag{6.36}$$

$$\begin{bmatrix} Z_i & \hat{C}_{ri} \\ \hat{C}_{ri}^T & T \end{bmatrix} > 0 \tag{6.37}$$

$$\mathrm{tr}\{\hat{Q}_i X\} + \mathrm{tr}\{Z_i R_i\} < \bar{p}_0 \tag{6.38}$$

where $X = X^T$ is the leading $n \times n$ block of T^{-1}.

Proof. With the regenerative constraint outlined in Theorem 6.1.2, Theorem 6.3.1 is a standard result [9]. □

As in the previous section, the above optimization problem poses two problems. The LMIs above are non-convex and basis dependent. And, similar to the previous case, a coordinate transformation as in [87] is used. Define

$$T = \begin{bmatrix} Y & N \\ N^T & \times \end{bmatrix} \qquad T^{-1} = \begin{bmatrix} X & M \\ M^T & \times \end{bmatrix} \tag{6.39}$$

where $\times$ is a term that is unnecessary to define. Therefore, as previously done in Section 4.1.1, the LMIs can be redefined by this transformation. Additionally, A_0, B_0, C_{y0}, etc. terms are introduced. These can be any point within in the polytope, as long as each utilizes the same weighting factor α_0. The proof of this is not explained

here but is very similar to [28]. Denote a known $\alpha_0 = \{\alpha_{01}, \ldots, \alpha_{0N}\} \in \Delta_N$ to be a fixed set of scaling factors. Then, we have that $J < \gamma$ there exists optimization variables $\tilde{A}, \tilde{B}, \tilde{C}, X = X^T, Y = Y^T$, and $Z_i = Z_i^T$ such that for $i \in \{1...N\}$ and $j \in \{1...n_z\}$,

$$\begin{bmatrix} \Delta_{1i} + \Delta_{1i}^T & \bullet & \bullet \\ A_i^T + \tilde{A}^T & \Delta_{2i} + \Delta_{2i}^T & \bullet \\ B_w^T & B_w^T Y & -I \end{bmatrix} + \begin{bmatrix} 0 & \bullet & \bullet \\ Y\Delta_{3i} + \Delta_{4i} X & 0 & \bullet \\ 0 & 0 & 0 \end{bmatrix} < 0 \tag{6.40}$$

$$\begin{bmatrix} \gamma & \bullet & \bullet \\ XC_{z_{ij}}^T + \tilde{C}^T D_{z_{ij}}^T & X & \bullet \\ C_{z_{ij}}^T & I & Y \end{bmatrix} > 0 \tag{6.41}$$

$$\begin{bmatrix} Z_i & \bullet & \bullet \\ \tilde{C}^T - XG_i^T & X & \bullet \\ -G_i^T & I & Y \end{bmatrix} > 0 \tag{6.42}$$

$$\mathrm{tr}\{\hat{Q}_i X\} + \mathrm{tr}\{Z_i R_i\} < \bar{p}_0 \tag{6.43}$$

where

$$\Delta_{1i} = A_i X + B_i \tilde{C} \tag{6.44}$$

$$\Delta_{2i} = Y A_i + \tilde{B} C_{yi} \tag{6.45}$$

$$\Delta_{3i} = (B_i - B_0)\tilde{C} + \tfrac{1}{2}(A_i - A_0)X \tag{6.46}$$

$$\Delta_{4i} = \tilde{B}(C_{yi} - C_{y0}) + \tfrac{1}{2} Y (A_i - A_0) \tag{6.47}$$

and where α_0 is constant and $A_0 = A(\alpha_0)$, $B_0 = B(\alpha_0)$, and $C_{y0} = C_y(\alpha_0)$. The controller variables can then be backed out via the relationships

$$A_U = N^{-1}(\tilde{A}^T - Y B_0 \tilde{C} - \tilde{B} C_{y0} X - Y A_0 X) M^{-T} \tag{6.48}$$

$$B_U = N^{-1} \tilde{B} \tag{6.49}$$

$$C_U = M^{-T} \tilde{C} \tag{6.50}$$

$$D_U = \tilde{D} \tag{6.51}$$

With this optimization being presented, a few details must be distinguished:

- As before, M, N can be solved via the relationship $I - XY = MN^T$.
- The choice of α_0 is arbitrary, but must be held constant throughout. In the examples in this section, it is assumed $\alpha_{0i} = 1/N$, $i = 1, \ldots, N$. This assumption allows our design points to be centered in the polytopic domain, lessoning the time to find the next set of optimal points.
- Once again, to force a finite solution measurement noise on the signal y must be assumed. This modifies (6.40) to

$$\begin{bmatrix} \Delta_{1i} + \Delta_{1i}^T & \bullet & \bullet & \bullet \\ A_i^T + \tilde{A}^T & \Delta_{2i} + \Delta_{2i}^T & \bullet & \bullet \\ B_w^T & B_w^T Y & -I & \bullet \\ 0 & \tilde{B}^T & 0 & -\Xi^{-1} \end{bmatrix} + \begin{bmatrix} 0 & \bullet & \bullet & \bullet \\ Y\Delta_{3i} + \Delta_{4i} X & 0 & \bullet & \bullet \\ 0 & 0 & 0 & \bullet \\ 0 & 0 & 0 & 0 \end{bmatrix} < 0 \tag{6.52}$$

The optimization problem is then to minimize γ over the optimization variables $\{X, Y, Z_1 ... Z_N, \tilde{A}, \tilde{B}, \tilde{C}\}$ subject to (6.41)-(6.43),(6.52). As stated, the BMI in (6.52) is non-convex and no known coordinate transformation recovers convexity. Therefore, nonlinear convexification methods developed in Section 5.1.1 must be utilized. It is noteworthy that in the case when all of the vertices converge towards one point, i..e $A_i = A_j$, $B_i = B_j$ and $C_{yi} = C_{yj}$ for all $\{i, j\} \subset \{1...N\}$, the convexification technique outputs the same optimal controller developed in Chapter 3. In this case, irrespective of the α_0 chosen, $A_i - A_0$, $B_i - B_0$, and $C_{yi} - C_{y0}$ are zero. This means $\Delta_{3i}, \Delta_{4i} = 0$ and the optimization is the same as in Chapter 3. Therefore, any conservatism vanishes when the polytopic vertices converge to one point.

With this being said, (6.40) is equivalent, through Schur complements and the

convexification technique, to the convex LMI

(6.53)
$$\begin{bmatrix} \Delta_{1i}+\Delta_{1i}^T & \bullet & \bullet & \bullet & \bullet & \bullet & \bullet & \bullet \\ A_i^T+\tilde{A}^T+\Delta_{5i} & \Delta_{2i}+\Delta_{2i}^T & \bullet & \bullet & \bullet & \bullet & \bullet & \bullet \\ B_w^T & B_w^TY & -I & \bullet & \bullet & \bullet & \bullet & \bullet \\ 0 & Y-\bar{Y} & 0 & -W_1^{-1} & \bullet & \bullet & \bullet & \bullet \\ 0 & (\Delta_{4i}-\bar{\Delta}_{4i})^T & 0 & 0 & -W_2^{-1} & \bullet & \bullet & \bullet \\ \Delta_{3i}-\bar{\Delta}_{3i} & 0 & 0 & 0 & 0 & -W_1 & \bullet & \bullet \\ X-\bar{X} & 0 & 0 & 0 & 0 & 0 & -W_2 & \bullet \\ 0 & \tilde{B}^T & 0 & 0 & 0 & 0 & 0 & -\Xi^{-1} \end{bmatrix} < 0$$

where

(6.54)
$$\Delta_{5i} = -[\bar{Y}\bar{\Delta}_{3i}+\bar{\Delta}_{4i}\bar{X}]+[Y\bar{\Delta}_{3i}+\bar{\Delta}_{4i}X]+[\bar{Y}\Delta_{3i}+\Delta_{4i}\bar{X}]$$

The proof is not shown but the same methods as in Section 4.2.1 are used. Now, the convexificaition points $\bar{B}, \bar{C}, \bar{X}, \bar{Y}$ are invoked in the expressions for $\bar{\Delta}_3, \bar{\Delta}_4$. The optimization problem now becomes to minimize γ over $\{X, Y, Z_1...Z_N, \tilde{A}, \tilde{B}, \tilde{C}\}$ subject to (6.41)-(6.43), (6.53). The above is now convex in both the optimization variables and the uncertainty parameters, and can be solved iteratively via LMI optimization techniques.

6.3.1 Design of Optimization Algorithm

As stated in Section 5.1.1, there are two main hindrances of the convexification algorithm. There must be a feasible starting point and it may take many iterations to converge to the optimal solution. To alleviate some of the computational burden and initialize a feasible starting point, an optimization strategy is proposed below, with the implicit assumption that a solution exists and has been solved for optimization (6.29).

1. For $i = 1, \ldots, N$, set $A_i = A_0$, $B_i = B_0$, $C_i = C_0$, etc. for all network

characteristics which change over the polytopic region. This is equivalent to collapsing all the vertices to a single point, in the examples done, α_0 was assumed to be in the middle of the polytopic region, i.e., $\alpha_{0i} = 1/N$, $i = 1, \ldots, N$. Now, $\Delta_{4i} = \Delta_{5i} = 0$ and the optimization problem (6.41)-(6.43), (6.52) is convex as stated. It should be noted that the robust regenerative optimization problem is now the same as (3.37)-(3.40). Minimize γ over $\{X, Y, Z_1..Z_{n_z}, \tilde{A}, \tilde{B}, \tilde{C}\}$ subject to (6.41), (6.42), (6.43), and (6.52).

2. Now, reset the network characteristics from the collapsed vertices (i.e., A_0, B_0, C_0, etc) to their original values $A_1, \ldots, A_N, B_1, \ldots, B_N, C_1, \ldots, C_N$, etc. Set the right hand side of (6.53) to ϵI and (6.41), (6.42) to $-\epsilon I$. When $\epsilon > 0$, the feasibility of these three LMIs is relaxed. Initialize the convexification points $\bar{X}, \bar{Y}$, etc as the values obtained in Step 1 and specify some value of γ sufficiently large enough. Iteratively run an optimization problem that minimizes ϵ, each time using the previous solution as the next design point. Continue this process until $\epsilon < 0$ and thus the three constraints are overbounded. This homotopy approach results in a feasible starting point for the minimization of γ.

3. Set the design points equal to the previous optimization variable values from the last iteration of Step 2. Now, minimize γ over $\{X, Y, Z_1..Z_{n_z}, \tilde{A}, \tilde{B}, \tilde{C}\}$ subject to (6.41)-(6.43),(6.53). Use the values of the previous optimization as design points for the next iteration. Repeat this process until the change in γ from one iteration to the next is less than some specified value.

At the end of the optimization, an optimal regenerative controller over an unknown polytopic domain is generated.

6.4 Example

To formulate an example, the three-degree of freedom structure shown in Figure 2.1 is considered, with all system values as stated in Chapter 2, with the exception of the disturbance characteristics. For the purpose of the example, the scope of the polytopic region is limited to the case when there is uncertainty in the disturbance characterization $\mathcal{A}$ and nowhere else. Further uncertainty will be discussed in the future work section, but for the purposes of this example there is no uncertainty assumed in the network $\mathcal{N}$. Once again the feedback variable y is collocated with the voltage v via (3.48).

To ease the feasibility of the power generation, the system was converted to its self-dual form. This conversion is assumed to be known and will not be shown. The resulting system $\mathcal{N}$ can be characterized as

$$A_N = \text{diag}\left\{ \begin{bmatrix} 0 & \omega_p \\ -\omega_p & -\rho\omega_p^2 \end{bmatrix}, \quad p = 1, 2, 3 \right\} \tag{6.55}$$

$$B_{N_u} = \begin{bmatrix} 0 & -0.328 & 0 & 0.737 & 0 & -0.591 \end{bmatrix}^T \tag{6.56}$$

$$B_{N_a} = \begin{bmatrix} 0 & 1.6560 & 0 & -0.4740 & 0 & 0.182 \end{bmatrix}^T \tag{6.57}$$

$$C_{Nv} = B_{N_u}^T \tag{6.58}$$

$$D_{Nv} = 0 \tag{6.59}$$

where

$$\omega_1 = 0.445,\ \omega_2 = 1.247,\ \omega_3 = 1.8019,\ \rho = 0.01 \tag{6.60}$$

The performance vector z was assumed to be the absolute acceleration of the three

masses and the control input, i.,e.

$$z = \begin{bmatrix} \ddot{x}_1 + \ddot{x}_0 \\ \ddot{x}_2 + \ddot{x}_0 \\ \ddot{x}_3 + \ddot{x}_0 \\ u \end{bmatrix} \tag{6.61}$$

Additionally, the fictitious noise $\Xi = 1 \times 10^{-6}$ and the parasitic parameters were assumed to be $p_d = 0, R_d = 0.1$. Again, the power spectral density $a = \ddot{x}_0$ is assumed to be a stationary stochastic sequence of the form

$$S_a(\omega) = \frac{\omega^2}{(\omega^2 - \omega_a^2)^2 + (\zeta_a \omega_a \omega)^2} \tag{6.62}$$

where ω_a is the natural frequency and ζ_a is the damping ratio of the power spectral density. The above transfer function translates to the space space representation of the form

$$A_A = \begin{bmatrix} 0 & \omega_a \\ -\omega_a & -2\zeta_a \omega_a \end{bmatrix} \tag{6.63}$$

$$B_A^T = C_A = \begin{bmatrix} 0 & 1 \end{bmatrix} \tag{6.64}$$

It was assumed these disturbance parameters would vary, i.e. varied values of

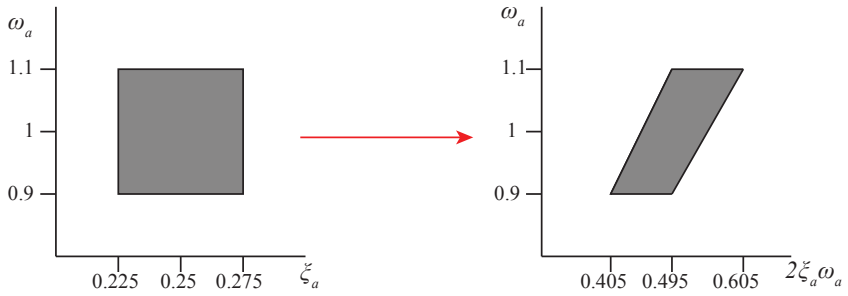

Figure 6.2: Polytopic uncertainty of exogenous disturbance parameters

$\{\omega_a, \zeta_a\}$ make up the polytopic domain. For this example, there was assumed to be a variance $= \pm\delta/2$ % from the nominal values $\omega_a = 1, \zeta_a = 0.25$ of the disturbance

characteristics, where $\delta \in \{0, 20\}$. This translates to the relationship shown in Figure 6.2. For example, the natural frequency ω_a, at its maximum variance, has values of $\omega_a = [0.9, 1.1]$. In the same respect the damping ratio has values $\zeta_a = [0.225, 0.275]$ at its maximum variance $\pm 10\%$. These two polytopic regions were assumed to vary independently, i.e., ω_a varies by some $\delta_\omega \in [0, 20]$ and ζ_a varies by some $\delta_\zeta \in \{0, 20\}$. The resulting polytopic region is composed of four vertices composed of the combination of $\{\omega_a + \delta_\omega/2, \omega_a - \delta_\omega/2\} \times \{\zeta_a + \delta_\zeta/2, \zeta_a - \delta_\zeta/2\}$. These vertices are additionally shown on the left hand side of Figure 6.2. The right hand of Figure 6.2 shows the transformed space of ω_a vs. $2\zeta_a\omega_a$, i.e., the polytopic region described by A_A.

Using values of δ_ω and δ_ζ of 5,10,15,20 %, the procedure described in Section 6.3.1 could be run and optimal γ values could be found. This value was then nominalized by γ_0 the performance of the regenerative controller when $\{\delta_\omega, \delta_\zeta\} = \{0, 0\}$. This manifests itself in the ratio

$$\gamma_R = \frac{\gamma(\delta_\omega, \delta_\zeta)}{\gamma(0, 0)} \tag{6.65}$$

For each value of δ, the optimization was run and γ_R was found. The result is the table is shown below, which details the amount of uncertainty in each parameter and the resulting γ_R value.

Table 6.1: Performance ratios over different values of uncertainty in the disturbance parameters

δ_{ω_a} \ δ_{ζ_a}	5	10	15	20
5	1.1881	1.2624	1.3461	1.4413
10	1.3605	1.4562	1.5657	1.6923
15	1.5896	1.7181	1.8685	2.0468
20	1.9107	2.0947	2.3174	2.5641

From the table, it is easy to see uncertainty in ω_a produces a much larger per-

formance drop compared to uncertainty in ζ_a. This makes sense, as ω_a is present in all three non-zero terms of A_A and uncertainty in ζ_a is only manifested in the (2,2) term of A_A. Additionally, the performance starts to severely degrade when both parameters have uncertainty larger than 10%. But, for a small δ the performance of the robust controller is comparable (within 20%) with the controller at the nominal values. Therefore, for small enough uncertainty, the regenerative controller is serviceable. It remains to be seen how this compares with the passive case.

CHAPTER 7

Conclusion

7.1 Current Conclusions

Through the last six chapters, the viability and feasibility of a regenerative controller has been explored. To do this, we have compared a regenerative controller with the baseline option, a passive controller. The passive controller represents the cheapest option and also provides energy autonomy. A regenerative controller theoretically provide the energy-autonomy of a passive controller, but with increased performance. The regenerative controller makes use of a local energy supply (battery, supercapacitor, etc.). The regenerative control device can then utilize energy from the local supply at times, and extract energy from the network to replenish the local energy storage at other times. The regenerative control law is constrained such that more energy is extracted from the network than taken from the local energy supply. Regenerative control devices also possess parasitics, which limit the flow of energy from the network into the local energy supply. Therefore, the regenerative controller must outperform a passive controller in the presence of parasitics.

To ensure an accurate, fair comparison, theoretical techniques for optimizing both regenerative and passive control laws have been found. The regenerative control law optimization, through a basis change, is convex and easy to solve using many com-

mercial solvers. Examples have also been shown which demonstrate the degradation in performance in the regenerative control law in the presence of parasitics. The passive control law optimization is non-convex, and requires nonlinear methods to be developed to solve the optimization. To this end, a technique called Iterative Convex OverBounding (ICO) has been proposed and developed to solve nonconvex problems. This technique requires initial feasible points and many iterations to solve, but converges to an optimal solution with little conservatism. This allows for optimal passive and regenerative control laws to be compared over a variety of examples. A study has also been performed to assess the robustness of a regenerative controller under uncertainty in system parameters. Using the ICO algorithm, the performance of a regenerative controller to be assessed over a polytopic region and quadratic stability to be ensured throughout the region.

Throughout the chapters, it has been found that optimal regenerative and passive control laws can be derived. It was also found that the ICO algorithm can solve for an optimal passive control law, and a variation on the ICO technique provided faster and smoother convergence characteristics in some cases. Through numerous examples, the regenerative control law was found to outperform the passive control law in structural applications. This advantage ranges from 10% - 1700%, but remains steady throughout the structural examples. The regenerative control law also showed an advantage when compared to a viscous damper in an automotive application. Therefore, theoretically a regenerative controller is viable in structural and automotive applications as long as parasitics are kept at a reasonable value. Lowering parasitics may be difficult and is dependent on the physical structure of the control device, and therefore may be a topic for future work. However, if parasitics can be brought down a regenerative controller presents a clear performance advantage over

a passive controller. It was also found that uncertainty in disturbance characteristics creates performance degradation ranging from 18-156%, depending on the level of uncertainty.

7.2 Future Work

First and foremost, experimental verification must be done for a regenerative controller. As of now, a hybrid hydraulic actuator is being set up. In order for the effect of the theory developed in this paper to be fully realized, experimental results must be shown. With an experimental setup in place, real data can be seen and the parasitics can be measured. The parasitics represent the main limiting factor of a regenerative controller, and an experimental model can showcase just how large we can expect the parasitic parameters to be.

On this topic, a more complete representation of parasitics may prove itself useful. We have developed a model that captures static and dynamic parasitics, but have no experimental results which showcase the values of the actual parasitic parameters or that our model is correct. A more complete study would give an idea as to the nature of the parasitic parameters, the range we should be considering, and the feasibility of various examples and the regenerative controller as a whole.

Something that is currently being developed is new theory behind optimizing a passive controller. The current solution we have solves for an optimal passive controller without conservatism, but requires a large number of iterations. In some cases, the code takes days and sometimes weeks to run. Finding a way to make the passive control optimization convex, through a small amount of conservatism, would be a great advance. This would allow for more complex examples and networks to be analyzed quickly.

More work can also be done with the ICO algorithm. The ICO algorithm was the last study performed, and it may be advantageous to consider the implications of the two ICO algorithms on the optimal passive control laws from Chapter 4. It may be the case that the passive controller can converge to another local solution, via the new ICO technique, which has a lower cost than that of the controller optimized via the previous technique. The regenerative control advantage may be smaller than originally anticipated. Additionally, work should be done to try to understand the jumps in cost value which are occurring in the cost convergence. Theoretically, these jumps should not occur and have thus far been attributed to precision errors within MatLab. In the future, the numerical robustness of the ICO algorithm must be increased. One suggestion is, rather than using the built in solvers in cvx, implement an interior point method of our own. This would speed up optimization time, and possibly help improve convergence characteristics.

Appendix

Proof of conversion from (4.3-4.4) to (4.5-4.6).

We are given (4.3-4.4). Rewriting A_K, B_K, C_K using

$$\tilde{A} = NA_pM^T + NB_pC_yX + YBC_pM^T + YAX \tag{7.1}$$

$$\tilde{B} = NB_p \tag{7.2}$$

$$\tilde{C} = C_pM^T \tag{7.3}$$

produces the new LMI constraints

$$\begin{bmatrix} M^{-1}\bar{A}^TN^{-T}T_p + T_pN^{-1}\bar{A}M^{-T} & \bullet & \bullet \\ \tilde{B}^{*T}N^{-T}T_p & -\epsilon I & \bullet \\ C_p - \tilde{C}M^{-T} & D_p & -\epsilon I \end{bmatrix} < 0 \tag{7.4}$$

$$\begin{bmatrix} M^{-1}\bar{A}^TN^{-T}W_p + W_pN^{-1}\bar{A}M^{-T} & \bullet \\ \tilde{B}^{*T}N^{-T}W_p + C_p & D_p^T + D_p \end{bmatrix} < 0 \tag{7.5}$$

Define M_p =diag$\{M, I, I\}$, and pre and post-multiply the above by M_p, which yields

$$\begin{bmatrix} \bar{A}^T N^{-T} T_p M^T + M T_p N^{-1} \bar{A} & \bullet & \bullet \\ \tilde{B}^{*T} N^{-T} T_p M^T & -\epsilon I & \bullet \\ C_p - \tilde{C} & D_p & -\epsilon I \end{bmatrix} < 0 \tag{7.6}$$

$$\begin{bmatrix} \bar{A}^T N^{-T} W_p M^T + M W_p N^{-1} \bar{A} & \bullet \\ \tilde{B}^{*T} N^{-T} W_p M^T + C_p M^T & D_p^T + D_p \end{bmatrix} < 0 \tag{7.7}$$

Next, redefine $\tilde{T}_p = N^T T_p N$, $\tilde{W}_p = N^T W_p N$ and set $G = N M^T = I - YX$ which yields

$$\begin{bmatrix} \bar{A}^T \tilde{T}_p G + G^T \tilde{T}_p \bar{A} & \bullet & \bullet \\ \tilde{B}^{*T} \tilde{T}_p G & -\epsilon I & \bullet \\ \tilde{C}_p - \tilde{C}^* & \tilde{D}_p & -\epsilon I \end{bmatrix} < 0 \tag{7.8}$$

$$\begin{bmatrix} \bar{A}^T \tilde{W}_p G + G^T \tilde{W}_p \bar{A} & \bullet \\ \tilde{B}^{*T} \tilde{W}_p G + \tilde{C}_p & \tilde{D}_p^T + \tilde{D}_p \end{bmatrix} < 0 \tag{7.9}$$

Proof of Redefined Variables in (4.16)**,** (4.21)**,** (4.13)

Eliminating the controller basis

We first change to the basis-independent optimization variables from [87], we have that in the optimization domain $\{\tilde{A}, \tilde{B}, \tilde{C}, \tilde{D}, X, Y\}$ we would like to minimize

$\gamma = \text{tr}\{Q\}$, subject to

$$\begin{bmatrix} AX + XA^T + B\tilde{C} + (B\tilde{C})^T & \tilde{A}^T + (A + B\tilde{D}B^T) & B_w \\ \tilde{A} + (A + B\tilde{D}B^T)^T & A^TY + YA + \tilde{B}B^T + (\tilde{B}B^T)^T & YB_w \\ B_w^T & (YB_w)^T & -I \end{bmatrix} < 0 \tag{7.10}$$

$$\begin{bmatrix} X & I & (C_zX + D_z\tilde{C})^T \\ I & Y & (C_z + D_z\tilde{D}B^T)^T \\ C_zX + D_z\tilde{C} & C_z + D_z\tilde{D}B^T & Q \end{bmatrix} > 0 \tag{7.11}$$

$$\begin{bmatrix} A_p^TW_p + W_pA_p & W_pB_p + C_p^T \\ B_p^TW_p + C_p & D_p^T + D_p \end{bmatrix} < 0 \tag{7.12}$$

From a previous section, we know the controller variables $\{A_K, B_K, C_K, D_K\}$ are related to the optimization domain through

$$D_p = \tilde{D} \tag{7.13}$$

$$C_p = (\tilde{C} - D_pB^TX)M^{-T} \tag{7.14}$$

$$B_p = N^{-1}(\tilde{B} - YBD_p) \tag{7.15}$$

$$\begin{aligned} A_p &= N^{-1}(\tilde{A} - NB_pB^TX - YBC_pM^T - Y(A + BD_pB^T)X)M^{-T} \\ &= N^{-1}(\tilde{A} - YAX - \tilde{B}B^TX - YB\tilde{C} + YBD_pB^TX)M^{-T} \end{aligned} \tag{7.16}$$

and where N and M can be any matrices satisfying

$$MN^T = I - XY \tag{7.17}$$

Different solutions result in different state-space realizations of the same controller. Substituting the above into (7.12) gives the SPR LMI in terms of the optimization domain variables, together with M, N, and W_p, as

(7.18)
$$\begin{bmatrix} \begin{pmatrix} M^{-1}(\tilde{A} - YAX - \tilde{B}B^TX - YB\tilde{C} + YB\tilde{D}B^TX)^TN^{-T}W_p \\ +W_pN^{-1}(\tilde{A} - YAX - \tilde{B}B^TX - YB\tilde{C} + YB\tilde{D}B^TX)M^{-T} \end{pmatrix} & \begin{pmatrix} W_pN^{-1}(\tilde{B} - YB\tilde{D}) \\ +M^{-1}(\tilde{C} - \tilde{D}B^TX)^T \end{pmatrix} \\ (\tilde{B} - YB\tilde{D})^TN^{-T}W_p + (\tilde{C} - \tilde{D}B^TX)M^{-T} & \tilde{D}^T + \tilde{D} \end{bmatrix} < 0$$

Premultiplying by $\begin{bmatrix} M & 0 \\ 0 & I \end{bmatrix}$ and postmultiplying by $\begin{bmatrix} M^T & 0 \\ 0 & I \end{bmatrix}$ gives the equivalent condition

(7.19)
$$\begin{bmatrix} \begin{pmatrix} (\tilde{A} - YAX - \tilde{B}B^TX - YB\tilde{C} + YB\tilde{D}B^TX)^TN^{-T}W_pM^T \\ +MW_pN^{-1}(\tilde{A} - YAX - \tilde{B}B^TX - YB\tilde{C} + YB\tilde{D}B^TX) \end{pmatrix} & \begin{pmatrix} MW_pN^{-1}(\tilde{B} - YB\tilde{D}) \\ +(\tilde{C} - \tilde{D}B^TX)^T \end{pmatrix} \\ (\tilde{B} - YB\tilde{D})^TN^{-T}W_pM^T + (\tilde{C} - \tilde{D}B^TX) & \tilde{D}^T + \tilde{D} \end{bmatrix} < 0$$

Define $P = N^{-T}W_pN^{-1}$ and, noting that $MW_pN^{-1} = (I - XY)P$, we eliminate M and N from the condition, we redefine our LMI in terms of our optimization variables

$\{\tilde{A}, \tilde{B}, \tilde{C}, \tilde{D}, X, Y, P\}$, as

(7.20)
$$\begin{bmatrix} \begin{pmatrix} (\tilde{A} - YAX - \tilde{B}B^TX - YB\tilde{C} + YB\tilde{D}B^TX)^TP(I - YX) \\ +(I - XY)P(\tilde{A} - YAX - \tilde{B}B^TX - YB\tilde{C} + YB\tilde{D}B^TX) \end{pmatrix} & \begin{pmatrix} (I - XY)P(\tilde{B} - YB\tilde{D}) \\ +(\tilde{C} - \tilde{D}B^TX)^T \end{pmatrix} \\ (\tilde{B} - YB\tilde{D})^TP(I - YX) + (\tilde{C} - \tilde{D}B^TX) & \tilde{D}^T + \tilde{D} \end{bmatrix} < 0$$

Let $Z = Y^{-1}$. Then the three optimization matrix inequalities, (7.10), (7.11), and (7.20) become

(7.21)
$$\begin{bmatrix} AX + XA^T + B\tilde{C} + (B\tilde{C})^T & \tilde{A}^TZ + (AZ + B\tilde{D}B^TZ) & B_w \\ Z\tilde{A} + (AZ + B\tilde{D}B^TZ)^T & ZA^T + AZ + Z\tilde{B}B^TZ + (Z\tilde{B}B^TZ)^T & B_w \\ B_w^T & B_w^T & -I \end{bmatrix} < 0$$

(7.22)
$$\begin{bmatrix} X & Z & (CX + D\tilde{C})^T \\ Z & Z & (CZ + D\tilde{D}B^TZ)^T \\ CX + D\tilde{C} & CZ + D\tilde{D}B^TZ & Q \end{bmatrix} > 0$$

(7.23)
$$\begin{bmatrix} \begin{pmatrix} (Z\tilde{A} - AX - Z\tilde{B}B^TX - B\tilde{C} + B\tilde{D}B^TX)^TYPY(Z - X) \\ +(Z - X)YPY(Z\tilde{A} - AX - Z\tilde{B}B^TX - B\tilde{C} + B\tilde{D}B^TX) \end{pmatrix} & \begin{pmatrix} (Z - X)YPY(Z\tilde{B} - B\tilde{D}) \\ +(\tilde{C} - \tilde{D}B^TX)^T \end{pmatrix} \\ (Z\tilde{B} - B\tilde{D})^TYPY(Z - X) + (\tilde{C} - \tilde{D}B^TX) & \tilde{D}^T + \tilde{D} \end{bmatrix} < 0$$

So if we redefine $\tilde{A} \leftarrow Z\tilde{A}$, $\tilde{B} \leftarrow Z\tilde{B}$, $P \leftarrow YPY$ and $\Theta = B_w B_w^T$ then, the above are reformulated as

(7.24)

$$\begin{bmatrix} \Theta + AX + XA^T + B\tilde{C} + (B\tilde{C})^T & \Theta + \tilde{A}^T + (AZ + B\tilde{D}B^T Z) \\ \Theta + \tilde{A} + (AZ + B\tilde{D}B^T Z)^T & \Theta + ZA^T + AZ + \tilde{B}B^T Z + (\tilde{B}B^T Z)^T \end{bmatrix} < 0$$

(7.25)

$$\begin{bmatrix} X & Z & (CX + D\tilde{C})^T \\ Z & Z & (CZ + D\tilde{D}B^T Z)^T \\ CX + D\tilde{C} & CZ + D\tilde{D}B^T Z & Q \end{bmatrix} > 0$$

(7.26)

$$\begin{bmatrix} \begin{pmatrix} (\tilde{A} - AX - \tilde{B}B^T X - B\tilde{C} + B\tilde{D}B^T X)^T P(Z - X) \\ +(Z - X)P(\tilde{A} - AX - \tilde{B}B^T X - B\tilde{C} + B\tilde{D}B^T X) \end{pmatrix} & \begin{pmatrix} (Z - X)P(\tilde{B} - B\tilde{D}) \\ +(\tilde{C} - \tilde{D}B^T X)^T \end{pmatrix} \\ (\tilde{B} - B\tilde{D})^T P(Z - X) + (\tilde{C} - \tilde{D}B^T X) & \tilde{D}^T + \tilde{D} \end{bmatrix} < 0$$

where we have used a Schur complement in the first LMI.

All three matrix inequalities above are nonlinear. In the following subsections, we create (convex) over-bounding LMIs for each of these, which are linearized about $\{\tilde{A}_0, \tilde{B}_0, \tilde{C}_0, \tilde{D}_0, X_0, Z_0, P_0\}$. (Note that no linearization is necessary in the Q variable, which already participates linearly. Through the analysis, the following definition will make the notation a lot more concise.

Convexification of (4.10)-(4.12)

Inequality (4.10)

Matrix inequality (4.10) is currently bilinear in variables Z, $\tilde{B}$, and $\tilde{D}$. First, we isolate the bilinear terms:

$$0 > \begin{bmatrix} \Theta + AX + XA^T + B\tilde{C} + (B\tilde{C})^T & \Theta + \tilde{A}^T + (AZ + B\tilde{D}B^TZ) \\ \Theta + \tilde{A} + (AZ + B\tilde{D}B^TZ)^T & \Theta + ZA^T + AZ + \tilde{B}B^TZ + (\tilde{B}B^TZ)^T \end{bmatrix}$$

$$= \begin{bmatrix} \Theta + AX + XA^T + B\tilde{C} + \tilde{C}^TB^T & \Theta + \tilde{A}^T + AZ \\ \Theta + \tilde{A} + ZA^T & \Theta + ZA^T + AZ \end{bmatrix} + \begin{bmatrix} 0 \\ ZB \end{bmatrix} \begin{bmatrix} B\tilde{D} \\ \tilde{B} \end{bmatrix}^T + \begin{bmatrix} B\tilde{D} \\ \tilde{B} \end{bmatrix} \begin{bmatrix} 0 \\ ZB \end{bmatrix}^T$$

Referencing the inequality to design point $\{Z_0, \tilde{B}_0, \tilde{D}_0\}$ gives

$$0 > \begin{bmatrix} \Theta + AX + XA^T + +B\tilde{C} + \tilde{C}^TB^T & \Theta + \tilde{A}^T + AZ \\ \Theta + \tilde{A} + ZA^T & \Theta + ZA^T + AZ \end{bmatrix} + \mathcal{G}_0 \left(\begin{bmatrix} 0 \\ ZB \end{bmatrix}, \begin{bmatrix} B\tilde{D} \\ \tilde{B} \end{bmatrix} \right)$$

$$+ \begin{bmatrix} 0 \\ (Z - Z_0)B \end{bmatrix} \begin{bmatrix} B(\tilde{D} - \tilde{D}_0) \\ (\tilde{B} - \tilde{B}_0) \end{bmatrix}^T + \begin{bmatrix} B(\tilde{D} - \tilde{D}_0) \\ (\tilde{B} - \tilde{B}_0) \end{bmatrix} \begin{bmatrix} 0 \\ (Z - Z_0)B \end{bmatrix}^T$$

where

$$\mathcal{G}_0(Q, R) = Q_0R^T + RQ_0^T + QR_0^T + R_0Q^T - Q_0R_0^T - R_0Q_0^T \tag{7.27}$$

Next, we use the convexification algorithm to introduce a weighting matrix W_1 such that our constraint is now

(7.28)

$$0 > \begin{bmatrix} \Theta + AX + XA^T + +B\tilde{C} + \tilde{C}^T B^T & \Theta + \tilde{A}^T + AZ \\ \Theta + \tilde{A} + ZA^T & \Theta + ZA^T + AZ \end{bmatrix} + \mathcal{G}_0 \left(\begin{bmatrix} 0 \\ ZB \end{bmatrix}, \begin{bmatrix} B\tilde{D} \\ \tilde{B} \end{bmatrix} \right) + \begin{bmatrix} 0 \\ (Z - Z_0)B \end{bmatrix} W_1 \begin{bmatrix} 0 \\ (Z - Z_0)B \end{bmatrix}^T + \begin{bmatrix} B(\tilde{D} - \tilde{D}_0) \\ (\tilde{B} - \tilde{B}_0) \end{bmatrix} W_1^{-1} \begin{bmatrix} B(\tilde{D} - \tilde{D}_0) \\ (\tilde{B} - \tilde{B}_0) \end{bmatrix}^T$$

we have, through Schur complements, the conservative LMI

(7.29)

$$\begin{bmatrix} \left(\begin{bmatrix} \Theta + AX + XA^T + +B\tilde{C} + \tilde{C}^T B^T & \Theta + \tilde{A}^T + AZ \\ \Theta + \tilde{A} + ZA^T & \Theta + ZA^T + AZ \end{bmatrix} + \mathcal{G}_k \left(\begin{bmatrix} 0 \\ ZB \end{bmatrix}, \begin{bmatrix} B\tilde{D} \\ \tilde{B} \end{bmatrix} \right) \right) & \begin{bmatrix} 0 \\ (Z - Z_0)B \end{bmatrix} & \begin{bmatrix} B(\tilde{D} - \tilde{D}_0) \\ \tilde{B} - \tilde{B}_0 \end{bmatrix} \\ \bullet & -W_1^{-1} & 0 \\ \bullet & \bullet & -W_1 \end{bmatrix} < 0$$

We can make W_1 a design variable as well, by recognizing that for $W_1 > 0$,

(7.30)
$$W_1^{-1} > W_{10}^{-1}(2W_{10} - W_1)W_{10}^{-1}$$

Substituting the conservative approximation of W_1^{-1}, which is linear in W_1, we arrive at an LMI in all the unknown variables, which now includes our weighting matrix W_1. We can eliminate the need to invert W_{10} by multiplying the third block row

from the left by W_{10}, and the third block column from the right by W_{10}, to get

(7.31)

$$\begin{bmatrix} \left(\begin{bmatrix} \Theta + AX + XA^T + +B\tilde{C} + \tilde{C}^T B^T & \Theta + \tilde{A}^T + AZ \\ \Theta + \tilde{A} + ZA^T & \Theta + ZA^T + AZ \end{bmatrix} + \mathcal{G}_0 \left(\begin{bmatrix} 0 \\ ZB \end{bmatrix}, \begin{bmatrix} B\tilde{D} \\ \tilde{B} \end{bmatrix} \right) \right) & \begin{bmatrix} 0 \\ (Z - Z_0)BW_{10} \end{bmatrix} & \begin{bmatrix} B(\tilde{D} - \tilde{D}_0) \\ \tilde{B} - \tilde{B}_0 \end{bmatrix} \\ * & -2W_{10} + W_1 & 0 \\ * & * & -W_1 \end{bmatrix} < 0$$

Inequality (4.11)

Convexification of LMI (4.11) is the same as in the previous section We begin by isolating the bilinear terms:

$$0 < \begin{bmatrix} X & Z & (C_z X + D_z \tilde{C})^T \\ Z & Z & ZC_z^T \\ C_z X + D_z \tilde{C} & C_z Z & Q \end{bmatrix} + \begin{bmatrix} 0 \\ 0 \\ D\tilde{D} \end{bmatrix} \begin{bmatrix} 0 \\ ZB \\ 0 \end{bmatrix}^T + \begin{bmatrix} 0 \\ ZB \\ 0 \end{bmatrix} \begin{bmatrix} 0 \\ 0 \\ D\tilde{D} \end{bmatrix}^T$$

Next we reference the above to a design point $\{Z_k, \tilde{D}_k\}$,

$$0 < \begin{bmatrix} X & Z & (C_z X + D_z \tilde{C})^T \\ Z & Z & Z C_z^T \\ C_z X + D_z \tilde{C} & C_z Z & Q \end{bmatrix} + \mathcal{G}_k \left(\begin{bmatrix} 0 \\ ZB \\ 0 \end{bmatrix}, \begin{bmatrix} 0 \\ 0 \\ D\tilde{D} \end{bmatrix} \right)$$
$$+ \begin{bmatrix} 0 \\ 0 \\ D(\tilde{D} - \tilde{D}_0) \end{bmatrix} \begin{bmatrix} 0 \\ (Z - Z_0)B \\ 0 \end{bmatrix}^T + \begin{bmatrix} 0 \\ (Z - Z_0)B \\ 0 \end{bmatrix} \begin{bmatrix} 0 \\ 0 \\ D(\tilde{D} - \tilde{D}_0) \end{bmatrix}^T$$

Next we proceed with the convexification in the same manner as in the previous section with weighting matrix W_2 defined as an optimization variable

$$0 < \begin{bmatrix} \left(\begin{bmatrix} X & Z & (C_z X + D_z \tilde{C})^T \\ Z & Z & Z C_z^T \\ C_z X + D_z \tilde{C} & C_z Z & Q \end{bmatrix} + \mathcal{G}_0 \left(\begin{bmatrix} 0 \\ ZB \\ 0 \end{bmatrix}, \begin{bmatrix} 0 \\ 0 \\ D\tilde{D} \end{bmatrix} \right) \right) & \begin{bmatrix} 0 \\ (Z - Z_0)B \\ 0 \end{bmatrix} & \begin{bmatrix} 0 \\ 0 \\ D(\tilde{D} - \tilde{D}_0) \end{bmatrix} \\ \bullet & W_2 & 0 \\ \bullet & \bullet & W_2^{-1} \end{bmatrix} \tag{7.32}$$

Last, we use the fact that $W_2^{-1} < 2W_{20}^{-1} - W_{20}^{-1}W_2W_{20}^{-1}$ to obtain

(7.33)

$$0 < \begin{bmatrix} \left(\begin{bmatrix} X & Z & (C_zX + D_z\tilde{C})^T \\ Z & Z & ZC_z^T \\ C_zX + D_z\tilde{C} & C_zZ & Q \end{bmatrix} + \mathcal{G}_0 \left(\begin{bmatrix} 0 \\ ZB \\ 0 \end{bmatrix}, \begin{bmatrix} 0 \\ 0 \\ D\tilde{D} \end{bmatrix} \right) \right) & \begin{bmatrix} 0 \\ (Z - Z_0)B \\ 0 \end{bmatrix} & \begin{bmatrix} 0 \\ 0 \\ D(\tilde{D} - \tilde{D}_0)W_{20} \end{bmatrix} \\ * & W_2 & 0 \\ * & * & 2W_{20} - W_2 \end{bmatrix}$$

Inequality (4.12)

Convexification of MI (4.12) is more complicated because it is quadrilinear. Thus, we need to convexify once to get a BMI, and then again to get an LMI. To get the

BMI, we have

$$\begin{bmatrix} \begin{pmatrix} (\tilde{A}-AX-\tilde{B}B^TX-B\tilde{C}+B\tilde{D}B^TX)^TP(Z-X) \\ +(Z-X)P(\tilde{A}-AX-\tilde{B}B^TX-B\tilde{C}+B\tilde{D}B^TX) \end{pmatrix} & \begin{pmatrix} (Z-X)P(\tilde{B}-B\tilde{D}) \\ +(\tilde{C}-\tilde{D}B^TX)^T \end{pmatrix} \\ (\tilde{B}-B\tilde{D})^TP(Z-X)+(\tilde{C}-\tilde{D}B^TX) & \tilde{D}^T+\tilde{D} \end{bmatrix}$$

$$= \begin{bmatrix} 0 & \tilde{C}^T \\ \tilde{C} & \tilde{D}+\tilde{D}^T \end{bmatrix} + \begin{bmatrix} 0 \\ -\tilde{D} \end{bmatrix} \begin{bmatrix} XB \\ 0 \end{bmatrix}^T + \begin{bmatrix} XB \\ 0 \end{bmatrix} \begin{bmatrix} 0 \\ -\tilde{D} \end{bmatrix}^T$$

$$+ \begin{bmatrix} (Z-X)P \\ 0 \end{bmatrix} \begin{bmatrix} \tilde{A}^T-XA^T-\tilde{C}^TB^T-XB(\tilde{B}-B\tilde{D})^T \\ (\tilde{B}-B\tilde{D})^T \end{bmatrix}^T$$

$$+ \begin{bmatrix} \tilde{A}^T-XA^T-\tilde{C}^TB^T-XB(\tilde{B}-B\tilde{D})^T \\ (\tilde{B}-B\tilde{D})^T \end{bmatrix} \begin{bmatrix} (Z-X)P \\ 0 \end{bmatrix}^T < 0$$

Following the convexification process as before, we get that the above is satisfied if

(7.34)

$$\begin{bmatrix} \begin{bmatrix} 0 & \tilde{C}^T \\ \tilde{C} & \tilde{D}+\tilde{D}^T \end{bmatrix} + \begin{bmatrix} 0 \\ -\tilde{D} \end{bmatrix} \begin{bmatrix} XB \\ 0 \end{bmatrix}^T + \begin{bmatrix} XB \\ 0 \end{bmatrix} \begin{bmatrix} 0 \\ -\tilde{D} \end{bmatrix}^T + R & * & * \\ \begin{bmatrix} P(Z-X)-P_k(Z_0-X_0) & 0 \end{bmatrix} & -W_3^{-1} & * \\ \begin{bmatrix} \begin{pmatrix} \tilde{A}-\tilde{A}_0-A(X-X_0)-B(\tilde{C}-\tilde{C}_0) \\ -(\tilde{B}-B\tilde{D})B^TX+(\tilde{B}_0-B\tilde{D}_0)B^TX_0 \end{pmatrix} & (\tilde{B}-B\tilde{D})-(\tilde{B}_0-B\tilde{D}_0) \end{bmatrix} & 0 & -W_3 \end{bmatrix} < 0$$

which is a BMI, where

$$
\begin{aligned}
R = \mathcal{G}_k \left(\begin{bmatrix} (Z-X)P \\ \\ 0 \end{bmatrix}, \begin{bmatrix} \tilde{A}^T - XA^T - \tilde{C}^T B^T - XB(\tilde{B} - B\tilde{D})^T \\ \\ (\tilde{B} - B\tilde{D})^T \end{bmatrix} \right) \\
= \begin{bmatrix} (Z-X)P \\ \\ 0 \end{bmatrix} \begin{bmatrix} \tilde{A}_0^T - X_0 A^T - \tilde{C}_0^T B^T - X_0 B(\tilde{B}_0 - B\tilde{D}_0)^T \\ \\ (\tilde{B}_0 - B\tilde{D}_0)^T \end{bmatrix}^T \\
+ \begin{bmatrix} \tilde{A}_0^T - X_0 A^T - \tilde{C}_0^T B^T - X_0 B(\tilde{B}_0 - B\tilde{D}_0)^T \\ \\ (\tilde{B}_0 - B\tilde{D}_0)^T \end{bmatrix} \begin{bmatrix} P(Z-X) & 0 \end{bmatrix} \\
+ \begin{bmatrix} (Z_0 - X_0)P_0 \\ \\ 0 \end{bmatrix} \begin{bmatrix} \tilde{A} - AX - B\tilde{C} - (\tilde{B} - B\tilde{D})B^T X & (\tilde{B} - B\tilde{D}) \end{bmatrix} \\
+ \begin{bmatrix} \tilde{A}^T - XA^T - \tilde{C}^T B^T - XB(\tilde{B} - B\tilde{D})^T \\ \\ (\tilde{B} - B\tilde{D})^T \end{bmatrix} \begin{bmatrix} (Z_0 - X_0)P_0 \\ \\ 0 \end{bmatrix}^T \\
- \begin{bmatrix} (Z_0 - X_0)P_0 \\ \\ 0 \end{bmatrix} \begin{bmatrix} \tilde{A}_0^T - X_0 A^T - \tilde{C}_0^T B^T - X_0 B(\tilde{B}_0 - B\tilde{D}_0)^T \\ \\ (\tilde{B}_0 - B\tilde{D}_0)^T \end{bmatrix}^T \\
- \begin{bmatrix} \tilde{A}_0^T - X_0 A^T - \tilde{C}_0^T B^T - X_0 B(\tilde{B}_0 - B\tilde{D}_0)^T \\ \\ (\tilde{B}_0 - B\tilde{D}_0)^T \end{bmatrix} \begin{bmatrix} (Z_0 - X_0)P_0 \\ \\ 0 \end{bmatrix}^T
\end{aligned}
$$

Define

$$T_k = (\tilde{B}_0 - B\tilde{D}_0)^T \tag{7.35}$$

$$U_k = (Z_0 - X_0)P_0 \tag{7.36}$$

$$V_k = \tilde{A}_0^T - X_0 A^T - \tilde{C}_0^T B^T - X_0 B T_0 \tag{7.37}$$

Then

$$
\begin{aligned}
R = &\begin{bmatrix} I \\ \\ 0 \end{bmatrix} (Z-X)P \begin{bmatrix} V_0^T & T_0^T \end{bmatrix} + \begin{bmatrix} V_0 \\ \\ T_0 \end{bmatrix} P(Z-X) \begin{bmatrix} I & 0 \end{bmatrix} \\
&+ \begin{bmatrix} I \\ \\ 0 \end{bmatrix} U_k \begin{bmatrix} \tilde{A} - AX - B\tilde{C} - (\tilde{B} - B\tilde{D})B^T X & (\tilde{B} - B\tilde{D}) \end{bmatrix} \\
&+ \begin{bmatrix} \tilde{A}^T - XA^T - \tilde{C}^T B^T - XB(\tilde{B} - B\tilde{D})^T \\ \\ (\tilde{B} - B\tilde{D})^T \end{bmatrix} U_0^T \begin{bmatrix} I & 0 \end{bmatrix} \\
&- \begin{bmatrix} I \\ \\ 0 \end{bmatrix} U_0 \begin{bmatrix} V_0^T & T_0^T \end{bmatrix} - \begin{bmatrix} V_0 \\ \\ T_0 \end{bmatrix} U_0 \begin{bmatrix} I & 0 \end{bmatrix} \\
= &\begin{bmatrix} U_0(\tilde{A} - AX - B\tilde{C}) + (\tilde{A} - AX - B\tilde{C})^T U_0^T & U_0(\tilde{B} - B\tilde{D}) \\ \\ (\tilde{B} - B\tilde{D})^T U_0^T & 0 \end{bmatrix} - \begin{bmatrix} I \\ \\ 0 \end{bmatrix} U_0 \begin{bmatrix} V_0^T & T_0^T \end{bmatrix} - \\
&\begin{bmatrix} V_0 \\ \\ T_0 \end{bmatrix} U_0^T \begin{bmatrix} I & 0 \end{bmatrix} + \begin{bmatrix} I \\ \\ 0 \end{bmatrix} (Z-X)P \begin{bmatrix} V_0^T & T_0^T \end{bmatrix} + \begin{bmatrix} V_0 \\ \\ T_0 \end{bmatrix} P(Z-X) \begin{bmatrix} I & 0 \end{bmatrix} \\
&+ \begin{bmatrix} -XB \\ \\ 0 \end{bmatrix} (\tilde{B} - B\tilde{D})^T U_0^T \begin{bmatrix} I & 0 \end{bmatrix} + \begin{bmatrix} I \\ \\ 0 \end{bmatrix} U_0(\tilde{B} - B\tilde{D}) \begin{bmatrix} -B^T X & 0 \end{bmatrix}
\end{aligned}
$$

The entire term (1,1) of the BMI is thus

$$\begin{bmatrix} U_0(\tilde{A}-AX-B\tilde{C})+(\tilde{A}-AX-B\tilde{C})^TU_0^T & \tilde{C}^T+U_0(\tilde{B}-B\tilde{D}) \\ \tilde{C}+(\tilde{B}-B\tilde{D})^TU_0^T & \tilde{D}+\tilde{D}^T \end{bmatrix}$$
$$- \begin{bmatrix} I \\ \\ 0 \end{bmatrix} U_0 \begin{bmatrix} V_0^T & T_0^T \end{bmatrix} - \begin{bmatrix} V_0 \\ \\ T_0 \end{bmatrix} U_0^T \begin{bmatrix} I & 0 \end{bmatrix}$$
$$+ \begin{bmatrix} I \\ \\ 0 \end{bmatrix} (Z-X)P \begin{bmatrix} V_0^T & T_0^T \end{bmatrix} + \begin{bmatrix} V_0 \\ \\ T_0 \end{bmatrix} P(Z-X) \begin{bmatrix} I & 0 \end{bmatrix}$$
$$+ \begin{bmatrix} -XB \\ \\ 0 \end{bmatrix} \begin{bmatrix} (\tilde{B}-B\tilde{D})^TU_0^T & \tilde{D}^T \end{bmatrix} + \begin{bmatrix} U_0(\tilde{B}-B\tilde{D}) \\ \\ \tilde{D} \end{bmatrix} \begin{bmatrix} -B^TX & 0 \end{bmatrix}$$

where we notice that the first line is linear, while the second and third lines are bilinear. The overall matrix inequality is therefore

$$
0 > \begin{bmatrix}
U_0(\tilde{A} - AX - B\tilde{C} - V_0^T) + (\tilde{A} - AX - B\tilde{C} - V_0)^T U_0^T & * & * & * \\
\tilde{C} + (\tilde{B} - B\tilde{D} - T_0^T)^T U_0^T & \tilde{D} + \tilde{D}^T & * & * \\
-U_0^T & 0 & -W_3^{-1} & * \\
\tilde{A} - AX - B\tilde{C} - V_0^T & \tilde{B} - B\tilde{D} - T_0^T & 0 & -W_3
\end{bmatrix}
$$

$$
+ \begin{bmatrix} -XB \\ 0 \\ 0 \\ 0 \end{bmatrix} \begin{bmatrix} U_0(\tilde{B} - B\tilde{D}) \\ \tilde{D} \\ 0 \\ \tilde{B} - B\tilde{D} \end{bmatrix}^T + \begin{bmatrix} U_0(\tilde{B} - B\tilde{D}) \\ \tilde{D} \\ 0 \\ \tilde{B} - B\tilde{D} \end{bmatrix} \begin{bmatrix} -XB \\ 0 \\ 0 \\ 0 \end{bmatrix}^T
$$

$$
+ \begin{bmatrix} V_0P \\ T_0P \\ P \\ 0 \end{bmatrix} \begin{bmatrix} Z - X \\ 0 \\ 0 \\ 0 \end{bmatrix}^T + \begin{bmatrix} Z - X \\ 0 \\ 0 \\ 0 \end{bmatrix} \begin{bmatrix} V_0P \\ T_0P \\ P \\ 0 \end{bmatrix}^T
$$

So the BMI is conservatively satisfied by the following inequality

(7.38)

$$
\begin{aligned}
0 > &\begin{bmatrix}
\begin{pmatrix} U_0(\tilde{A} - AX - B\tilde{C} - V_0^T) \\ +(\tilde{A} - AX - B\tilde{C} - V_0)^T U_0^T \end{pmatrix} & * & * & * \\
\tilde{C} + (\tilde{B} - B\tilde{D} - T_0^T)^T U_0^T & \tilde{D} + \tilde{D}^T & * & * \\
-U_0^T & 0 & -W_3^{-1} & * \\
\tilde{A} - AX - B\tilde{C} - V_0^T & \tilde{B} - B\tilde{D} - T_0^T & 0 & -W_3
\end{bmatrix} \\
&+ \mathcal{G}_0\left(\begin{bmatrix} U_0(\tilde{B} - B\tilde{D}) \\ \tilde{D} \\ 0 \\ \tilde{B} - B\tilde{D} \end{bmatrix}, \begin{bmatrix} -XB \\ 0 \\ 0 \\ 0 \end{bmatrix}\right) + \mathcal{G}_0\left(\begin{bmatrix} V_0 P \\ T_0 P \\ P \\ 0 \end{bmatrix}, \begin{bmatrix} Z - X \\ 0 \\ 0 \\ 0 \end{bmatrix}\right) \\
&+ \begin{bmatrix} (X - X_0)B \\ 0 \\ 0 \\ 0 \end{bmatrix} W_4 \begin{bmatrix} (X - X_0)B \\ 0 \\ 0 \\ 0 \end{bmatrix}^T + \begin{bmatrix} U_0(\tilde{B} - B\tilde{D} - T_0^T) \\ \tilde{D} - \tilde{D}_0 \\ 0 \\ \tilde{B} - B\tilde{D} - T_0^T \end{bmatrix} W_4^{-1} \begin{bmatrix} U_0(\tilde{B} - B\tilde{D} - T_0^T) \\ \tilde{D} - \tilde{D}_0 \\ 0 \\ \tilde{B} - B\tilde{D} - T_0^T \end{bmatrix}^T \\
&+ \begin{bmatrix} (Z - X) - (Z_0 - X_0) \\ 0 \\ 0 \\ 0 \end{bmatrix} W_5 \begin{bmatrix} (Z - X) - (Z_0 - X_0) \\ 0 \\ 0 \\ 0 \end{bmatrix}^T + \begin{bmatrix} V_0(P - P_0) \\ T_0(P - P_0) \\ (P - P_0) \\ 0 \end{bmatrix} W_5^{-1} \begin{bmatrix} V_0(P - P_0) \\ T_0(P - P_0) \\ (P - P_0) \\ 0 \end{bmatrix}^T
\end{aligned}
$$

Derivation of $\alpha_k, \beta_k, \gamma_k$ values in (5.17)

We assume our optimization cost fits the exponential curve:

$$\hat{\gamma}(i) = \gamma_k\big((1 - \alpha_k) + \alpha_k e^{-\beta_k(i-k)}\big)$$

Where k is the present point of the iteration, i is an iteration time index for our curve, and $\alpha_k, \beta_k, \gamma_k$ are the variables we wish to find. We compute a Least Squares Solution

$$g_k = \int_{-\infty}^{\infty} (\gamma_{k-p} - \hat{\gamma}_{k-p})^2 \tag{7.39}$$

Our new index for $\hat{\gamma}$ is $(k - p)$ instead of i. This alters $\hat{\gamma}(i)$ to:

$$\hat{\gamma}(k-p) = \gamma_k\big((1-\alpha_k) + \alpha_k e^{-\beta_k(k-p-k)}\big)$$

$$= \gamma_k\big((1-\alpha_k) + \alpha_k e^{\beta_k p}\big)$$

Taking the partial of g_k with respect to α_k and β_k, the following two partial derivatives must be minimized. We also redefine $\bar{\gamma}_{k-p} = \frac{\gamma_{k-p}}{\gamma_k}$.

$$\frac{\delta g_k}{\delta \alpha_k} = 2\int_{-\infty}^{\infty}(\gamma_{k-p} - \hat{\gamma}_{k-p})\frac{\delta \hat{\gamma}_k}{\delta \alpha_k} \tag{7.40}$$

$$= 2\textstyle\int_{-\infty}^{\infty}(\gamma_{k-p} - \hat{\gamma}_{k-p})(-\gamma_k + \gamma_k e^{\beta_k p})$$

$$= 2\textstyle\int_{-\infty}^{\infty}(\gamma_{k-p} - \gamma_k\big((1-\alpha_k) + \alpha_k e^{\beta_k p}\big))(-\gamma_k + \gamma_k e^{\beta_k p})$$

$$= 2\textstyle\int_{-\infty}^{\infty}(\bar{\gamma}_{k-p} - \big((1-\alpha_k) + \alpha_k e^{\beta_k p}\big))(-1 + e^{\beta_k p})$$

And our second partial derivative:

$$\frac{\delta g_k}{\delta \beta_k} = 2\int_{-\infty}^{\infty}(\gamma_{k-p} - \hat{\gamma}_{k-p})\frac{\delta \hat{\gamma}_k}{\delta \beta_k} \tag{7.41}$$

$$= 2\textstyle\int_{-\infty}^{\infty}(\gamma_{k-p} - \gamma_k\big((1-\alpha_k) + \alpha_k e^{\beta_k p}\big))(\gamma_k \alpha_k p e^{\beta_k p})$$

$$= 2\textstyle\int_{-\infty}^{\infty}(\bar{\gamma}_{k-p} - \big((1-\alpha_k) + \alpha_k e^{\beta_k p}\big))\alpha_k p e^{\beta_k p}$$

We would like to solve for α_k in terms of β_k in both equations. In $\frac{\delta g_k}{\delta \alpha_k}$, it can be shown:

$$\textstyle\int_{-\infty}^{\infty}(1-\bar{\gamma}_{k-p})(1-e^{\beta_k p}) = \left[\int_{-\infty}^{\infty}(1-e^{\beta_k p})^2\right]\alpha_k$$

$$\Rightarrow \alpha_k = \left[\int_{-\infty}^{\infty}(1-e^{\beta_k p})^2\right]^{-1}\int_{-\infty}^{\infty}(1-\bar{\gamma}_{k-p})(1-e^{\beta_k p}) \tag{7.42}$$

In the same respect, solving α_k in terms of β_k in $\frac{\delta g_k}{\delta \alpha_k}$ can be computed as:

$$\int_{-\infty}^{\infty}(1-\bar{\gamma}_{k-p})pe^{\beta_k p} = \left[\int_{-\infty}^{\infty}(1-e^{\beta_k p})pe^{\beta_k p}\right]\alpha_k \tag{7.43}$$

Subbing in 7.42 into 7.43, we come to the equation:

$$\int_{-\infty}^{\infty}(1-\bar{\gamma}_{k-p})pe^{\beta_k p} = \left[\int_{-\infty}^{\infty}(1-e^{\beta_k p})pe^{\beta_k p}\right]\left[\int_{-\infty}^{\infty}(1-e^{\beta_k p})^2\right]^{-1}\int_{-\infty}^{\infty}(1-\bar{\gamma}_{k-p})(1-e^{\beta_k p})$$

Or

(7.44)
$$0 = \left[\int_{-\infty}^{\infty}(1-e^{\beta_k p})pe^{\beta_k p}\right]\left[\int_{-\infty}^{\infty}(1-e^{\beta_k p})^2\right]^{-1}\int_{-\infty}^{\infty}(1-\bar{\gamma}_{k-p})(1-e^{\beta_k p})-\int_{-\infty}^{\infty}(1-\bar{\gamma}_{k-p})pe^{\beta_k p}$$

Redefining $\theta = e^{-\beta_k}$, the above equation can be simplified to:

(7.45)
$$0 = \left[\int_{-\infty}^{\infty}(1-\theta^{-p})p\theta^{-p}\right]\left[\int_{-\infty}^{\infty}(1-\theta^{-p})^2\right]^{-1}\int_{-\infty}^{\infty}(1-\bar{\gamma}_{k-p})(1-\theta^{-p})-\int_{-\infty}^{\infty}(1-\bar{\gamma}_{k-p})p\theta^{-p}$$

(7.46)
$$\Rightarrow \alpha_k = \left[\int_{-\infty}^{\infty}(1-\theta^{-p})^2\right]^{-1}\int_{-\infty}^{\infty}(1-\bar{\gamma}_{k-p})(1-\theta^{-p})$$

Brune Synthesis

When considering the practicality of a passive controller, one must consider the hardware specifications associated with installation. A passive configuration which creates extremely complicated network realizations proves problematic for a number of reasons. A complicated network is difficult to install and proves challenging to alter if the parameters of the network or disturbance change. Additionally, with so many mechanical components (springs, masses, inertial elements, levers), complete accuracy cannot be guaranteed. There will be rounding errors, errors in installation and construction, and others which will all prove the network realization suboptimal. These errors, while small for individual components, compound when many passive components are used.

Consider a passive controller which is realized via a strictly positive real (SPR) transfer function More specifically, the transfer function for an optimal passive controller where the performance output is the relative displacement and the control

force with a coefficient of one is considered, the passive controller in Figure 4.2c. Since the controller is assumed to be the same order of the plant, this translates to an eighth order transfer function. Additionally, since the controller is passive, there is guaranteed to be a set of mechanical components which can realize the passive transfer function [15]. In order to realize the network, one such decomposition method (Brune Synthesis [11]) is utilized. Once the impedance transfer function has been completely decomposed, the transfer function can be realized via positive inductors, resistors, capacitors, and transformers. This translates to springs, dampers, inerters, and levers, respectively, in a mechanical context. Shown in the coming section is an explanation of Brune Synthesis and the steps required to decompose a transfer function and an explination fo the resulting realization from the transfer function in Figure 4.2c.

Table 7.1: Electrical-Mechanical Relationship Between Components

Mechanical Comp.	**Force Relationship**	**Current Relationship**	**Electrical Comp.**
Spring	$\frac{dF}{dt} = k(v_2 - v_1)$	$\frac{di}{dt} = \frac{1}{L}(v_2 - v_1)$	Inductor
Inerter	$F = b\frac{d(v_2 - v_1)}{dt}$	$i = C\frac{d(v_2 - v_1)}{dt}$	Capacitor
Damper	$F = c(v_2 - v_1)$	$i = \frac{1}{R}(v_2 - v_1)$	Resistor

Step 1: Remove Minimum Resistance

This ensures that the cycle starts with as a minimum function. To complete this, the minimum of the real part of the Nyquist plot is subtracted from the transfer function, i.e,

$$Z_1(s) = Z(s) - R_1 \tag{7.47}$$

This step creates a resistor in series with $Z_1(s)$ of value $R_1 = min(Re(Z(j\omega))$. At this point, a minimum positive real function $Z_1(s)$ is obtained.

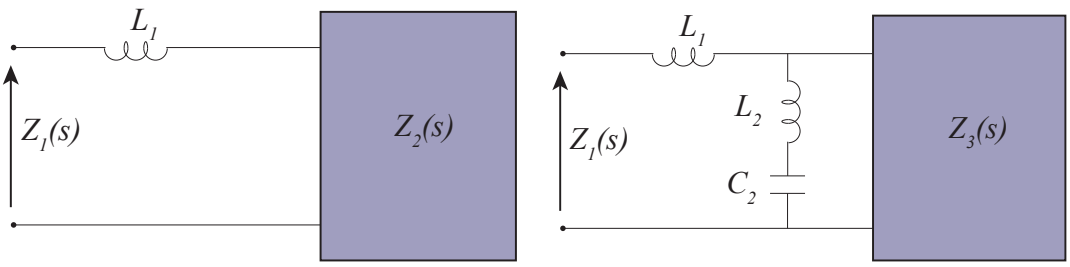

(a) Brune Synthesis after Step 2 (b) Brune Synthesis after Step 3

Figure 7.1: Progression of Electrical Setup after Step 2 of Brune Synthesis

Step 2: Remove Minimum Inductance

To remove the minimum inductance from the system, first ω_1 be the frequency such that $Re(Z(j\omega) = 0$, i.e., the network is purely reactive. Then, define X_1 such that

$$Z_1(j\omega_1) = X_1(j\omega_1) = jX_1 \tag{7.48}$$

This is now removed from the system via:

$$Z_2(s) = Z_1(s) - L_1 s, \quad L_1 = \frac{X_1}{\omega_1} \tag{7.49}$$

There will additionally be a case when $X_1 = 0$, in which $L_1 = 0$ and this step can be skipped. This step will introduce zeros at $z = \pm j\omega_1$ to $Z_2(s)$, which must be removed in the next step.

Step 3: Removal of Imaginary Zeros

Due to step 2, there will now be new zeros introduced at some point along the imaginary axis $z = \pm j\omega_1$. To remove these zeros, consider the three cases:

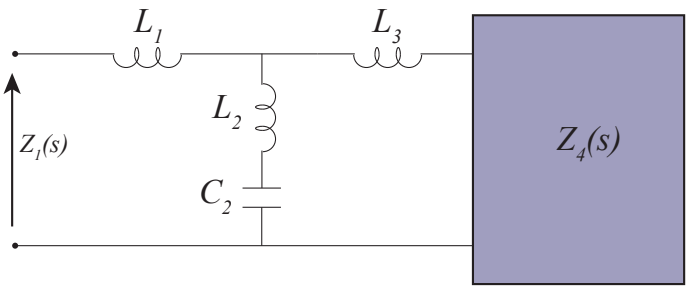

Figure 7.2: Brune Synthesis after Step 4

Case 1: $\omega_1 = 0$: In this case, one zero will be created at $z = 0$. In this case, the admittance $Y_2(s)$ will be of the form:

$$Y_1(s) = \frac{1}{Z_1(s)} = \frac{b_n s^n + b_{n-1}s^{n-1} + \cdots + b_1 s + b_0}{\bar{a}_n s^n + \bar{a}_{n-1}s^{n-1} + \cdots + \bar{a}_1 s} \tag{7.50}$$

and the Inductance term:

$$L_2 = \frac{b_0}{\bar{a}_1} \tag{7.51}$$

will reduce the order of the network via

$$Y_2(s) = Y_1(s) - \frac{L_2}{s} \tag{7.52}$$

At this point, the Brune process terminates and the Brune cycle starts up at Step 1.

Case 2: ω_1 =finite number: In this case, two zeros are created at $z = \pm j\omega_1$. To remove these, an shunt element composed of an inductor and a capacitor in series is introduced. In the network, this consists of a constant K_1 such that (given $Y_2(s) = 1/Z_2(s)$)

$$Y_3(s) = Y_2(s) - \frac{2K_1 s}{s^2 + \omega_1^2} \tag{7.53}$$

From this, the shunt element inductor ($L_2 = 1/2K_1$) and capacitor ($C_2 = 2K_1/\omega_1^2$) can be created, as shown in Figure [fig]. To compute the gain K_1, consider the

following reformulation of $Y_1(s)$. Since it is known that $\pm j\omega$ is a pole of $Y_1(s)$, it can be written:

$$Y_2(s) = \frac{1}{s^2 + \omega_1^2}\frac{N}{D} \tag{7.54}$$

and therefore

$$Y_3(s) = \frac{1}{s^2 + \omega_1^2}\left(\frac{N - 2DK_1 s}{D}\right) \tag{7.55}$$

It is not hard to see that ideally K_1 would be chosen such that $s^2 + \omega_1^2$ is a factor of $N - 2DK_1 s$. To achieve this, one can do long division with $s^2 + \omega_1^2$ as the divisor and $N - 2DK_1 s$ as the dividend. With this done, there will be a remainder which will be some function of K_1, and can be set equal to zero to solve for the gain K_1.

Now, we have some network $Y_2(s)$ which is not proper, since two poles have been removed with only one added. Therefore, the last step is to introduce another inductor $L_3 = -L_1/(1 + 2K_1 L_1)$ such that

$$1/Y_3(s) = Z_3(s) = sL_3 + Z_4(s) \tag{7.56}$$

At this point, we now have a proper, positive real system $Z_3(s)$ and the Brune cycle can start up again.

Case 3: $\omega_1 = \infty$: For this case, the goal of the Brune process (to create a zero at $z = \infty$) has already been completed. Therefore, the Brune's process would terminate here and the Brune cycle would start up at Step 1.

Step 4: Introduction of Transformer

In the above cases, either $L_1 < 0$ or $L_3 < 0$. What this translates to is a system that cannot be realized with mechanical components, since a negative spring is

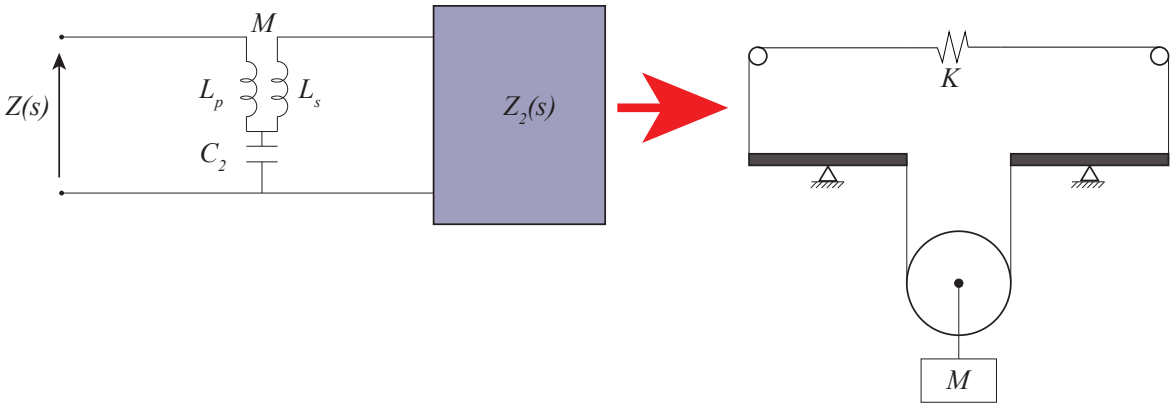

Figure 7.3: Relationship between Transformer and Lever

not physically possible. To alleviate this with electrical components, a transformer is introduced. The mechanical equivalent of a transformer is a lever system, e.g., the system shown in Figure [fig]. These would have to implemented wherever a transformer would be introduced. In the diagram, $L_p > 0$, $L_s > 0, M$ are picked such that

$$M = L_2, \quad \frac{M^2}{L_p L_s} = 1 \tag{7.57}$$

For this reason, Brune synthesis may be suboptimal for a mechanical realization. The lever system would complicate the realization and make it much more difficult to realize.

Resulting Realization

Brune synthesis was run on the transfer function created in Figure 4.2c. In this example, three full cycles of Brune Synthesis were run, with two capacitors being added into the mix. Due to negative inductance terms, the electrical implementation shown in Figure 7.4a had to be altered to the transformer implementation in Figure 7.4b. To be more precise, the realization required three transformers and five capacitors to realize the passive transfer function. This translates to three levers (see Figure 7.3 for a comparison between a transformer and a lever) and five inertial

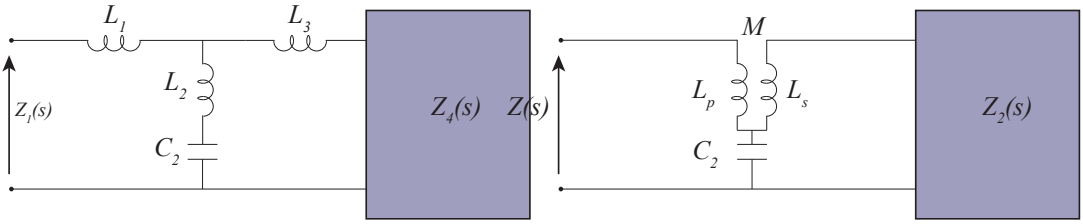

(a) Transfer Function after One Brune Cycle (b) Transformer in Brune Cycle

Figure 7.4: Example Brune Cycle Converted to Transformer

elements to realize the transfer function to be realized in a mechanical context.

BIBLIOGRAPHY

[1] M Abdelrohman. Effectiveness of active tmd for buildings control. *Transactions of the Canadian Society for Mechanical Engineering*, 8(4):179–184, 1984.

[2] Cristiano M Agulhari, Ricardo CLF Oliveira, and Pedro LD Peres. Static output feedback control of polytopic systems using polynomial lyapunov functions. In *49th IEEE Conference on Decision and Control (CDC)*, pages 6894–6901. IEEE, 2010.

[3] Cristiano M Agulhari, Ricardo CLF Oliveira, and Pedro LD Peres. Lmi relaxations for reduced-order robust control of continuous-time uncertain linear systems. *IEEE Transactions on Automatic Control*, 57(6):1532–1537, 2012.

[4] Brian Anderson and Sumeth Vongpanitlerd. *Network analysis and synthesis*. Dover Publications, 2013.

[5] P Apkarian and HD Tuan. Parameterized lmis in control theory. *SIAM Journal on Control and Optimization*, 38(4):1241–1264, 2000.

[6] Thomas Bailey and JE Ubbard. Distributed piezoelectric-polymer active vibration control of a cantilever beam. *Journal of Guidance, Control, and Dynamics*, 8(5):605–611, 1985.

[7] D Banjerdpongchai and JP How. Convergence analysis of a parametric robust h 2 controller synthesis algorithm. In *IEEE Conference on Decision and Control, 1997*, volume 2, pages 1020–1025. IEEE, 1997.

[8] Sam Behrens, Andrew J Fleming, SO Moheimani, et al. Passive vibration control via electromagnetic shunt damping. Institute of Electrical and Electronics Engineers, 2005.

[9] Stephen P Boyd, Laurent El Ghaoui, Eric Feron, and Venkataramanan Balakrishnan. *Linear matrix inequalities in system and control theory*, volume 15. SIAM, 1994.

[10] B Brogliato, R Lozano, B Maschke, and O Egeland. *Dissapative Systems Analysis and Control*. Springer-Verlag, London, 2 edition, 2007.

[11] Otto Brune. *Synthesis of a finite two-terminal network whose driving-point impedance is a prescribed function of frequency*. PhD thesis, Massachusetts Institute of Technology, 1931.

[12] James CH Chang and Tsu T Soong. Structural control using active tuned mass dampers. *Journal of the Engineering Mechanics Division*, 106(6):1091–1098, 1980.

[13] Inr J Conrr. Guaranteed margins for lqg regulators. 1972.

[14] Christopher J Damaren. Optimal strictly positive real controllers using direct optimization. *Journal of the Franklin Institute*, 343(3):271–278, 2006.

[15] Sidney Darlington. A history of network synthesis and filter theory for circuits composed of resistors, inductors, and capacitors. *IEEE transactions on circuits and systems*, 31(1):3–13, 1984.

[16] MC De Oliveira, JF Camino, and RE Skelton. A convexifying algorithm for the design of structured linear controllers. In *Proceedings of the 39th IEEE Conference on Decision and Control*, volume 3, pages 2781–2786. IEEE, 2000.

[17] JC Doyle. Synthesis of robust controllers and filters. In *IEEE Conference on Decision and Control*, pages 109–114. IEEE, 1983.

[18] SJ Dyke, BF Spencer Jr, MK Sain, and JD Carlson. Modeling and control of magnetorheological dampers for seismic response reduction. *Smart materials and structures*, 5(5):565, 1996.

[19] M Fazel, H Hindi, and S Boyd. Rank minimization and applications in system theory. In *American Control Conference*, volume 4, pages 3273–3278. IEEE, 2004.

[20] James Richard Forbes. Dual approaches to strictly positive real controller synthesis with a h2 performance using linear matrix inequalities. *International Journal of Robust and Nonlinear Control*, 23(8):903–918, 2013.

[21] Hermann Frahm. Device for damping vibrations of bodies., 1911. US Patent 989,958.

[22] T Fujinami, S Yamamoto, and A Sone. Dynamic absorber using lever and pendulum mechanism for vibration control of structure (the method of deciding parameters for the system). *Transactions of the Japan Society of Mechanical Engineers*, (Part C):3490–3496, 1991.

[23] T Fujita, T Kamada, and N Masaki. Fundamental study of active mass damper using multistage rubber bearing and hydraulic actuator for vibration control of tall buildings (2nd report, excitation tests for experimental model of building with mass damper). *Trans. Jpn. Soc. Mech. Eng., Ser. C*, 58(545):87–91, 1992.

[24] Pascal Gahinet, Pierre Apkarian, and Mahmoud Chilali. Affine parameter-dependent lyapunov functions and real parametric uncertainty. *IEEE Transactions on Automatic Control*, 41(3):436–442, 1996.

[25] JC Geromel, CC De Souza, and RE Skelton. Lmi numerical solution for output feedback stabilization. In *American Control Conference*, volume 1, pages 40–44. IEEE, 1994.

[26] JC Geromel and PB Gapski. Synthesis of positive real $\mathcal{H}_2$ controllers. *IEEE Transactions on automatic control*, 42(7):988–992, 1997.

[27] José C Geromel, Maurício C de Oliveira, and Liu Hsu. Lmi characterization of structural and robust stability. In *Proceedings of the American Control Conference*, volume 3, pages 1888–1892. IEEE, 1999.

[28] Jose C Geromel, Rubens H Korogui, and J Bernussou. $\mathcal{H}_2$ and $\mathcal{H}_\infty$ robust output feedback control for continuous time polytopic systems. *IET Control Theory & Applications*, 1(5):1541–1549, 2007.

[29] José Claudio Geromel and Rubens H Korogui. Analysis and synthesis of robust control systems using linear parameter dependent lyapunov functions. *IEEE Transactions on Automatic Control*, 51(12):1984–1989, 2006.

[30] K-C Goh, MG Safonov, and GP Papavassilopoulos. A global optimization approach for the bmi problem. In *Decision and Control, 1994., Proceedings of the 33rd IEEE Conference on*, volume 3, pages 2009–2014. IEEE, 1994.

[31] KC Goh, MG Safonov, and GP Papavassilopoulos. Global optimization for the biaffine matrix inequality problem. *Journal of global optimization*, 7(4):365–380, 1995.

[32] A Gonzalez-Buelga, LR Clare, A Cammarano, SA Neild, SG Burrow, and DJ Inman. An optimised tuned mass damper/harvester device. *Structural Control and Health Monitoring*, 21(8):1154–1169, 2014.

[33] KM Grigoriadis. Optimal h model reduction via linear matrix inequalities: continuous and discrete-time cases. In *IEEE Conference on Decision and Control*, volume 3, pages 3074–3079. IEEE, 1995.

[34] KM Grigoriadis and RE Skelton. Low-order control design for lmi problems using alternating projection methods. *Automatica*, 32(8):1117–1125, 1996.

[35] MM Haddad, Dennis S Bernstein, and Y William Wang. Dissipative $\mathcal{H}_2/\mathcal{H}_\infty$ controller synthesis. *IEEE Transactions on Automatic Control*, 39(4):827–831, 1994.

[36] Nesbitt W Hagood, Walter H Chung, and Andreas Von Flotow. Modelling of piezoelectric actuator dynamics for active structural control. *Journal of Intelligent Material Systems and Structures*, 1(3):327–354, 1990.

[37] James D Hart, Richard Sause, G Wyche Ford, and Lloyd D Brown. Pipeline vibration damper, 1993. US Patent 5,193,644.

[38] James D Hart, Richard Sause, G Wyche Ford, and Dennis G Row. Mitigation of wind-induced vibration of arctic pipeline systems. In *Proceedings of the International Conference on Offshore Mechanics and Artic Engineering*, pages 169–169. American Society of Mechanical Engineers, 1992.

[39] JP Den Hartog. *Mechanical vibrations*. Courier Corporation, 1985.

[40] Kumagai Toru Hashimoto, Ryoichi Wada, Mitsuo, Masato Tanaka, and Yoshida Yasuo. Control of an active mass damper using a neural network. *the Japan Society of Mechanical Engineers Part C*, 59(564):2305–2311, 1993.

[41] A Hassibi, J How, and S Boyd. A path-following method for solving bmi problems in control. In *American Control Conference*, volume 2, pages 1385–1389. IEEE, 1999.

[42] C Hol and C Scherer. A nonlinear sdp approach to fixed-order controller synthesis and comparison with two other methods applied to an active suspension system. *European Journal of Control*, 9, 2003.

[43] H Horisberger and PR Belanger. Regulators for linear, time invariant plants with uncertain parameters. *IEEE Transactions on Automatic Control*, 21(5):705–708, 1976.

[44] George William Housner, L_A Bergman, TK Caughey, AG Chassiakos, RO Claus, SF Masri, RE Skelton, TT Soong, BF Spencer, and James TP Yao. Structural control: past, present, and future. *Journal of engineering mechanics*, 123(9):897–971, 1997.

[45] Davor Hrovat. Survey of advanced suspension developments and related optimal control applications. *Automatica*, 33(10):1781–1817, 1997.

[46] Davorin Hrovat, Pinhas Barak, and Michael Rabins. Semi-active versus passive or active tuned mass dampers for structural control. *Journal of Engineering Mechanics*, 109(3):691–705, 1983.

[47] S Ibaraki and M Tomizuka. Rank minimization approach for solving bmi problems with random search. In *American Control Conference*, volume 3, pages 1870–1875. IEEE, 2001.

[48] Sedo Ichito, Koren Katsuhiko, and Saruwatari Katsumi. Vibration control of tower structure by a two-dimensional hybrid dynamic absorber. *the Japan Society of Mechanical Engineers Part C*, 59(559):721–726, 1993.

[49] Daniel J Inman and Ramesh Chandra Singh. *Engineering vibration*, volume 3. Prentice Hall Upper Saddle River, 2001.

[50] T Iwasaki. The dual iteration for fixed-order control. *IEEE transactions on automatic control*, 44(4):783–788, 1999.

[51] T Iwasaki and M Rotea. Fixed-order scaled synthesis. *Optimal Control Applications and Methods*, 18(6):381–398, 1997.

[52] T Iwasaki and RE Skelton. The xy-centring algorithm for the dual lmi problem: a new approach to fixed-order control design. *International Journal of Control*, 62(6):1257–1272, 1995.

[53] MR Jolly and DL Margolis. Regenerative systems for vibration control. *Journal of vibration and acoustics*, 119(2):208–215, 1997.

[54] S Kanev, C Scherer, M Verhaegen, and B De Schutter. Robust output-feedback controller design via local bmi optimization. *Automatica*, 40(7):1115–1127, 2004.

[55] Alireza Karimi and Mahdieh Sadabadi. Fixed-order controller design for state space polytopic systems by convex optimization. In *Proceddings of the IFAC Joint Conference*, number EPFL-CONF-176320, 2013.

[56] Koren Katsuhiko and Sedo Ichito. Vibration control of two-degree-of-freedom system using active dynamic absorber. *the Japan Society of Mechanical Engineers Part C*, 60(571):788–795, 1994.

[57] K Kawashima, S Unjoh, and K Shimizu. Experiments on dynamics characteristics of variable damper. In *Proc. of the Japan Nat. Symp. on Struct. Resp. Control*, 1992.

[58] James M Kelly. Aseismic base isolation: review and bibliography. *Soil Dynamics and Earthquake Engineering*, 5(4):202–216, 1986.

[59] Pramod P Khargonekar, Ian R Petersen, and Mario A Rotea. $\mathcal{H}_\infty$ optimal control with state-feedback. *IEEE Transactions on Automatic Control*, 33(8):786–788, 1988.

[60] Y KISHHVIOTO, DS Bernstein, and SR Hall. Energy flow control of interconnected structures: I. modal subsystems. 1995.

[61] Y KISHHVIOTO, DS Bernstein, and SR Hall. Energy flow control of interconnected structures: Ii. structural subsystems. 1995.

[62] M Kočvara, F Leibfritz, M Stingl, and D Henrion. A nonlinear sdp algorithm for static output feedback problems in compl e ib. *IFAC Proceedings Volumes*, 38(1):1055–1060, 2005.

[63] Huibert Kwakernaak and Raphael Sivan. *Linear optimal control systems*, volume 1. Wiley-interscience New York, 1972.

[64] E Lawler and D Wood. Branch-and-bound methods: A survey. *Operations research*, 14(4):699–719, 1966.

[65] F Leibfritz and EME Mostafa. An interior point constrained trust region method for a special class of nonlinear semidefinite programming problems. *SIAM Journal on Optimization*, 12(4):1048–1074, 2002.

[66] Zhongjie Li, Lei Zuo, George Luhrs, Liangjun Lin, and Yi-xian Qin. Electromagnetic energy-harvesting shock absorbers: Design, modeling, and road tests. *IEEE T. Vehicular Technology*, 62(3):1065–1074, 2013.

[67] R Lozano-Leal and SM Joshi. On the design of the dissipative lqg-type controllers. In *Proceedings of the 27th IEEE Conference on Decision and Control*, pages 1645–1646. IEEE, 1988.

[68] MatsuHisahiro, Sakae, OHisashi-kin, Nishihara Osamu Sato, and Susumu. Vibration control of a gondola by passive-type dynamic absorbers. *the Japan Society of Mechanical Engineers Part C*, 59(562):1717–1722, 1993.

[69] Takayuki Mizuno, Takuji Kobori, Jun-ichi Hirai, Yoshinori Matsunaga, and Naoki Niwa. Development of adjustable hydraulic dampers for seismic response control of large structure. In *Proc., ASME PVP Conf*, volume 229, pages 163–170, 1992.

[70] SO Reza Moheimani. A survey of recent innovations in vibration damping and control using shunted piezoelectric transducers. *IEEE Transactions on Control Systems Technology*, 11(4):482–494, 2003.

[71] Takehiro Mori and Hideki Kokame. A parameter-dependent lyapunov function for a polytope of matrices. *IEEE Transactions on Automatic Control*, 45(8):1516–1519, 2000.

[72] Kimihiko Nakano, Yoshihiro Suda, and Shigeyuki Nakadai. Self-powered active vibration control using a single electric actuator. *Journal of Sound and Vibration*, 260(2):213–235, 2003.

[73] P Narendra and K Fukunaga. A branch and bound algorithm for feature subset selection. *IEEE Transactions on Computers*, 100(9):917–922, 1977.

[74] AC Nerves and R Krishnan. A strategy for active control of tall civil structures using regenerative electric actuators. In *Engineering Mechanics*, pages 503–506. ASCE, 1996.

[75] Yohji Okada, Hideyuki Harada, and Kohei Suzuki. Active and regenerative control of an electrodynamic-type suspension. *JSME International Journal Series C*, 40(2):272–278, 1997.

[76] Ricardo CLF Oliveira, Maurício C de Oliveira, and Pedro LD Peres. Convergent lmi relaxations for robust analysis of uncertain linear systems using lifted polynomial parameter-dependent lyapunov functions. *Systems & Control Letters*, 57(8):680–689, 2008.

[77] Ricardo CLF Oliveira, Maurício C de Oliveira, and Pedro LD Peres. Robust state feedback lmi methods for continuous-time linear systems: Discussions, extensions and numerical comparisons. In *IEEE International Symposium on Computer-Aided Control System Design (CACSD)*, pages 1038–1043. IEEE, 2011.

[78] Ricardo CLF Oliveira and Pedro LD Peres. Lmi conditions for robust stability analysis based on polynomially parameter-dependent lyapunov functions. *Systems & Control Letters*, 55(1):52–61, 2006.

[79] Ricardo CLF Oliveira and Pedro LD Peres. Parameter-dependent lmis in robust analysis: characterization of homogeneous polynomially parameter-dependent solutions via lmi relaxations. *IEEE Transactions on Automatic Control*, 52(7):1334–1340, 2007.

[80] Junjiro Onoda, Kanjuro Makihara, and Kenji Minesugi. Energy-recycling semi-active method for vibration suppression with piezoelectric transducers. *AIAA journal*, 41(4):711–719, 2003.

[81] E Ostertag. An improved path-following method for mixed controller design. *IEEE Transactions on Automatic Control*, 53(8):1967–1971, 2008.

[82] Ian R Petersen. Disturbance attenuation and $\mathcal{H}_\infty$ optimization: A design method based on the algebraic riccati equation. *IEEE Transactions on Automatic Control*, 32(5):427–429, 1987.

[83] André Preumont. *Vibration control of active structures: an introduction*, volume 179. Springer Science & Business Media, 2011.

[84] Domingos CW Ramos and Pedro LD Peres. An lmi condition for the robust stability of uncertain continuous-time linear systems. *IEEE Transactions on Automatic Control*, 47(4):675–678, 2002.

[85] Mahdieh Sadat Sadabadi and Alireza Karimi. Fixed-order controller design of linear systems. Technical report, 2014.

[86] Arash Sadeghzadeh and Alireza Karimi. Fixed-structure $\mathcal{H}_2$ controller design for polytopic systems via lmis. *Optimal Control Applications and Methods*, 2014.

[87] Carsten Scherer, Pascal Gahinet, and Mahmoud Chilali. Multiobjective output-feedback control via lmi optimization. *IEEE Transactions on Automatic Contro*, 42(7):896–911, 1997.

[88] Jeff T Scruggs, Ian L Cassidy, and Sam Behrens. Multi-objective optimal control of vibratory energy harvesting systems. *Journal of Intelligent Material Systems and Structures*, page 1045389X12443015, 2012.

[89] Jeffrey Thomas Scruggs and WD Iwan. Structural control with regenerative force actuation networks. *Structural Control and Health Monitoring*, 12(1):25–45, 2005.

[90] JT Scruggs. Multi-objective optimization of regenerative damping systems in vibrating structures. In *American Control Conference*, pages 2672–2677. IEEE, 2007.

[91] Takashi Shimomura and Takao Fujii. Multiobjective control design via successive overbounding of quadratic terms. In *Proceedings of the 39th IEEE Conference on Decision and Control*, volume 3, pages 2763–2768. IEEE, 2000.

[92] Takashi Shimomura and Samuel P Pullen. Strictly positive real $\mathcal{H}_2$ controller synthesis via iterative algorithms for convex optimization. *Journal of guidance, control, and dynamics*, 25(6):1003–1011, 2002.

[93] M Shinozuka, MC Constantinou, and R Ghanem. Passive and active fluid dampers in structural applications. In *Proc. US/China/Japan Workshop on Struct. Control*, pages 507–516, 1992.

[94] Karl J Siwiecki. The full-scale experimental verification of an analytical model for evaluating methods of suppressing excessive bridge vibrations. Technical report, 1972.

[95] Malcolm C Smith. Synthesis of mechanical networks: the inerter. *IEEE Transactions on Automatic Control*, 47(10):1648–1662, 2002.

[96] BF Spencer Jr and S Nagarajaiah. State of the art of structural control. *Journal of structural engineering*, 2003.

[97] BF Spencer Jr, J Suhardjo, and MK Sain. Frequency domain optimal control strategies for aseismic protection. *Journal of Engineering Mechanics*, 120(1):135–158, 1994.

[98] JQ Sun, M Re Jolly, and MA Norris. Passive, adaptive and active tuned vibration absorbersa survey. *Journal of mechanical design*, 117(B):234–242, 1995.

[99] Frank Sup, Amit Bohara, and Michael Goldfarb. Design and control of a powered transfemoral prosthesis. *The International journal of robotics research*, 27(2):263–273, 2008.

[100] Onur Toker and Hitay Ozbay. On the np-hardness of solving bilinear matrix inequalities and simultaneous stabilization with static output feedback. In *American Control Conference*, volume 4, pages 2525–2526. IEEE, 1995.

[101] J VanAntwerp and R Braatz. A tutorial on linear and bilinear matrix inequalities. *Journal of process control*, 10(4):363–385, 2000.

[102] JG VanAntwerp, RD Braatz, and NV Sahinidis. Globally optimal robust control for systems with time-varying nonlinear perturbations. *Computers & chemical engineering*, 21:S125–S130, 1997.

[103] A Wahrburg and J Adamy. Parametric design of robust fault isolation observers for linear non-square systems. *Systems & Control Letters*, 62(5):420–429, 2013.

[104] EC Warner, IL Cassidy, and JT Scruggs. Regeneratively-constrained lqg control of passive networks. *energy*, 2(v1):x2, 2014.

[105] EC Warner and JT Scruggs. Control of vibratory networks with passive and regenerative systems. In *American Control Conference*, pages 5502–5508. IEEE, 2015.

[106] EC Warner and JT Scruggs. Regeneratively-constrained lqg control of vibration networks with polytopic model uncertainty. In *IEEE Conference on Control Applications (CCA)*, pages 1498–1504. IEEE, 2015.

[107] H Yamaura, K Ono, and K Toyota. Optimal tuning method for swing reduction of gondola lift by an inclined pendulum-type dynamic absorber. *Transactions of the Japan Society of Mechanical Engineers*, (Part C):3071–3077, 1993.

[108] Kemin Zhou and Pramod P Khargonekar. An algebraic riccati equation approach to h optimization. *Systems & Control Letters*, 11(2):85–91, 1988.